

Road surface noise research
Porous asphalt variability study – preliminary results



Prepared for
NZ Transport Agency

Victoria Arcade
50 Victoria Street
Wellington 6141

Date: 30 June 2019
Ref: 18-103/R11/A

Prepared for (the Client):
NZ Transport Agency

Prepared by (the Consultant):
Altissimo Consulting Ltd (NZBN 9429046516350)

Project: Road surface noise
Report: Porous asphalt thickness and variability study
Reference: 18-103/R11/A

Prepared by:

John Bull
Acoustics Engineer

Version history:

Version	Date	Comment
A	30/06/2019	Preliminary results

Executive Summary

This report presents preliminary results of the 2018-19 study into the effects of porous asphalt thickness on noise generation, and potential causes of variability of noise generation along a 'uniform' section of road (longitudinal variability). Some analysis is incomplete and further work required before this report is finalised in the second half of 2019. This preliminary report should be read on this basis.

Data collected

The below table summarises the data that forms the basis of the current work.

Property	Parameter	Measured by	Spatial resolution	Comments
Tyre/road noise	L _{CPX} (80 km/h)	CPX trailer	1 metre 20 metre	Raw audio data processed into 1 and 20 metre road segments.
Macrotexture	Mean profile depth ("MPD")	WDM*	1 metre 10 metre	The standardised MPD parameter captures texture wavelength between 0.5 and 50 mm. Tyre/road noise generation is affected by a narrower range of texture wavelengths.

Property	Parameter	Measured by	Spatial resolution	Comments
Void content	Dielectric constant	Ground penetrating radar	0.25 metre	Averaged over 1 and 20 metre segments. Relationship between dielectric constant and void content not yet determined.
Thickness	<i>direct</i>	Lidar	0.25 metre	Averaged over 1 metre road segments.
		Ground penetrating radar	0.25 metre	Averaged over 1 metre road segments.
		Tracesheet	Varies (20-50 metres)	
Roughness	NAASRA count	WDM*	20 metre	Not usually associated with tyre/road noise. Included for material transfer vehicle ("MTV") and construction property investigations.
Paving temperature	<i>direct</i>	Infrared sensor	2 seconds (~0.2 metre)	GPS accuracy 3-5 metres. Averaged over 20 metre road segments.
		Hand-held infrared camera	~10 metres	Unprocessed
		Paver mounted infrared camera	60 seconds (~5 metre)	Unprocessed
Paving speed, stops	<i>direct</i>	GPS	2 seconds (~0.2 metre)	GPS accuracy 3-5 metres. Averaged over 20 metre road segments.
Rolling temperature	<i>direct</i>	Infrared sensor	2 seconds (~0.2 metre)	Unprocessed
Rolling speed, passes	<i>direct</i>	GPS	2 seconds (~0.2 metre)	Unprocessed

* WDM high-speed data collection truck

Thickness study

Sections of differing asphalt thickness (30 mm, 40 mm and 50 mm) were constructed as part of the Western Belfast Bypass project ("WBB") in Christchurch in November 2018. The average thickness effect was found to be a noise reduction of -2.3 dB L_{CPX} (80 km/h) per 10 mm, which represents a significant acoustic effect.

Differences in L_{CPX} (80 km/h) of up to 1.4 dB were seen between the lanes for sections with the same nominal thickness; however, the lane differences are not consistent between each thickness section or between the two test tyres. The previous high-void trials at Sawyers to Groyne (2017) contained left-right lane mean profile depth differences that correlated with L_{CPX} . No significant variations in mean profile depth exist between the lanes at the WBB

thickness trial sections indicating that macrotexture is not the main driver of the L_{CPX} lane differences.

There is a relationship between the one-third octave band shape and surface thickness. A visual review of left and right lane spectrum data does not indicate a difference in thickness between the lanes.

Longitudinal variability study

Effect of material transfer vehicle

A material transfer vehicle ("MTV") was used on the majority of the WBB project to investigate its effect on longitudinal variability. While consistency of macrotexture, void content (measured through surface dielectric constant) and paving temperature were increased with the MTV, no significant differences in average $L_{CPX:P1,80}$ and acoustic variability were directly measured. This indicates that use of the MTV has no effect on $L_{CPX:P1,80}$.

Effect of local surface properties on tyre/road noise

The 20 metre road segment data for WBB with the MTV was used to investigate the effect of local mean profile depth and surface dielectric constant on tyre/road noise.

A regression of $L_{CPX:P1,80}$ on mean profile depth and surface dielectric constant showed a weak negative relationship between surface dielectric constant and $L_{CPX:P1,80}$, indicating that an increase in air-void content (decrease in dielectric constant) is related to an increase in tyre/road noise. The previous high-void trials exhibited higher tyre/road noise in the high-void mix than the standard mix due to an increase in macrotexture with void content. The current finding is consistent with the high-void trial finding, however, unlike the high-void trial, the change in void content has not resulted in a measurable change in mean profile depth.

Effect of construction properties on tyre/road noise

The 20 metre road segment data for WBB with the MTV was also used to investigate the effect of local paving temperature, paving speed and paver stops on tyre/road noise.

A regression of $L_{CPX:P1,80}$ on paving temperature, paving speed and paver stoppage provided no evidence of a relationship between 20 metre $L_{CPX:P1,80}$ and the available construction properties.

Thickness as determined by L_{CPX}

The spectrum shapes were reviewed at selected locations along WBB. The spectrum shape to thickness relationship suggests that the as-built thickness deviates significantly from the target thickness. In the case of the WBB project area (excluding the thickness trial sections) the average thickness is calculated to be 38 mm with values ranging between 25 mm and 50 mm.

Executive Summary	ii
1 Introduction	1
1.1 Background	1
1.2 Aim.....	2
1.3 Previous trials.....	2
1.4 Current trials.....	4
1.5 Report structure.....	4
2 Project details	4
2.1 Project area.....	4
2.2 Surface design details.....	5
2.3 Construction methodology and scheduling.....	6
3 Methodology	8
3.1 Surface thickness.....	8
3.2 Material transfer vehicle effects.....	8
3.3 Longitudinal variability.....	8
3.4 Data collection, storage and pre-processing	10
4 Thickness trial results	16
4.1 Overall thickness effect.....	16
4.2 Left-right lane differences in L_{CPX}	18
5 Longitudinal variability trial results	21
5.1 Heatmaps	21
5.2 $L_{CPX:P1,80}$, surface properties and construction properties with and without MTV	26
5.3 Effect of local surface properties on $L_{CPX:P1,80}$	36
5.4 Effect of local construction properties on $L_{CPX:P1,80}$	39
5.5 Thickness as determined by $L_{CPX:P1,80}$	42
6 Conclusions	48
Acknowledgements	49
References	50
Appendix A Results of previous trials	51
Appendix B Construction observations	57
Appendix C Ground Penetrating Radar	66
Appendix D Temperature and position loggers	76
Appendix E 3D Lidar Scan Data	82
Appendix F 1 metre Mean Profile Depth Data	84

1 Introduction

1.1 Background

The NZ Transport Agency has an ongoing research programme to reduce road surface noise. Work in this programme conducted between 2016 and June 2018, together with a summary of previous work, is set-out in Transport Agency report “Road surface noise research 2016-2018” [1]. Further to that report, in the current financial year (2018/2019) the research programme includes four main investigations being undertaken by WSP-Opus and Altissimo Consulting. This report sets out the current findings of one of those investigations relating to porous asphalt surfaces and a trial conducted during the surfacing of the Western Belfast Bypass (“WBB”) project in Christchurch. This report summarises the aspects of previous work that led to the trial. Other road surface noise investigations in 2018/2019 are reported separately (Table 1).

For context, Table 1 provides a summary of the road-surface noise research programme since 2017, which is when the Transport Agency began use and development of a close-proximity (“CPX”) road-surface noise measurement trailer. The CPX trailer measures sound levels with microphones mounted adjacent to the moving test wheel.

Table 1 Road surface noise research activities (following delivery of CPX trailer)

Date	Activity	Documentation
2017-2019	On-going development and improvement to CPX trailer (John Bull).	2016-2018 report [1] CPX trailer guide [2]
Feb 2017	High-void and texture trial sections constructed at Sawyers to Groynes, Christchurch.	2016-2018 report [1]
Mar 2017	CPX testing of Sawyers to Groynes trial sections (John Bull).	2016-2018 report [1]
Jun-Oct 2017	CPX testing of new North Island expressway sections and chipseal in Tairua (John Bull).	2016-2018 report [1] M2PP report [3] Tairua report [4]
Nov 2017	Western Belfast Bypass (WBB) pre-construction EPA7 trial section constructed at Clearwater to Groynes (Christchurch).	2016-2018 report [1]
Jan-Feb 2018	Biennial certification of CPX trailer (John Bull).	2016-2018 report [1] CPX trailer guide [2]
Mar 2018	EPA7 trial section constructed at Memorial Ave bridge (Christchurch).	2016-2018 report [1]
Mar 2018	CPX testing of WBB pre-construction EPA7 and Memorial Ave bridge EPA7 (John Bull).	2016-2018 report [1]
Jul-Dec 2018	Way-side and tyre investigation using CPX and SPB methods (Richard Jackett).	WSP-Opus report [5]
Sep-Oct 2018	CPX testing of North Island motorway asphalt surfaces (Robin Wareing).	Altissimo report [6]
Nov 2018 – Jun 2019	Western Belfast Bypass porous asphalt variability study.	This report
Feb-Jun 2019	Chipseal investigation using CPX and SPB methods (Richard Jackett).	WSP-Opus Research (in progress)
Jun 2019	CPX testing of Auckland Motorways (Robin Wareing).	Altissimo (in progress)

1.2 Aim

Existing data in New Zealand and internationally has shown significant variations in road surface noise from porous asphalt surfaces, both along the same section of road and between different sections of road having nominally the same surface [3] [6].

Since acquiring the CPX trailer in 2017, the Transport Agency has had two main goals for porous asphalt research:

1. To understand how bulk changes to the physical properties of a road surface (through mix design) affects the road surface noise of porous asphalt surfaces, in the interest of finding an improved low-noise porous asphalt mix design.
2. To investigate causes of longitudinal variability in porous asphalt surface noise and identify methods to reduce variability.

A number of the noise generating and amplification mechanisms associated with porous asphalt road surfaces are affected by surface macrotexture, void content and thickness [7]. These three surface properties often form the basis of international research into road surface noise [8] [9] [10]. The surface macrotexture, void content and thickness are in direct control of the surfacing engineer (through mix design) and the construction contractor (through construction methodology and quality control).

This report details the latest research activities undertaken in 2018/2019 to address the above two goals. Central to this work has been trials conducted on the WBB.

1.3 Previous trials

High-void and texture trials

A set of trial sections involving epoxy-modified porous asphalt (EPA) were commissioned by the Transport Agency in late 2016 to investigate the influence of void content on road surface noise (see Appendix A for details). Originally four porous asphalt mix designs were planned, however, one mix failed to pass the pre-construction lay-down trial resulting in that mix being excluded from the field trials. The final mix designs are described in Table 2 below.

Table 2 Details of the high-void and texture trial sections

Surface	Details
EPA10 (30 mm)	Epoxy-modified porous asphalt with 10 mm chip and 30 mm nominal surface thickness.
EPA10HV (30 mm)	Epoxy-modified porous asphalt with 10 mm chip, a lower ratio of fine aggregate to achieve a more open mix and 30 mm nominal surface thickness.
EPA14 (30 mm)	Epoxy-modified porous asphalt with a 14 mm chip and 30 mm nominal surface thickness.

The three trial sections were constructed by Downer New Zealand in February 2017 on both lanes of the northbound carriageway at the Sawyers to Groynes section of Johns Road (SH1) in Christchurch. CPX and macrotexture (mean profile depth) testing followed in March 2017 and the results revealed a linear relationship between mean profile depth and $L_{CPX:P1,80}$ (Figure 1). The graph has a separate data point for each lane for each trial surface.

Due to the differing macrotexture properties of the EPA10 and EPA10HV trial sections, the effect of the increased void content in the EPA10HV section could not be isolated from

macrotexture and no improvement due to the increased void content could be seen. Statistical pass-by (“SPB”) testing was performed by WSP-Opus in July 2018 to check for noise reduction effects at the way-side that may not be detectable using the CPX method; no additional way-side noise reduction was observed [5].

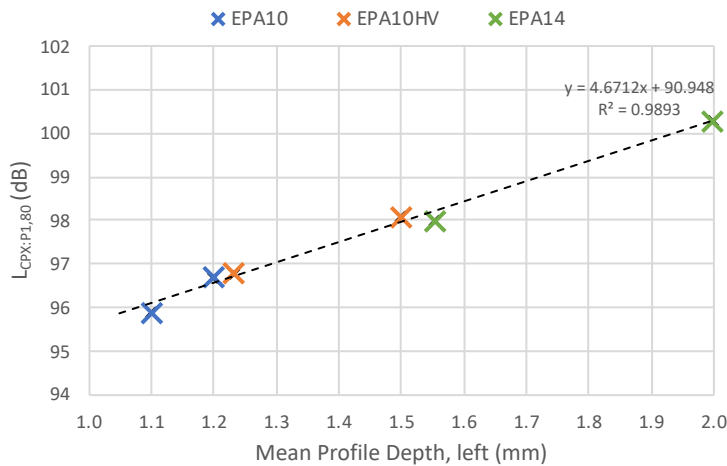


Figure 1 Macrotexture (mean profile depth) vs L_{CPX:P1,80} at the high-void trial sections

The results of the Sawyers to Groyne trail demonstrated how macrotexture is a strong driver of differences in tyre/road noise between different porous asphalt mixes. It also showed how an increase in void content results in an increase in macrotexture, and that any noise reduction due to increased void content appears to be insufficient to make up for the increase in noise due to macrotexture. These surfaces are subject to ongoing monitoring to identify any differences with wearing/aging, such as through voids clogging.

Small chip porous asphalt trials

To reduce the macrotexture of porous asphalt surfaces smaller chip mixes were trialled at two locations on SH1 in Christchurch (Table 3) (see Appendix A for details).

CPX testing on an initial WBB trial section showed a decrease of 4–5dB between an EPA7 surface and an existing EPA10 surface, although the EPA7 surface was 10 mm thicker than the EPA10 surface and in the order of half the noise reduction may have been caused by the increased thickness.

A second trial section on the Memorial Ave bridge did not show a difference in L_{CPX:P1,80} between the EPA7 and EPA10 surfaces, with both being nominally 30 mm thick. In this case the trial site was located on the approaches to the bridge and there is a possibility that the paver behaved differently on the sloped sections of road compared to its behaviour on level sections of road. The CPX measurements may also have been affected by the additional engine noise associated with the tow vehicle travelling uphill.

Both trial sections of EPA7 used aggregate from the same source (Fulton Hogan quarry).

Table 3 Small chip porous asphalt trial sections

Location	Surface	Details
Western Belfast Bypass pre-construction trial	EPA7 (40 mm) (laid October 2017, Fulton Hogan)	Epoxy-modified porous asphalt with 7 mm chip and 40 mm nominal surface thickness.
	EPA10 (30 mm) (laid March 2017, Downer)	Epoxy-modified porous asphalt with 10 mm chip and 30 mm nominal surface thickness.
Memorial Ave bridge trial (laid April 2017, Downer)	EPA7 (30 mm)	Epoxy-modified porous asphalt with 7 mm chip and 30 mm nominal surface thickness.
	EPA10 (30 mm)	Epoxy-modified porous asphalt with 10 mm chip and 30 mm nominal surface thickness.

1.4 Current trials

On the basis of the above trials the main surfacing works for WBB have been used to investigate changes to surface thickness and causes of longitudinal variability.

From the previous work, an EPA7 mix was selected for the main WBB surfacing, with a 40 mm nominal surface thickness. Within the works, trial sections of lesser (30 mm) and greater (50 mm) surface thickness were introduced. The surfacing process was closely scrutinised with various parameters measured during and after the works to investigate root causes of variability.

1.5 Report structure

A description of the project area, surface mix design, construction equipment and construction methodology are detailed in Section 2. The research methodology and surface and construction parameters being considered are outlined in Section 3. The results and discussion of results are presented together in Section 4. Where appropriate additional information has been included in the appendices.

2 Project details

2.1 Project area

The Western Belfast Bypass project forms a new part of SH1 in the northwest of Christchurch. Fulton Hogan was responsible for the construction of the WBB project.

The thickness trial sections were constructed on a section of the northbound carriageway (in both lanes) (see Figure 2). The thickness trial sections are short sections of road, approximately 260 metre in length. These sections form a continuous part of the rest of the WBB project, with thickness modification happening during a continuous paving run including gradual ramps (10 mm over 20-30 metres) between sections of differing thickness. The longitudinal variability study includes the whole of the WBB project area.

Details of the project area are provided in Table 4 below. In addition to the sections listed below, there were three bridge decks paved with a SMA surface (at an earlier date) and several EPA7 ramp sections before, after and between the thickness trial sections. All SMA and EPA7 ramp sections have been excluded from the analysis.

Table 4 Project area (all on State highway 01S)

Study	Carriageway	Lane	Thickness	Start	End	Length
Thickness trial sections	Northbound	Both	30 mm	0327/04.864	0327/05.126	262 m
			40 mm	0327/04.585	0327/04.845	260 m
			50 mm	0327/04.292	0327/04.566	274 m
Longitudinal variability	Northbound ⁺	Left	40 mm	0327/02.400	0333/0.316	2,500 m
		Right		0327/02.400	0333/0.316	2,500 m
	Southbound ⁺	Left	40 mm	0327/02.472	0333/0.507	3,600 m
		Right		0327/02.472	0333/0.510	3,600 m

† 30mm and 50mm thickness trial sections and joining ramps excluded.

+ SMA bridge decks excluded.

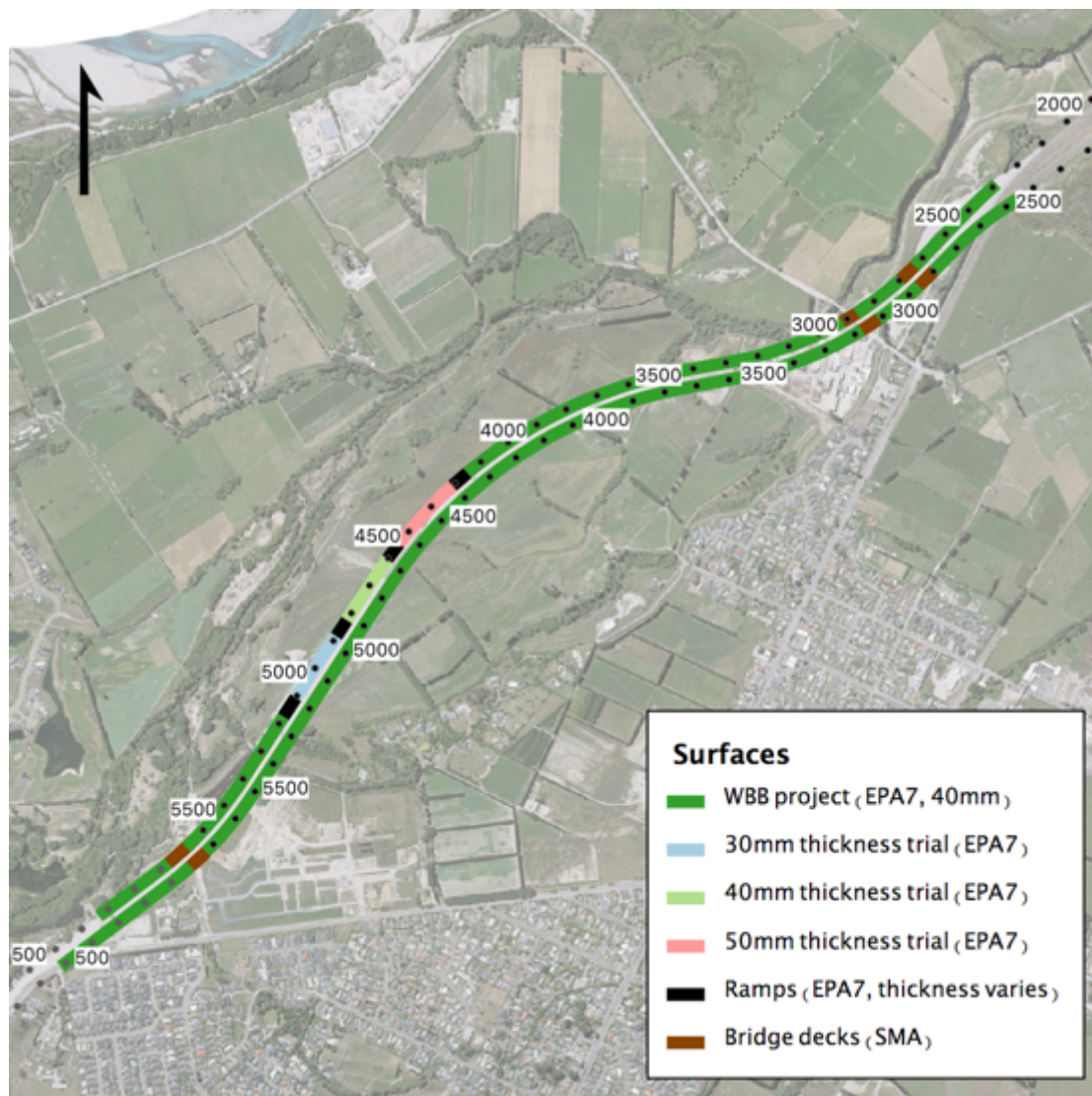


Figure 2 Project area and trial sections

2.2 Surface design details

The porous asphalt mix used on the entire WBB project was an epoxy modified porous asphalt with a nominal chip size of 7 mm. Specific details are provided in Table 5 below.

Table 5 Surface mix details

Property	Target
Asphalt plant temperature	120°C
Air void content	20%
Binder content	5.3 – 6.3%
Bitumen grade	80/100
Binder epoxy content	25%
Aggregate (sieve size)	% passing
13.2 mm	100 – 100
9.5 mm	95 – 100
6.7 mm	91 – 100
4.75 mm	45 – 55
2.36 mm	13 – 19
75 µm	1 – 5

2.3 Construction methodology and scheduling

A material transfer vehicle (MTV) was used on all but one construction shift to investigate whether it reduced variations in asphalt temperature and whether it would avoid artefacts caused as trucks offload into the paver. Normal practice in most of New Zealand does not include use of a MTV.

A list of construction equipment used by the paving contractor is provided in Table 6. The paver worked at a nominal speed of 5 metres/minute although at times was operated at other speeds. Once the surface temperature had dropped below 90°C the break-down roller performed one pass (both forward and reverse directions), with one of the directions being under vibration. The secondary roller then performed one pass (both forward and reverse directions) after the surface temperature had dropped below 50°C. The temperature was measured by the contractor QC staff using a hand-held infrared temperature probe.

Specific notes on the construction activities and temporary traffic management for each shift are provided in Appendix B. The construction schedule is provided in Table 7 below. Figure 3 shows the extents of each paving shift.

Table 6 Construction equipment

Category	Make/model	Details
Paver	Vogele 1803-3	Wheeled paver, capable of 8 metre wide runs.
Material transfer vehicle (MTV)	Roadtec SB-1500-C	Material transfer only (no on-board reheating).
Break-down roller	Bomag BW 151 AD-4	9.2t, 1.68 metre wide drum, tandem vibratory.
Secondary roller	HAMM HD75	8t, 1.68 metre wide drum, tandem vibratory.

Table 7 Construction schedule

Shift no.	Date	Direction and lane	Start	End	Length*	Notes
1	Tue, 23/10/18	SB right lane	0327/2.472	0327/4.400	1,798 m	No MTV
2	Wed, 24/10/18	SB left lane	0327/2.472	0327/4.439	1,836 m	
3	Fri, 26/10/18	SB right lane	0327/4.400	0333/0.510	1,802 m	
4	Sun, 28/10/18	SB left lane	0327/4.439	0333/0.507	1,763 m	
5	Sun, 4/11/18	NB right lane	0333/0.310	0327/2.998	2,898 m	
6	Mon, 5/11/18	NB left lane	0333/0.310	0327/3.624	2,274 m	
7	Tue, 6/11/18	NB left lane	0327/3.624	0327/2.386	1,116 m	
8	Wed, 7/11/18	NB right lane	0327/2.945	0327/2.387	494 m	

* Excludes SMA bridge decks.

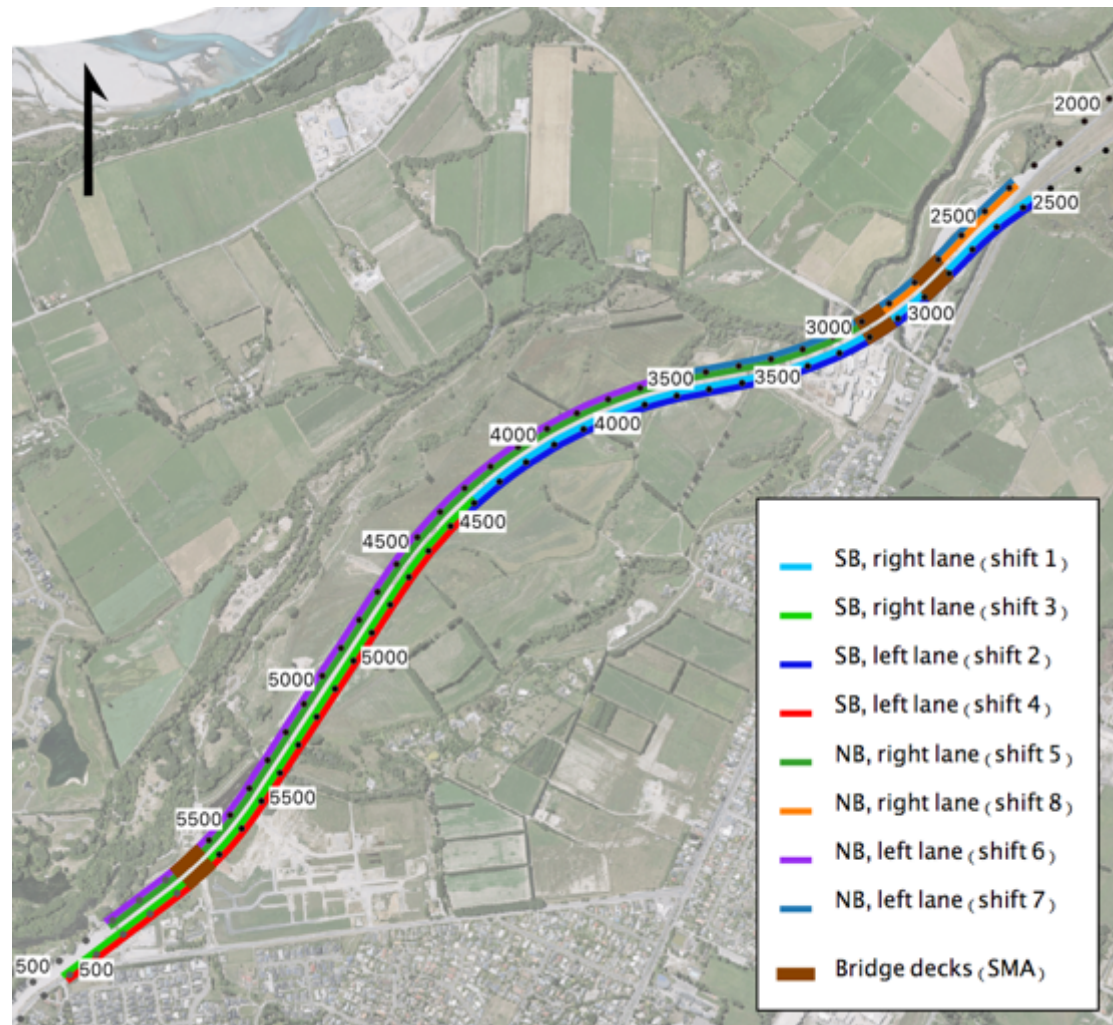


Figure 3 Extent of paving shifts. The displacement values are the Rp in metres from Rs 01S-0327 (black marks) and Rs 01S-0333 (grey marks).

3 Methodology

3.1 Surface thickness

CPX measurements were taken over the thickness trial sections using two test tyres (P1 and H1) and on two measurement dates (December 2018 and March 2019). The relationship between surface thickness and tyre/road noise is found using the average L_{CPX} in each lane for each target thickness (30 mm, 40mm and 50 mm). The one-third octave band L_{CPX} data is also investigated to determine whether or not there are any distinct differences in the spectral characteristics of the tyre/road noise between surfaces with differing thicknesses.

3.2 Material transfer vehicle effects

The effects of the material transfer vehicle on L_{CPX} , surface properties (macrotexture, dielectric constant and roughness) and construction properties (paving temperature, paving speed and paver stops) are investigated by considering the distributions of each property with and without the MTV (Section 5.2).

3.3 Longitudinal variability

Tyre/road noise is affected by macrotexture, void content and asphalt layer thickness (surface properties). In turn the surface properties are affected by the design and construction properties (see Figure 4). The design properties have remained constant across the WBB project (excluding thickness trial sections), meaning that any variability in tyre/road noise is due to the construction properties.

Three approaches are used for the longitudinal variability study:

1. Quantifying the local surface properties and construction properties and relating these to the local tyre/road noise (L_{CPX}). This is performed using 20 metre road segments and a multiple linear regression of L_{CPX} on the surface (Section 5.3) and construction (Section 5.4) properties.
2. Identifying 20 metres road segments having high, medium and low L_{CPX} and comparing their one-third octave band spectra to the average spectra from each thickness in the thickness trial area (Section 5.5).
3. Identifying areas of interest (having high and low L_{CPX}) of several hundred metres in length and investigating the differences in surface and construction properties (in progress, not reported).

While the success of first approach is strongly influenced by measurement uncertainty and missing parameters, it has been included as a first attempt towards finding properties that affect L_{CPX} . The second approach attempts to determine whether or not a variation in thickness is the primary cause of the L_{CPX} variability given that reliable measurements of the as-built thickness are not available.

The third approach represents a higher-level investigation and assumes that the wider areas of interest, comprising several hundred metres of road, will be less affected by measurement uncertainty (in particular repeatability and location issues).

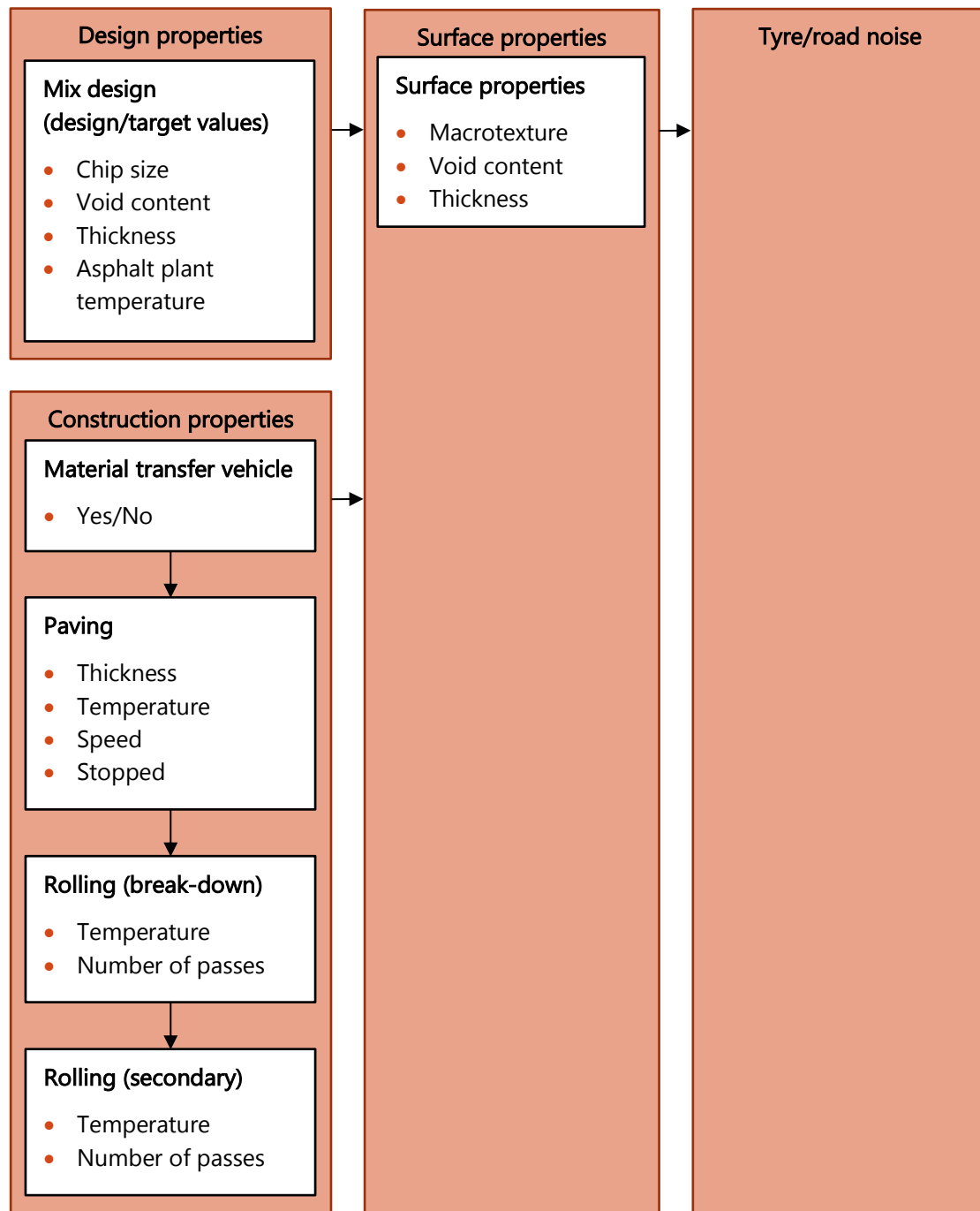


Figure 4 Relationship between tyre/road noise, surface properties and design and construction properties.

3.4 Data collection, storage and pre-processing

All of the raw data is GPS located and stored in a SQL database. The GPS coordinates of each row in the database are projected onto the RAMM [11] centreline model to find the linear reference associated with each raw data point (i.e. Rs/Rp). The linear references are then used to aggregate the raw data into discrete road segments. The data was processed at two scales for the current work. The 20 metre road segment lengths provide road segments consistent with ISO 11819-2 [12], while the 1 metre road segments provide a more detailed picture of the L_{CPX} distribution.

Tyre/road noise

The tyre/road noise was measured in December 2018 and March 2019 using the Transport Agency's CPX trailer. The CPX system records the raw audio data for each measurement run and outputs overall and one-third octave band CPX levels at the chosen road segment length.

For the current work the raw audio data was used instead of the 20 metre road segment values calculated directly and output by the CPX system. The raw audio data was processed into 1 and 20 metre road segments that align appropriately with the RAMM Rs/Rp points.

Three measurement runs were performed in each lane during each measurement session, and both the P1 and H1 test tyres were used.

Macrotexture

Surface macrotexture was measured in January 2019 using the vehicle mounted laser on the WDM high speed data collection truck as part of their annual network-wide survey. The macrotexture is reported as both mean profile depth over 1 metre and 10 metre road segments. The 1 metre road segment data was provided for the northbound carriageway only (see Figure 5); the detailed data does not form part of WDM's high-speed data collection contract with the Transport Agency and was provided in addition to the standard 10 metre road segments required under their contract. The 10 metre road segment data was available for the entire project area through RAMM.

The mean profile depth parameter contains no information concerning the texture wavelengths, which can be a critical piece of information when investigating road surface noise [13]. A 1 mm texture profile was provided by WDM; however, more work is needed to correctly process and align the profile with the other datasets. Only the 1 metre and 10 metre mean profile depth data has been included in the analyses to date.

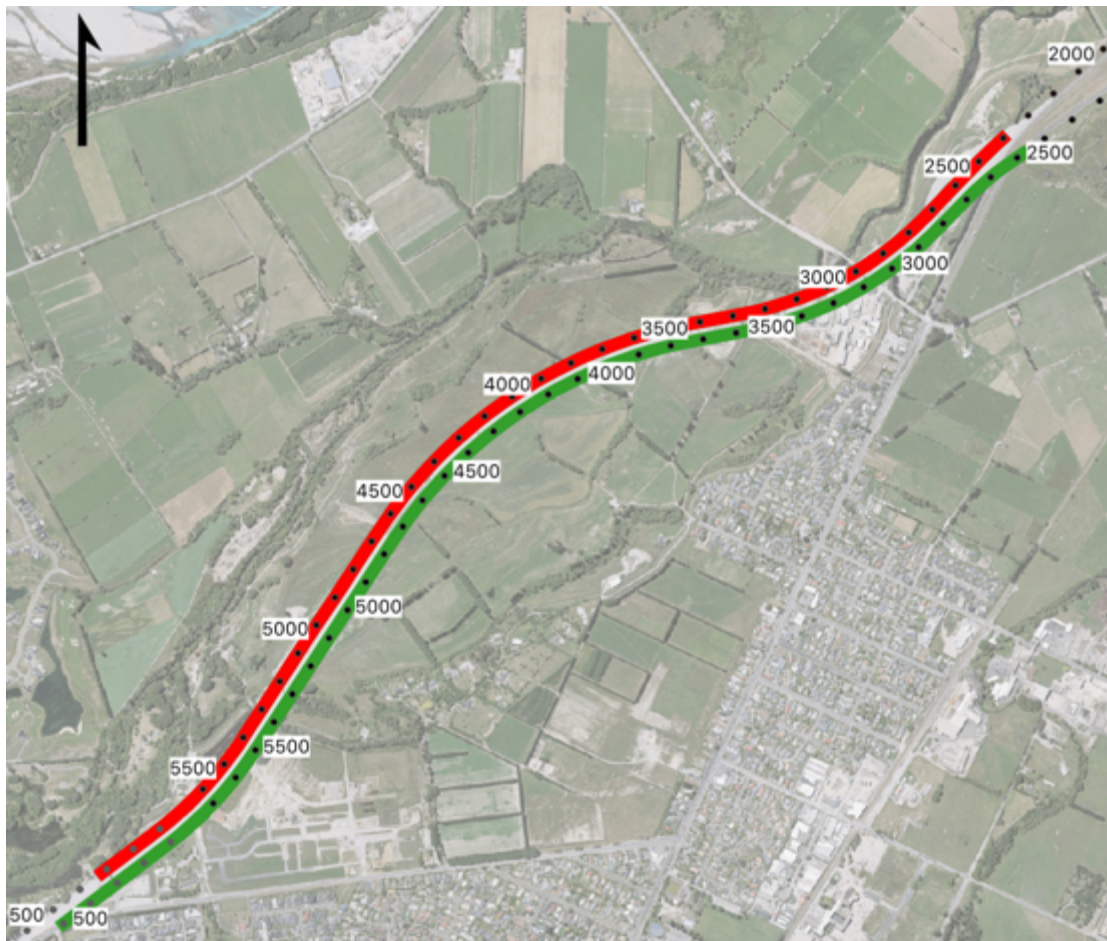


Figure 5 Extent of the detailed mean profile depth (1 metre road segments) and profile data is shown in red.

Void content

The air void content of the asphalt surface was measured by proxy using a vehicle mounted ground penetrating radar ("GPR"), which measures a material's dielectric constant.

In order to quantify the absolute air void content of the surface from the measured dielectric constants a calibration process must be performed (i.e. ground-truthing). Ground-truthing is achieved by extracting several core samples from the constructed surface and measuring the air void content in a laboratory. The core sampling process introduces a weakness in the road structure and has not yet been conducted on the WBB project. No calibration of the ground penetrating radar dielectric constants has been performed as part of the current analysis – this is a significant limitation and is intended to be addressed in the future analysis. The current analysis takes the dielectric constants at face-value and uses the assumption that an increase in dielectric constant indicates a decrease in air void content.

GPR testing was performed in December 2018 using Fulton Hogan's 2GHz GPR system over the entire project area. The raw reflection amplitudes were converted to dielectric constants and then arithmetically averaged over the desired road segment lengths.

Roughness

Roughness is defined as road texture with wavelengths between 50 mm and 500 mm and is quantified by the NAASRA count parameter. Tyre/road noise is widely considered to be most influenced by texture in the macrotexture range (wavelengths between 0.5 mm and 50 mm);

however, roughness is an important parameter for assessing ride quality and is expected to be influenced by the use of the material transfer vehicle. Roughness has therefore been included in the no-MTV / MTV analysis to determine the influence of the material transfer vehicle on roughness. 20 metre road segment data taken by WDM in January 2019 was available through RAMM.

Lidar thickness

A pre and post-construction height survey using a Lidar 3D scan was conducted by WSP-Opus over the thickness trial sections on the northbound carriageway (see Figure 6). WSP-Opus provided a detailed point cloud of both the original chipseal surface and the porous asphalt surface as well as cross-sections at 10 metre spacings.

The supplied point cloud data was used to generate long-section profiles for both the chipseal and porous asphalt surfaces. The thickness of the porous asphalt layer was found by subtracting the height of the chipseal surface from the height of the porous asphalt surface. The Altissimo results (calculated from the WSP-Opus point cloud data) were verified by comparing the calculated thicknesses to those in the 10 metre cross-sections supplied by WSP-Opus.

The thickness profiles are presented in Figure 7 below for the left and right lanes over the thickness trial sections. Inspection of the Lidar results shows that there is insufficient accuracy to assess small (<5mm) variations in surface thickness. In particular:

- The measured left lane asphalt thickness drops to 5 mm at its thinnest point. This is impossible given the mix design and visual inspection of the surface following paving. Assuming the surface is at least 20 mm thick, a measured thickness of 5 mm would suggest a measurement error of at least 15 mm.
- The measured left and right lane surface thicknesses show some correlation, at the 50-metre scale. Since the two lanes were paved in separate runs, correlation of surface thickness at the 50-metre scale is unlikely. While the base (chipseal) surface may contain bumps that run across the full width of the road, the paver's built in level control is only capable of smoothing out bumps up to 5-10 metres in length. The paver is unable to detect larger scale bumps in the base surface and hence will not correct for them. The observed correlation is most likely to be due to measurement error.
- The results show no difference between the 40 mm and 50 mm trial sections. The CPX measurement results presented in the later sections show a clear difference in L_{CPX} between the 40 mm and 50 mm trial sections and this difference can only be explained by a change in thickness.

Due to the above issues the Lidar thickness data is not considered an appropriate tool for determination of asphalt layer thickness and it has not been used in the current analysis.

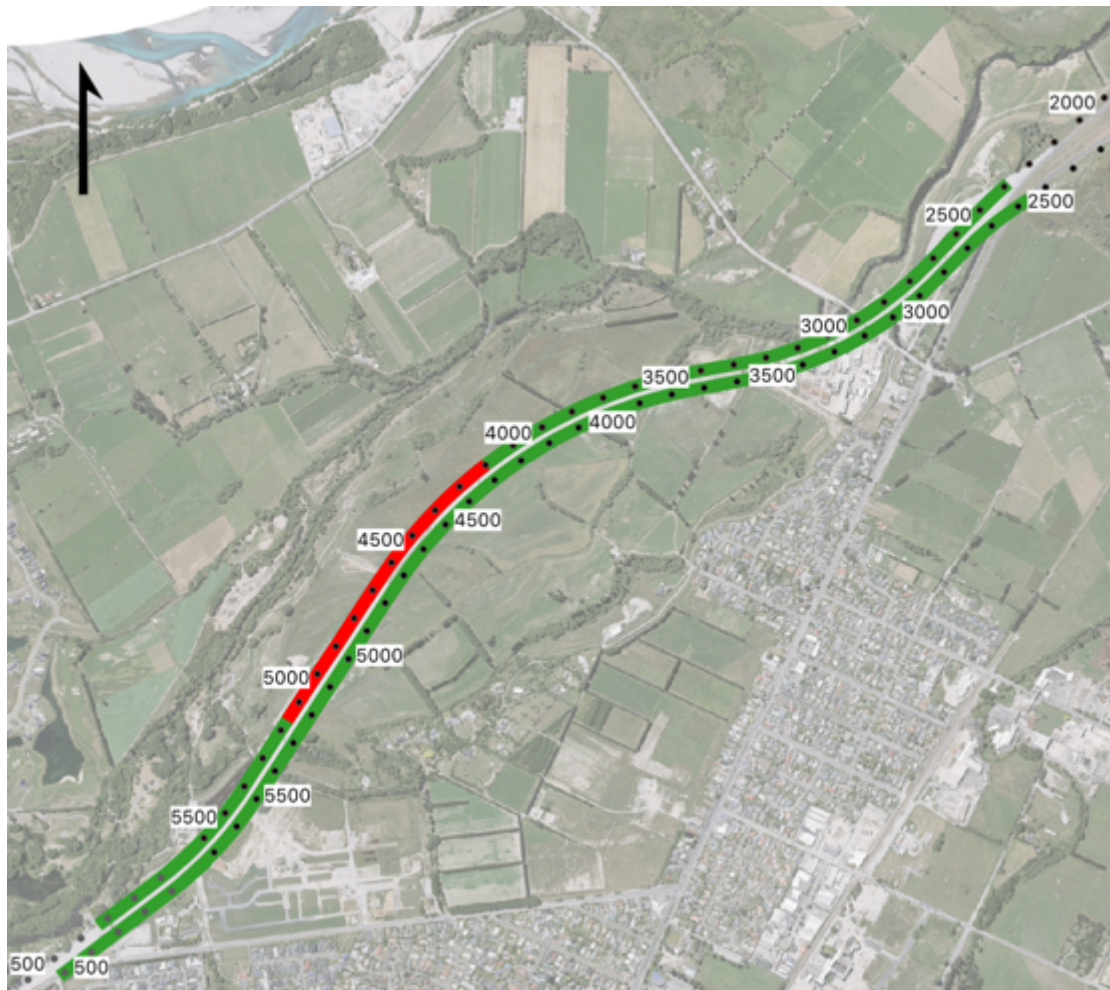


Figure 6 Extent of the WSP-Opus Lidar scan (limited to thickness trial sections).

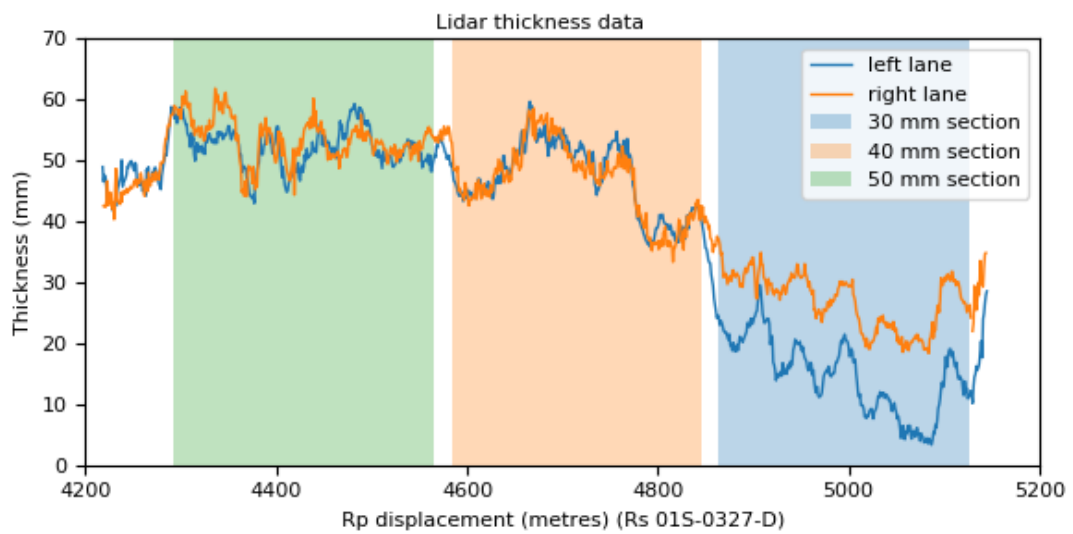


Figure 7 Left wheel path surface thickness profile

Ground penetrating radar thickness

An alternative thickness measurement technique made use of the reflection return times from the ground penetrating radar measurements. When combined with the local dielectric constant, the reflection return times can be used to calculate the distance travelled by the radar pulse.

Significant effort was put into checking the validity of this technique and automating the processing of the raw radar measurements to provide a detailed survey of the asphalt thickness (every 0.25 metres). At the time of writing the results have not proven reliable; a summary of the findings is presented in Appendix C along with a discussion of ground penetrating radar measurements in general.

Tracesheet thickness

After failure of the Lidar and ground penetrating radar thickness measurement techniques a third method was trialled to calculate the average asphalt thickness between truck loads. This technique relied on GPS records of the paver position and manual records by contractor QC staff noting the arrival and departure times of each asphalt truck and the paving width (included in the tracesheet records).

During steady operation it can be assumed that the system (paver and MTV) is completely full of asphalt at the departure of each asphalt truck. Therefore, an amount of asphalt equivalent to the load of the current truck is laid between the departure of the previous truck and the departure of the current truck. Assuming a constant asphalt density of $1,800 \text{ kg/m}^3$ and knowing the paving width at each truck departure, the average layer thickness can be calculated.

Again, the results of this technique proved unreliable, with the calculated asphalt thicknesses ranging from 10 mm to 150 mm. The main sources of error are thought to be the assumption that the MTV is full at the departure of each truck (the "full" condition is dependent on how the MTV is operated) and the manual recording of the truck departure times.

Paving temperatures and speed

Temperature and position loggers were developed specifically for the current work (see Appendix D for details). One logger unit was installed on the paver, with up to three non-contact infrared temperature sensors directed at the surface 2 metres behind the paver. The surface temperatures, paver position and paver speed were logged every 2 seconds throughout each construction shift over the entire project area. The GPS records were also used in the tracesheet thickness calculations described above.

The GPS receiver used was a low-cost consumer-grade GPS. The absolute positioning accuracy of consumer grade GPS receivers is generally considered to be 3-5 metres.

Rolling temperatures, speed and number of passes

Two additional temperature and position loggers were installed on each of the two rollers, with a single non-contact infrared temperature sensor directed 2 metres in front of each roller. The surface temperatures, paver position and paver speed were logged every 2 seconds throughout each shift. Additional processing of the roller temperature and position data is required to extract useful parameters since each roller must make several passes across the width of the lane and is able to make multiple passes over the same patch of surface. The processing steps are yet to be developed and rolling information has not been included in the current analysis.

Infrared photographs

Infrared photographs were taken approximately every 10 metres along the length of the project using a hand-held infrared camera. These photographs provide a detailed record of the surface temperature distribution beyond that provided by the spot measurements of the paver temperature logger.

An infrared camera was mounted on the paver during shifts 5 to 8 to provide an alternative record of the temperature distribution. The photographs from the paver-mounted camera provide meaningful absolute temperatures.

The infrared photographs are yet to be reviewed. They will be considered as part of the future analysis.

Contractor QC information

QC information was provided by the contractor following construction. The QC data included asphalt lab test reports, compaction tests (during construction) and tracesheets. The tracesheets included the following information for each asphalt truck:

- Asphalt plant docket number
- Truck load time
- In MTV time
- Out MTV time
- Paving width
- Length of load
- Load size (tonnes)
- Average depth

Only the “truck load time”, “in MTV time”, “load size” and “paving width” information was used in the current analysis. The “truck load time” and “in MTV time” were used to determine the average elapsed time between truck loading at the asphalt plant and unloading into the MTV for each shift.

Both the “length of road” and “average depth” information is based on the project chainages, marked on the ground at a 10 metre spacing. There is a high chance of error due to the low precision of the chainage marks, manual error from reading the incorrect mark and error due to the staff member responsible being unavailable at the required time and estimating the distance upon their return. The tracesheet “length of road” and “average depth” has not been used in the current analysis.

Construction observations

Written notes were taken by John Bull (Altissimo Consulting) during all eight paving shifts. These included equipment details, general observations and events such as equipment breakdowns. See Appendix B for details.

Summary of data collected

Table 8 provides a summary of the data collected.

Table 8 Summary of data collected

	Parameters	Details
Macrotecture	1 metre mean profile depth 10 metre mean profile depth 1 mm texture profile	WDM annual high-speed data survey. (January 2019)
Void content	Dielectric constant (GPR reflection amplitudes)	Part of the current work, using Fulton Hogan 2.0GHz GPR unit. (December 2018)
Roughness	20 metre NAASRA count	WDM annual high-speed data survey. (January 2019)
Thickness	Pre and post-construction height survey	WSP-Opus Lidar scan. (November 2018)
	Layer thickness (GPR reflection return times)	Part of the current work, using Fulton Hogan 2.0GHz GPR unit. (December 2018)
	Tracesheet thickness	Calculated for paver GPS records and truck departure times (contractor QC documentation).
Paver monitoring	Surface temperature (~2 metres behind paver)	Custom built loggers and non-contact IR temperature sensors. (taken during construction shifts)
	GPS position and speed	
Roller monitoring	Surface temperature (~2 metres in front of roller)	Custom built loggers and non-contact IR temperature sensors. (taken during construction shifts)
	GPS position and speed	
Infrared cameras	Hand-held camera	Flir One (hand-held) and Flir E4 (paver-mounted). (taken during construction shifts)
	Paver-mounted camera	
Construction trace sheets	Asphalt truck load details.	From contractor QC documentation.
Asphalt test reports	Asphalt laboratory test results (e.g. particle size distributions, air void content)	From contractor QC documentation.
Construction observations	Details of stops, breakdowns.	Written notes. (taken during construction shifts)

4 Thickness trial results

4.1 Overall thickness effect

At the time of writing, neither the Lidar scan nor ground penetrating radar techniques have been able to provide a reliable measurement of the asphalt layer thickness. The current analysis has been conducted using the target thickness that the construction crew aimed for during construction rather than a surveyed as-built thickness.

The overall L_{CPX} is presented below for each trial thickness, split by lane and test tyre for the December 2018 measurements. Figure 8 presents the data for the P1 test tyre. Figure 9 presents the data for the H1 test tyre.

There is a clear thickness effect, with L_{CPX} decreasing by 1.8–3.1 dB for each 10 mm increase in target thickness. The thickness effect is present for all combinations of lane and tyre; however, the magnitude of the effect varies. The magnitude of the changes are presented in Table 9 for both test tyres.

The overall thickness to L_{CPX} (80 km/h) relationship for the December 2018 measurements is included below, for thickness t in millimetres. The thickness effect is -2.3 dB L_{CPX} per 10 mm increase in thickness when considering the results from the P1 and H1 test tyres together.

$$L_{CPX} = -0.23t + 101.8$$

The thickness to $L_{CPX:P1,80}$ relationship for the December 2018 measurements will be used in the longitudinal variability study and is included here for reference:

$$L_{CPX:P1,80} = -0.24t + 102.0$$

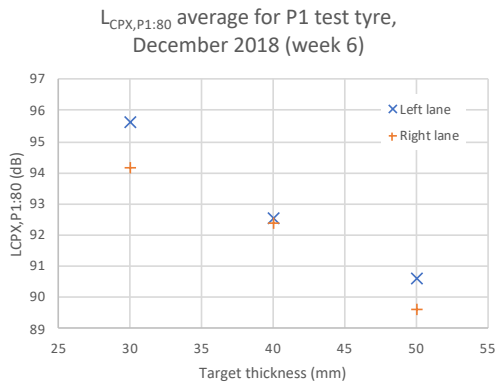


Figure 8 Average $L_{CPX:P1,80}$ for the thickness trial sections (December 2018).

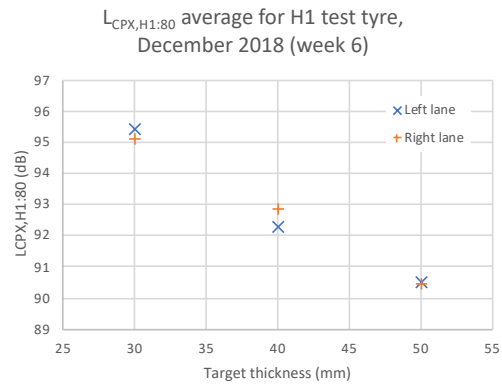


Figure 9 Average $L_{CPX:H1,80}$ for the thickness trial sections (December 2018).

Table 9 Thickness effect for P1 and H1 test tyres with 40 mm reference thickness

Lane	Target thickness	$L_{CPX,P1,80}$	$L_{CPX,H1,80}$
Left	30 mm	95.6 dB (+3.1)	95.4 dB (+3.1)
	40 mm	92.5 dB	92.3 dB
	50 mm	90.6 dB (-1.9)	90.5 dB (-1.8)
Right	30 mm	94.1 dB (+1.8)	95.1 dB (+2.3)
	40 mm	92.3 dB	92.8 dB
	50 mm	89.6 dB (-2.8)	90.5 dB (-2.4)

4.2 Left-right lane differences in L_{CPX}

The left-right lane differences in L_{CPX} are presented in Table 10 for the December 2018 measurements. The P1 test tyre measurements show the left lane to have higher $L_{CPX:P1,80}$ than the right lane for the 30 mm and 50 mm sections. The H1 test tyre measurements show the right lane to have higher $L_{CPX:H1,80}$ for the 40 mm section, with insignificant lane differences for the 30mm and 50 mm sections.

Table 10 Left-right lane difference in L_{CPX} for the December 2018 measurements.

Measurement date	Target thickness	Left-right lane difference in L_{CPX}	
		P1 test tyre ($L_{CPX,P1,80}$)	H1 test tyre ($L_{CPX,H1,80}$)
December 2018 (week 6)	30 mm	+1.4 dB	+0.3 dB
	40 mm	+0.2 dB	-0.6 dB
	50 mm	+1.0 dB	+0.0 dB

Differences in macrotexture between lanes

Both the surface macrotexture and void content were kept as constant as possible during construction by maintaining the same asphalt mix design on all trial sections and constructing the trial sections in one continuous paving run per lane.

In previous studies it was hypothesised that any left-right lane differences in L_{CPX} were due to differences in macrotexture caused by differences in early trafficking between the lanes, with left lanes generally experiencing higher traffic volumes than right lanes.

The average and standard deviation of the 1 metre road segment mean profile depth (macrotexture) are presented in Table 11 below for each thickness and lane (measured 12 weeks after construction). The results show no significant variations in mean profile depth between trial thicknesses or between lanes and provide no evidence of differences in macrotexture.

Table 11 Mean profile depth by lane and trial thickness (measured 12 weeks after construction)

Lane	Target thickness	Mean profile depth (mm)	
		Average	Standard deviation
Left	30 mm	1.19	0.07
	40 mm	1.13	0.07
	50 mm	1.12	0.08
Right	30 mm	1.18	0.06
	40 mm	1.17	0.06
	50 mm	1.20	0.09

Differences in thickness between lanes

While the target thickness is known for each trial section, there is a possibility that the left-right lane thicknesses differed slightly during construction. With an average L_{CPX} -thickness effect of -2.3 dB per 10mm increase in thickness, a 5 mm difference in surface thickness between lanes could cause a 1.2 dB difference in L_{CPX} .

The average and 95% confidence interval one-third octave band $L_{CPX:P1,80}$ values from the December 2018 measurements are presented in Figure 10 to Figure 12 for each thickness.

While there are clear differences in the frequency content of the $L_{CPX:P1,80}$ between the three target thicknesses, there are no substantial differences in frequency content between the lanes that would support the hypothesis that the lane differences are the result of differences in thickness. Additional measurements are required to determine whether or not there are differences in thickness between the lanes.

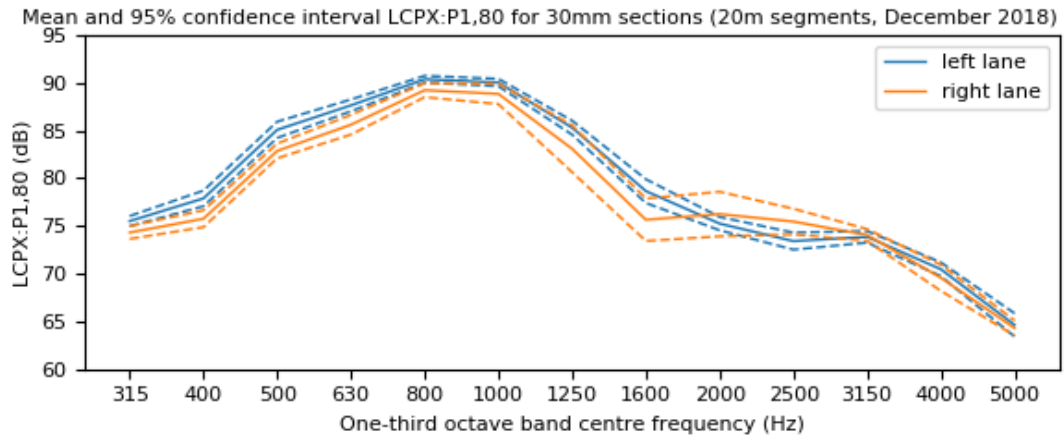


Figure 10 One-third octave band $L_{CPX:P1,80}$ (December 2018) for the 30 mm thickness sections.

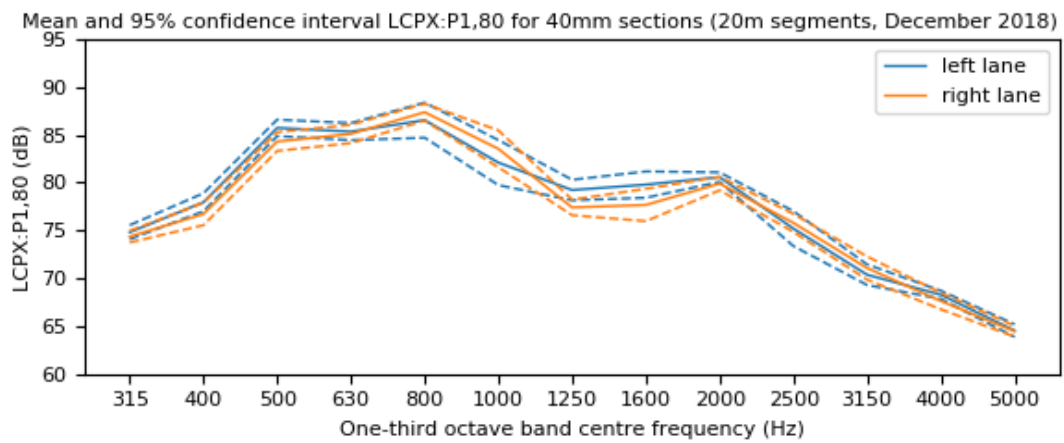


Figure 11 One-third octave band $L_{CPX:P1,80}$ (December 2018) for the 40 mm thickness sections.

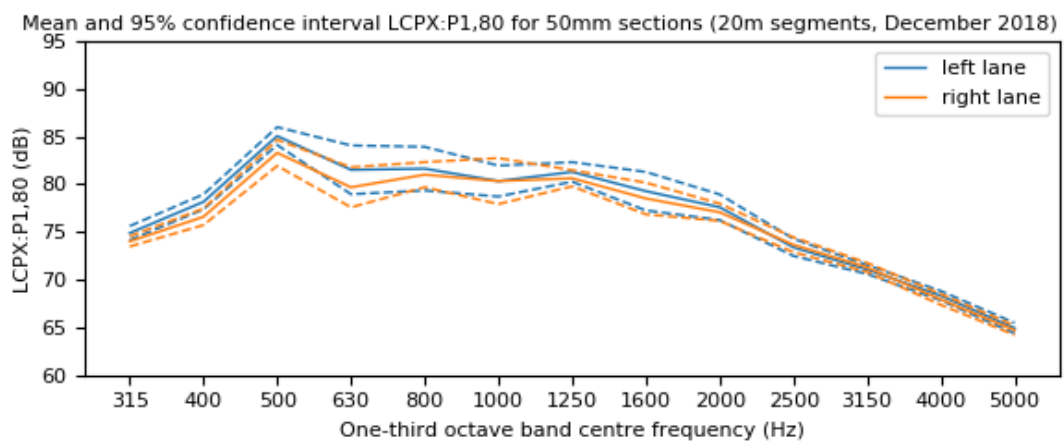


Figure 12 One-third octave band $L_{CPX:P1,80}$ (December 2018) for the 50 mm thickness sections.

5 Longitudinal variability trial results

5.1 Heatmaps

The L_{CPX} , surface properties and construction properties are shown as “heatmaps” below to provide an overview of the dataset. Each property includes a left and right lane measurement in both carriageways. The longitudinal variability study has only made use of the $L_{CPX:P1,80}$ data from the December 2018 measurements.

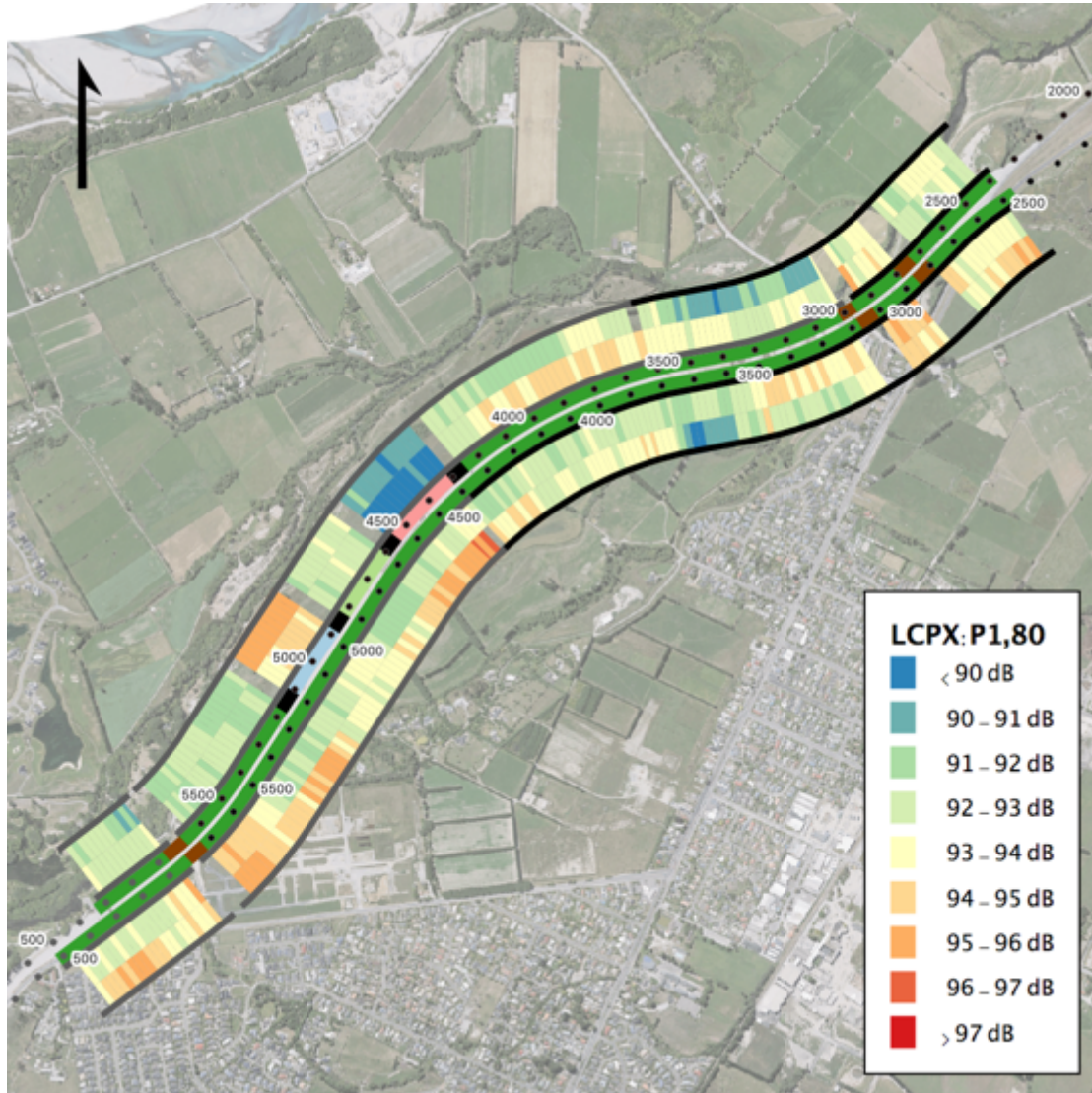


Figure 13 $L_{CPX:P1,80}$ for WBB (20 metre segments). The thickness trial sections are marked on the dotted centreline as pale blue (30 mm), pale green (40 mm) and pale red (50 mm). The construction shifts are marked as northern half (black) and southern half (grey).

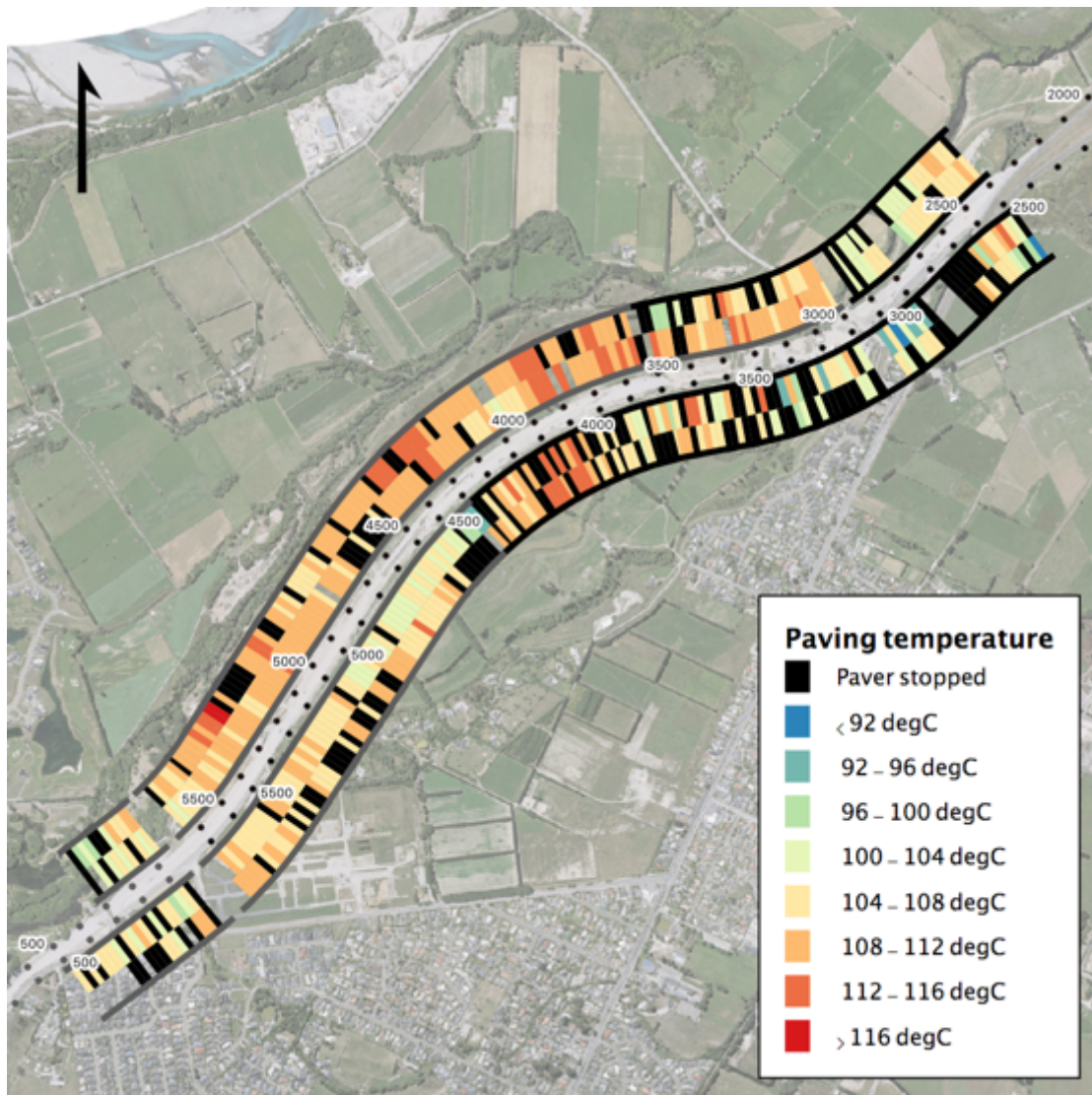


Figure 14 Paving temperature and stops for WBB (20 metre segments). The construction shifts are marked as northern half (black) and southern half (grey).



Figure 15 Paving speed and stops for WBB (20 metre segments). The construction shifts are marked as northern half (black) and southern half (grey).

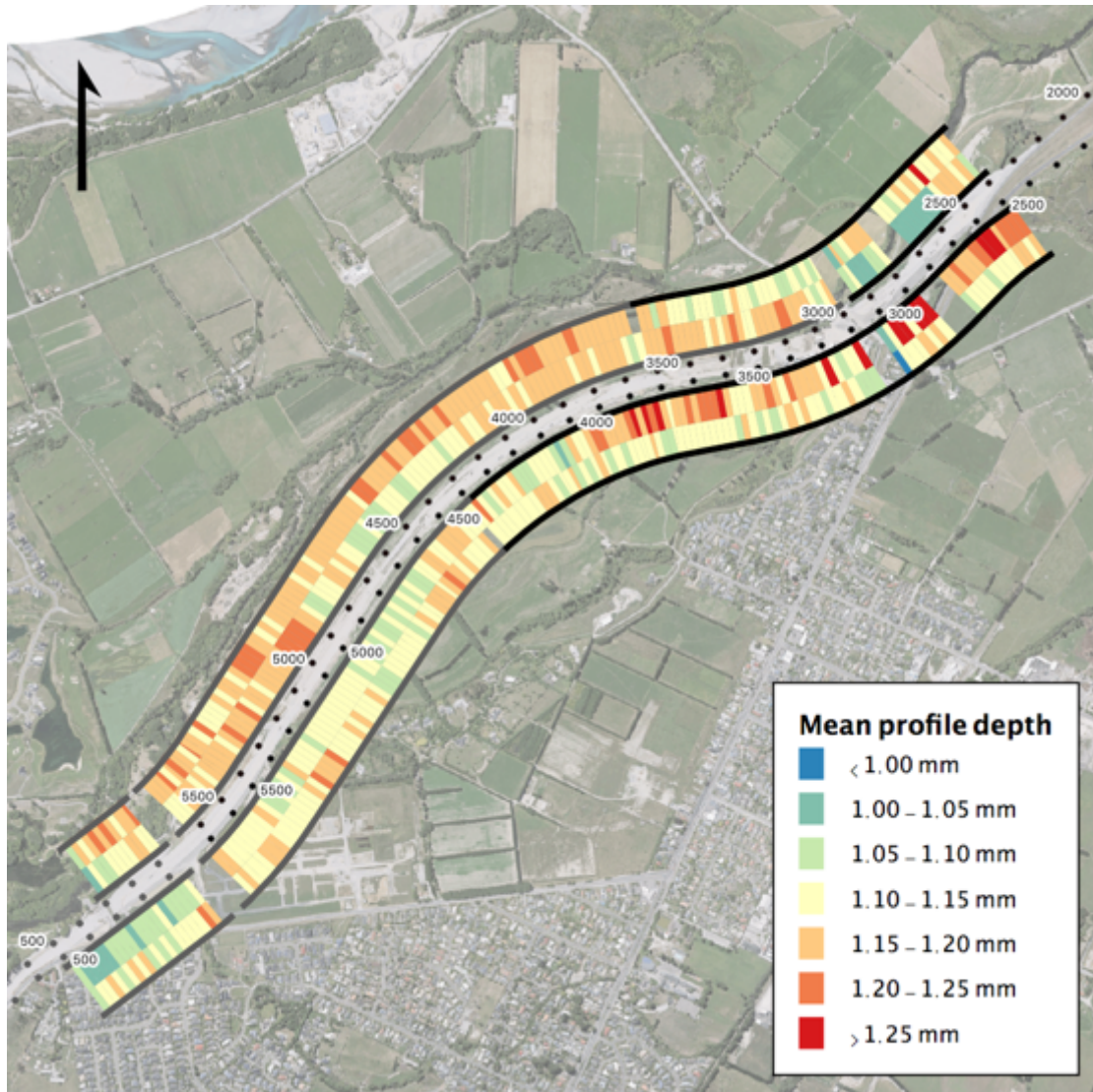


Figure 16 Left wheel path mean profile depth for WBB (20 metre segments), calculated from 2019 WDM 10 metre dataset. The construction shifts are marked as northern half (black) and southern half (grey).

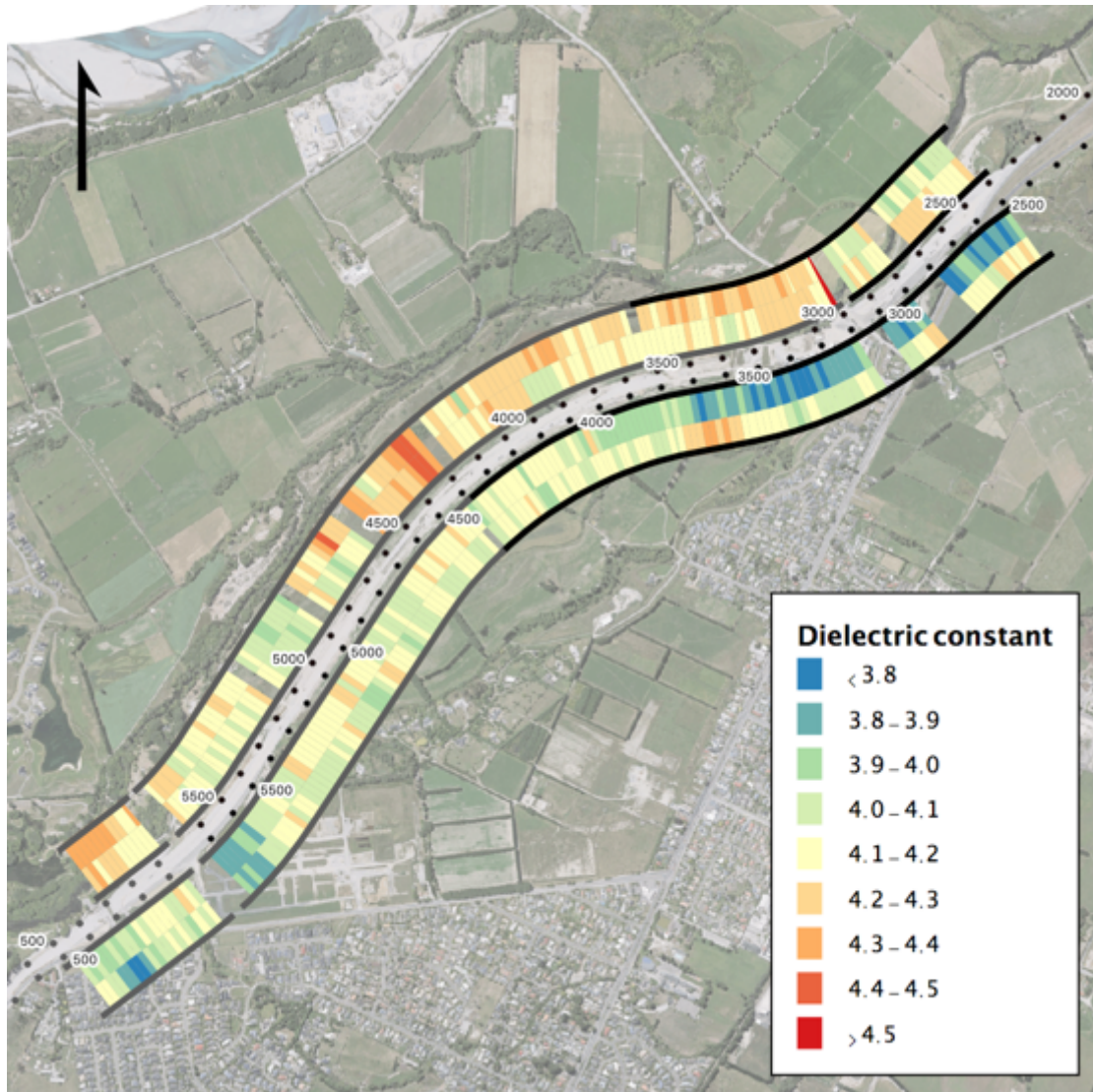


Figure 17 Surface dielectric constant for WBB (20 metre segments). The construction shifts are marked as northern half (black) and southern half (grey).

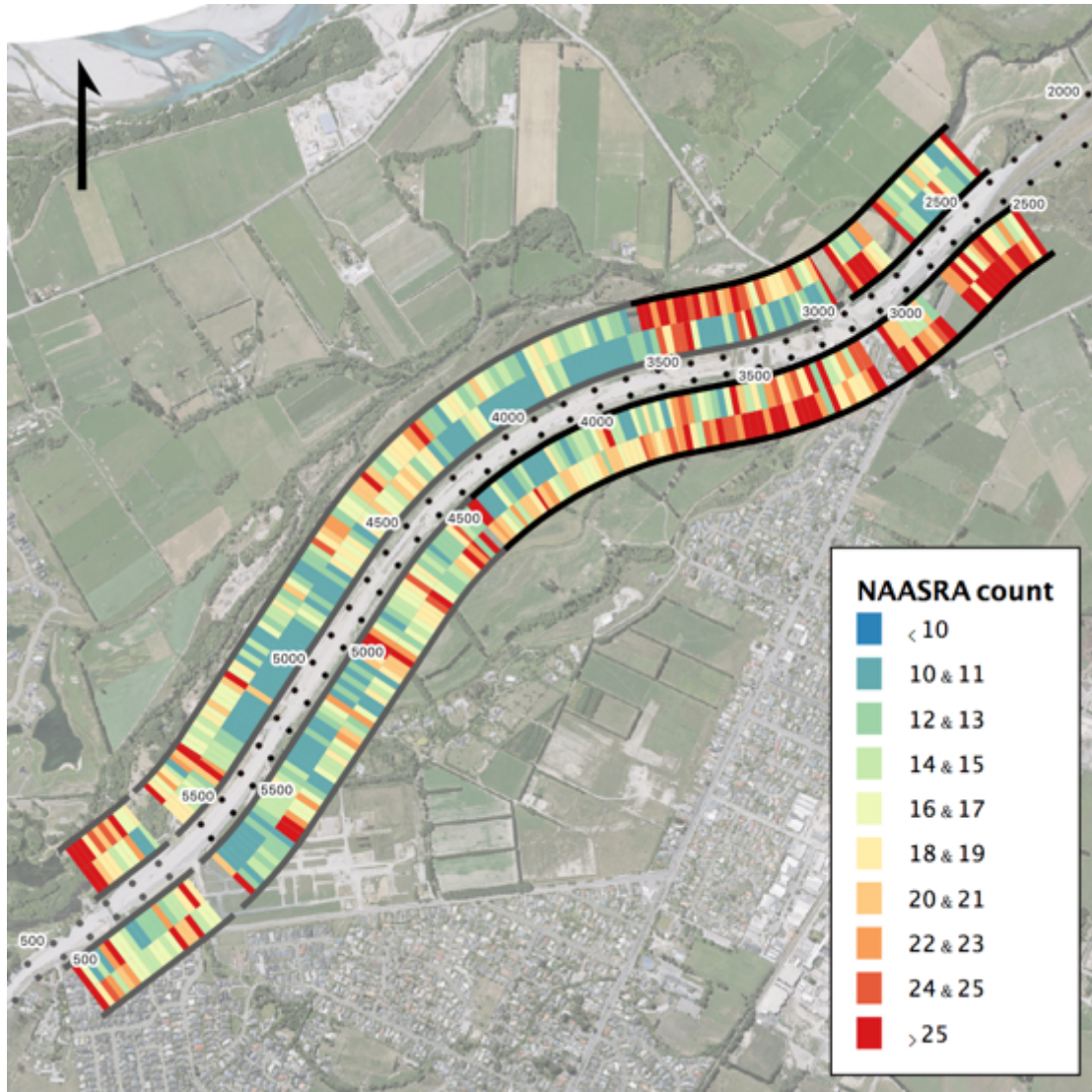


Figure 18 NAASRA count for WBB (20 metre segments). The construction shifts are marked as northern half (black) and southern half (grey).

5.2 LCPX:P1,80, surface properties and construction properties with and without MTV

The effects of the material transfer vehicle on tyre/road noise, road surface properties and operating behaviour of the paver are investigated using the right lane southbound carriageway between Dickey's Road bridge and Groynes Road bridge.

The section of road was chosen for the following reasons:

- It is free from features that would usually cause the paving process to slow or stop (key-ins, manholes and complex edge detailing),
- Both MTV and no-MTV sections lie in the same lane (and carriageway) so experience similar traffic behaviour, and
- There are approximately equal numbers of MTV and no-MTV 20 metre road segments.

Table 12 lists the start and end positions of the no-MTV and MTV sections. The segments within 50 metres of each bridge key-in have been excluded as these generally involve some edge detailing. Similarly, the segments within 50 metres of the junction between the two shifts have been excluded due to the slow paving and paver stops usually associated with the start and end of paving shifts.

Table 12 Start and end Rs/Rp for the no-MTV and MTV sections.

	Start Rs/Rp	End Rs/Rp	Length
No MTV section (shift 1)	01S-0327/03.150-I	01S-0327/04.350-I	1,200 metres
MTV section (shift 3)	01S-0327/04.450-I	01S-0327/05.700-I	1,250 metres

Table 13 provides a summary of the mean and standard deviation for each available surface and construction property. Also included in the table are details of the number of paver stops, asphalt plant-to-paver time, truck load size and the total number of trucks. Where applicable the distributions of each property are plotted (see Figure 19 to Figure 32).

Key differences between the no-MTV and MTV sections are as follows:

- The results show that there is no significant difference in $L_{CPX:P1,80}$ between the no-MTV and MTV sections, both in terms of average level and standard deviation.
- The average and standard deviation of the mean profile depth for the MTV section is slightly lower than the no-MTV section. It is unclear whether or not this is a significant difference. Analysis of a similar system provided mean profile depth repeatability of 0.1 mm [14].
- The average surface dielectric constant is slightly higher for the MTV section, suggesting that the MTV section has a lower void content than the no-MTV section. More work is needed to determine if this is a real difference or due to measurement uncertainty. Work is also needed to relate the measured surface dielectric constant to air void content.
- There is a small change in average NAASRA count between the no-MTV and MTV sections. The magnitude of the change is minimal and should not represent a perceptible difference in ride quality.
- The average paving temperature is slightly lower for the MTV section. This could be explained by the fact that the asphalt has to travel through the MTV (without reheating) before reaching the paver; however, there was also a difference in ambient air temperature between the two paving shifts (11°C for no-MTV, 7°C for MTV), which may be another reason for the faster asphalt cooling within the MTV section. The 20 metre segments within the MTV section experienced lower variations in paving temperature than those within the no-MTV section, which can be explained by the temperature smoothing effect caused by the large thermal mass of the MTV.
- The no-MTV section involved more paver stops. This is due to the paver being stopped at every truck change-over, compared to the MTV section that generally involved continuous paving.
- The 20 metre segment paving speed is consistent for both no-MTV and MTV sections. The paving speed calculation includes paver stops, hence, the no-MTV section has more <4 metre/minute segments due to the higher number of stops.

- The average asphalt plant-to-paver time is significantly longer for the no-MTV section, which is put down to the reasons listed below and supported by the piecemeal distribution in Figure 31.
 1. The no-MTV section was the first paving shift of the project and there were multiple delays getting paving underway while staff and equipment settled in to their roles. Later paving shifts involved fewer start-of-shift delays.
 2. The no-MTV section follows on from a complex area involving bridge key-ins and edge detailing that caused the paving process to slow and significant wait times for the asphalt trucks.
- The truck load size was consistent between the no-MTV and MTV sections. With the MTV section using three more trucks, which is consistent with it being slightly longer.

Table 13 Summary statistics for the no-MTV and MTV sections.

Property	Statistic	No-MTV (shift 1)	MTV (shift 3)
L _{CPX:P1,80} (20 metre segments, December 2018)	Mean	92.7 dB	92.7 dB
	Std. dev.	0.87 dB	0.97 dB
Mean profile depth (20 metre segments, WDM January 2019)	Mean	1.17 mm	1.12 mm
	Std. dev.	0.06 mm	0.03 mm
Surface dielectric constant (20 metre segments, December 2018)	Mean	3.96	4.11
	Std. dev.	0.13	0.09
NAASRA count (20 metre segments, WDM January 2019)	Mean	16.2	14.3
	Std. dev.	5.2	4.4
Paving temperature (1 metre segments, excludes stops)	Mean	107.5°C	105.6°C
	Std. dev.	6.7°C	3.0°C
Paving speed (20 metre segments, includes stops)	Mean	6.8 metres/minute	6.6 metres/minute
	Std. dev.	1.7 metres/minute	1.5 metres/minute
Paver stops (1 metre segments)	Total	40	8
Asphalt plant-to-paver time	Mean	79.5 minutes	36.8 minutes
	Std. dev.	43.3 minutes	5.3 minutes
Asphalt truck load size	Mean	12.8 tonnes	13.1 tonnes
	Std. dev.	3.6 tonnes	3.3 tonnes
Number of trucks	Total	32	35
Paved length per truck load	Average	37.5 metres	35.7 metres

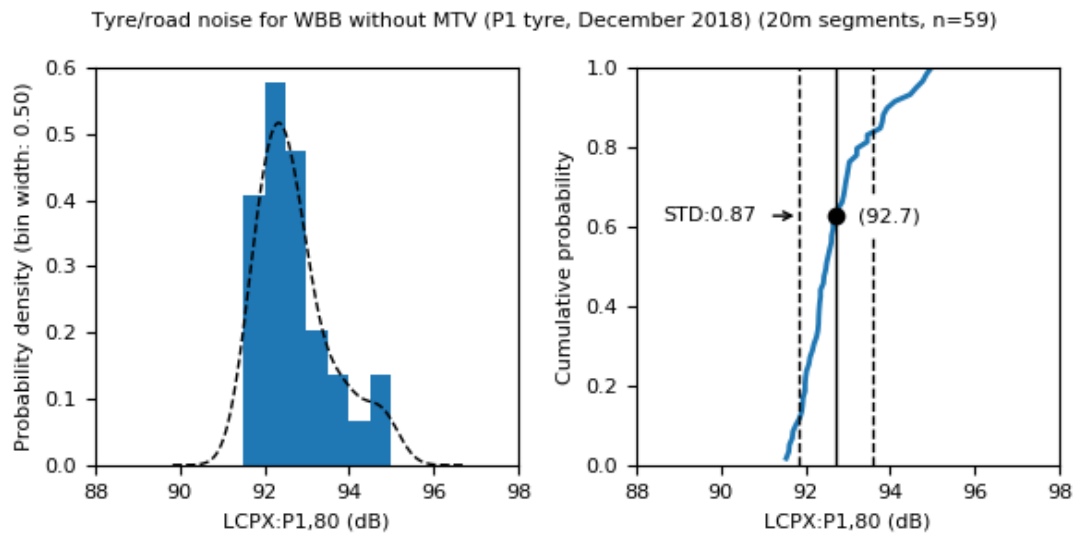


Figure 19 $L_{CPX:P1,80}$ (December 2018) for the no-MTV section.

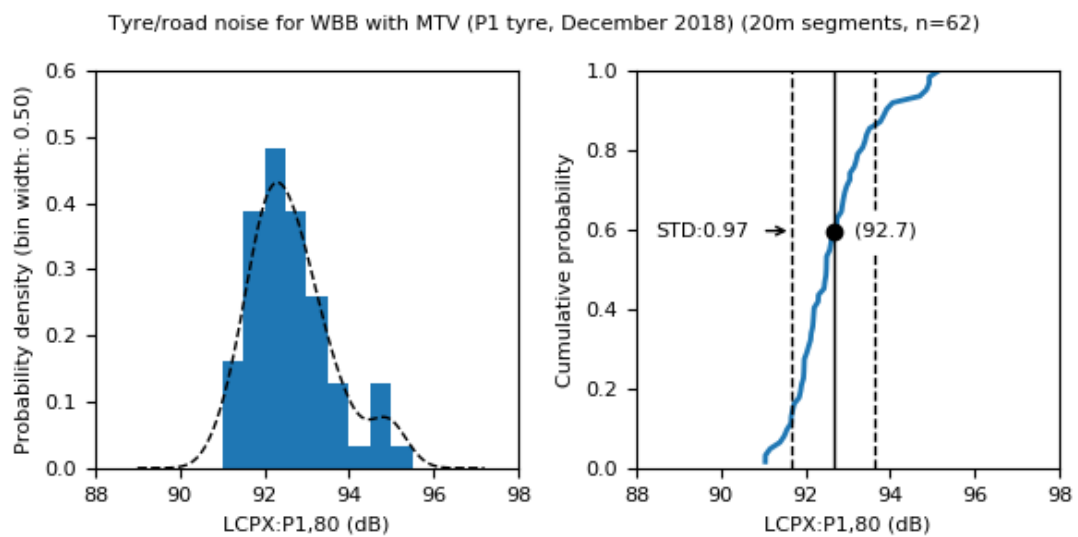


Figure 20 $L_{CPX:P1,80}$ (December 2018) for the MTV section.

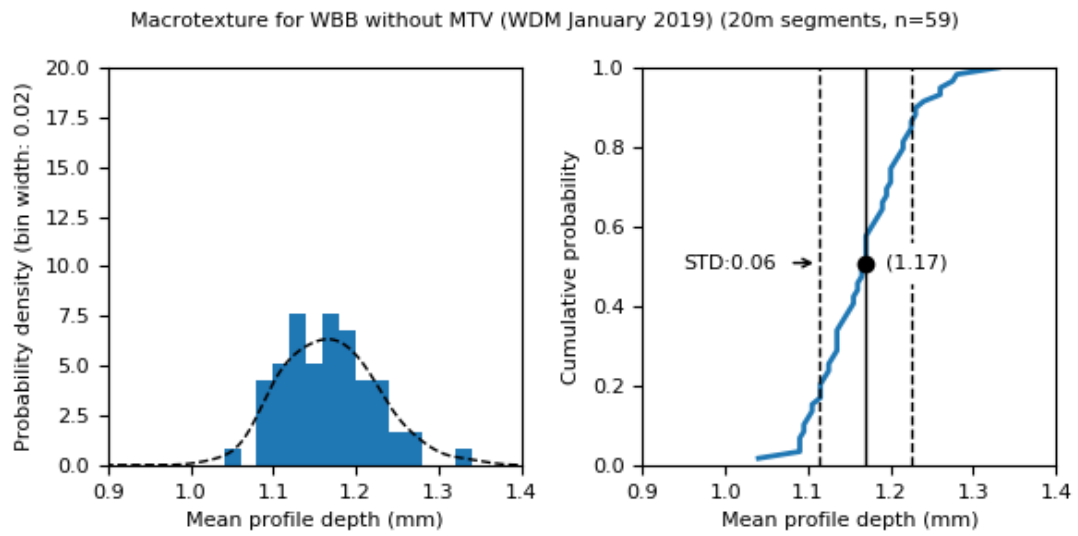


Figure 21 Mean profile depth (WDM, January 2019) for the no-MTV section.

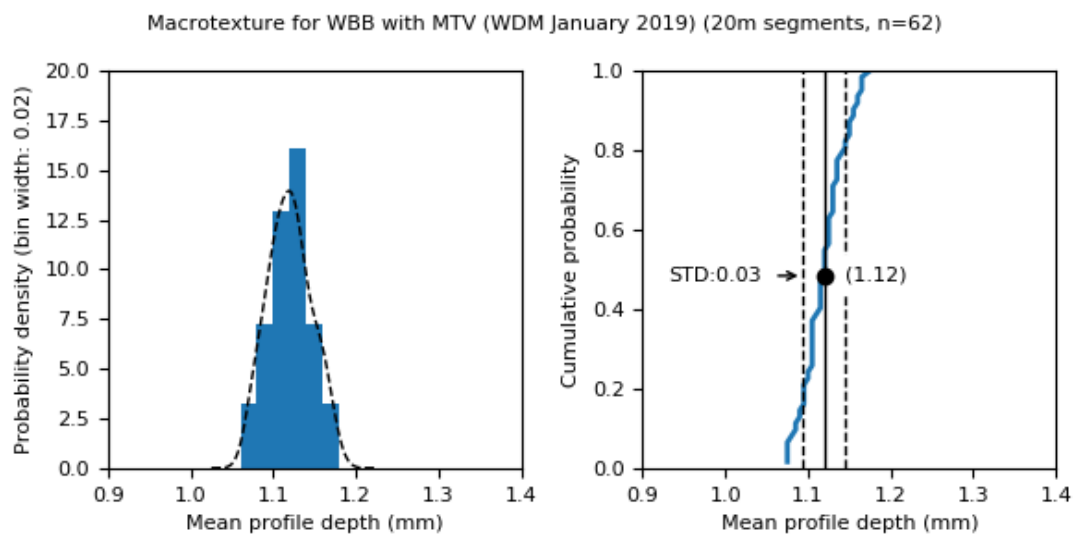


Figure 22 Mean profile depth (WDM, January 2019) for the MTV section.

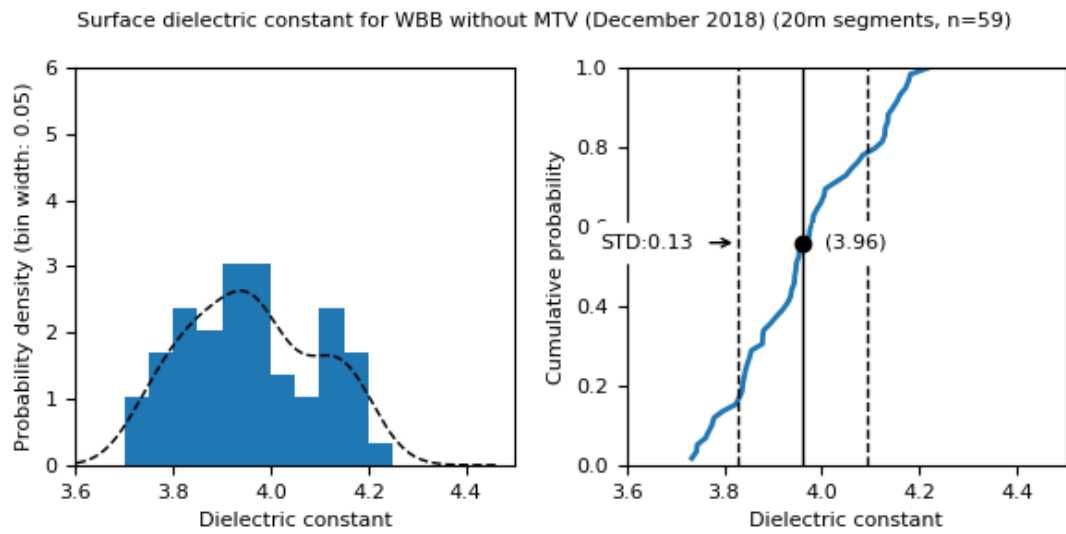


Figure 23 Surface dielectric constant (December 2018) for the no-MTV section.

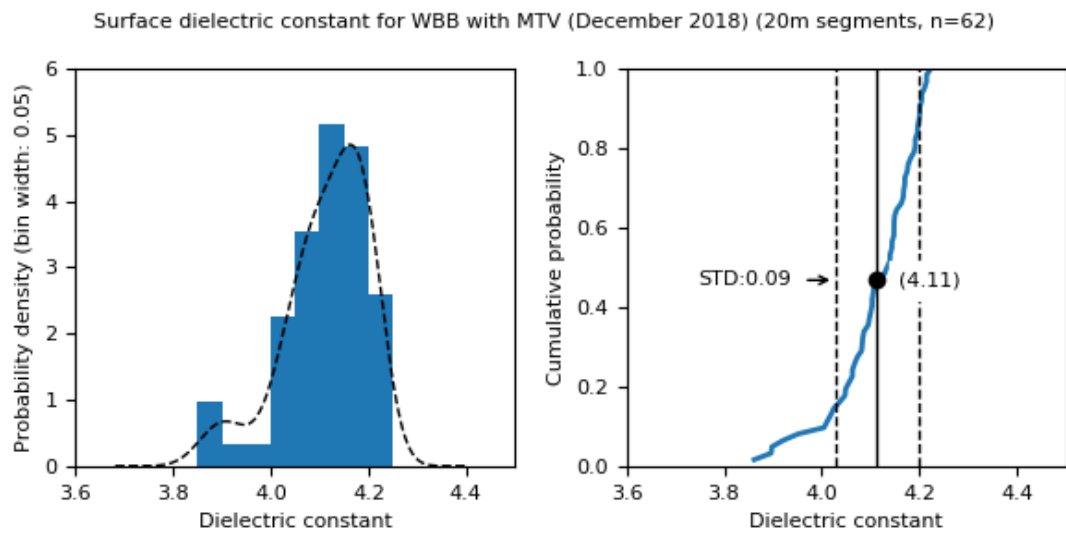


Figure 24 Surface dielectric constant (December 2018) for the MTV section.

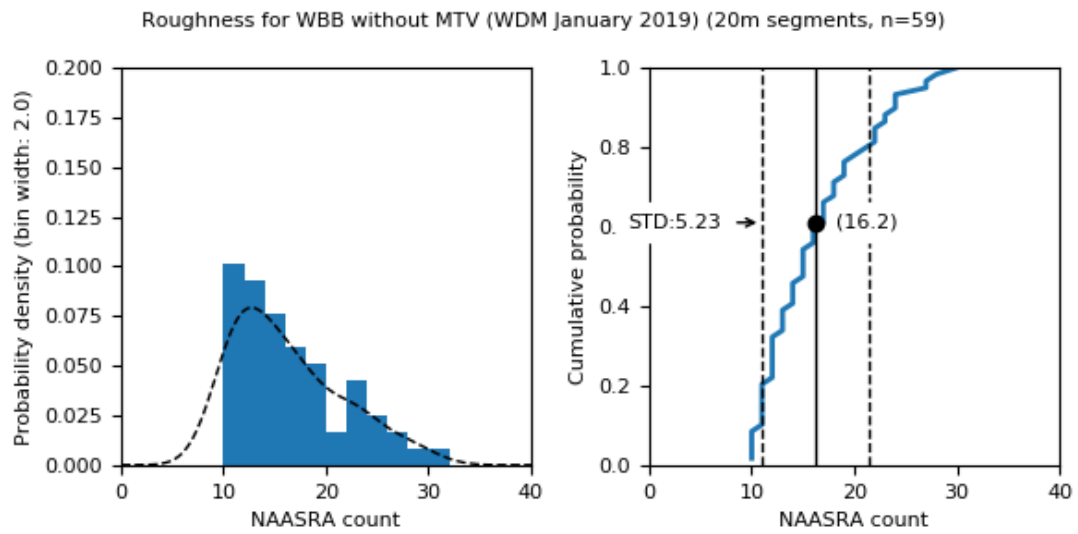


Figure 25 NAASRA count (WDM, January 2019) for the no-MTV section.

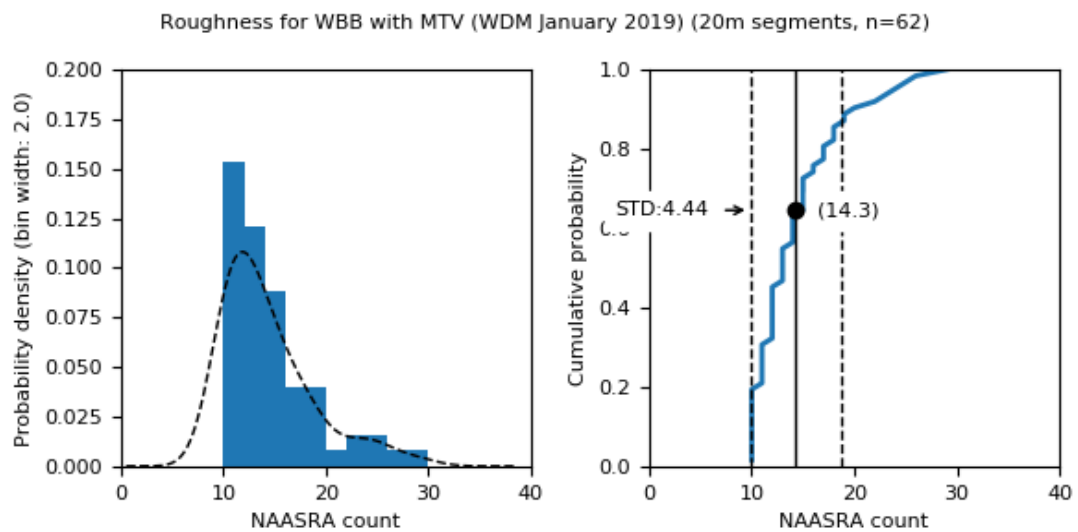


Figure 26 NAASRA count (WDM, January 2019) for the MTV section.

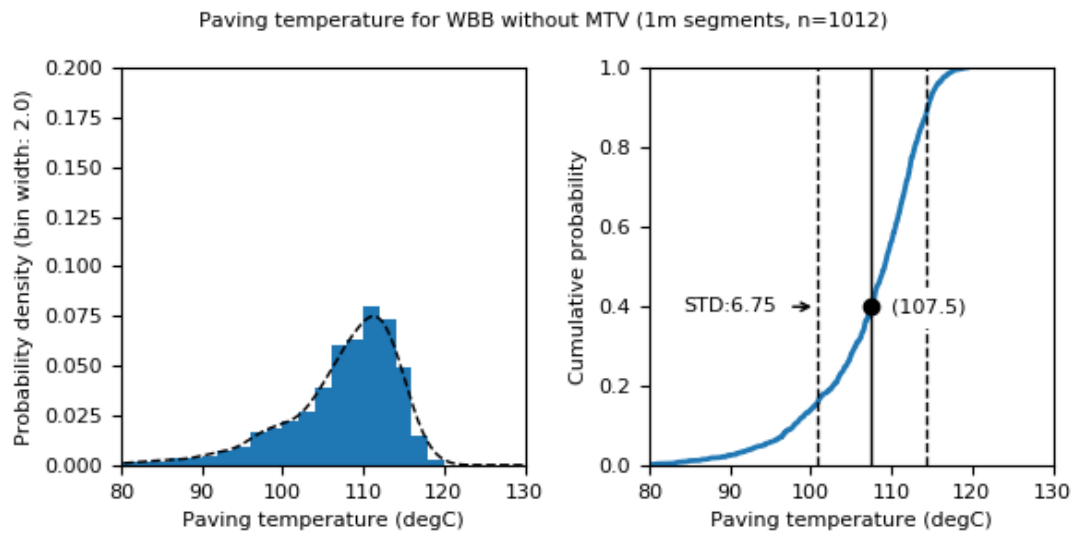


Figure 27 Paving temperature, 1 metre segments excluding stops for the no-MTV section.

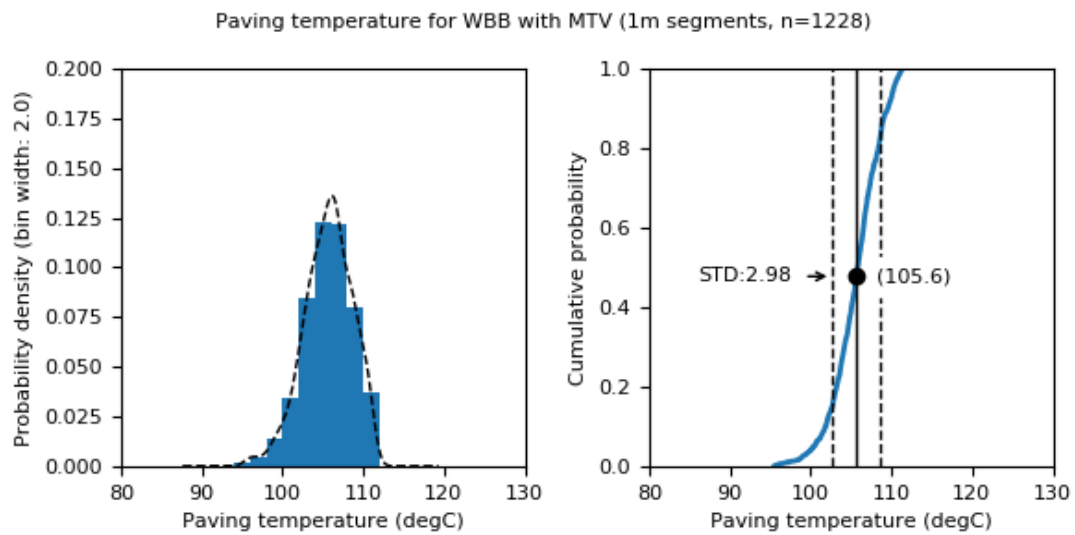


Figure 28 Paving temperature, 1 metre segments excluding stops for the MTV section.

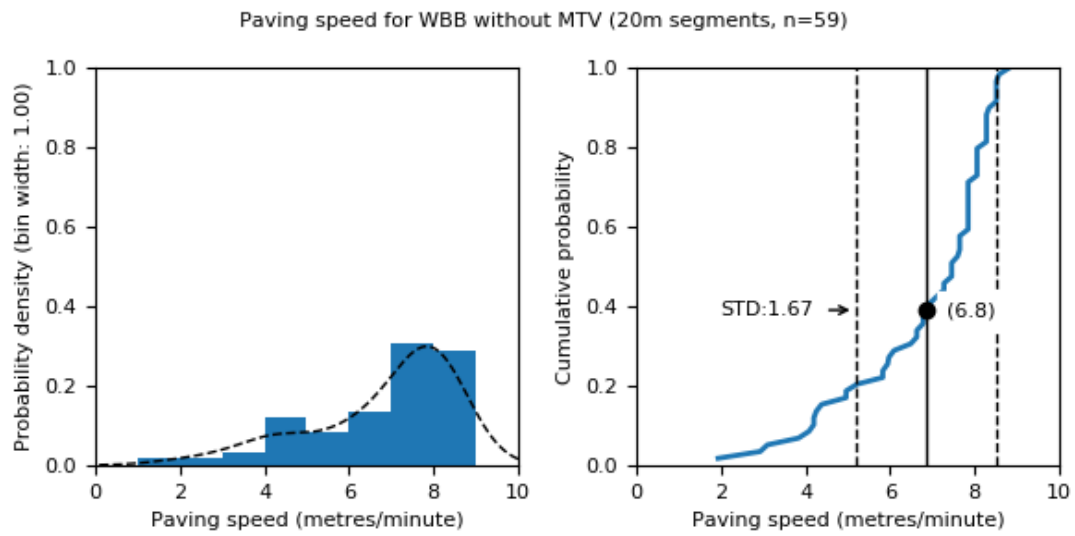


Figure 29 Paving speed, 20 metre segments including stops for the no-MTV section.

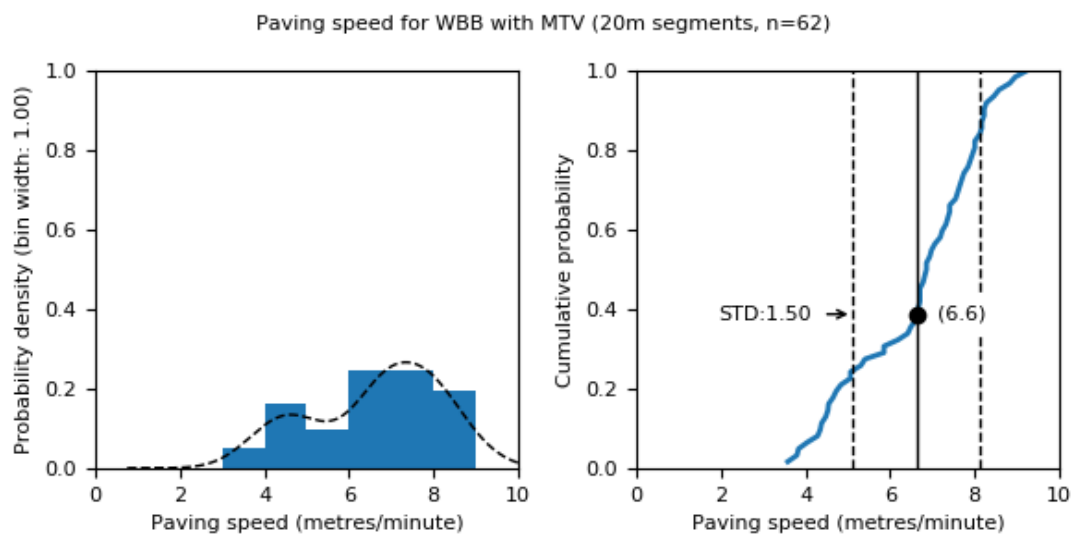


Figure 30 Paving speed, 20 metre segments including stops for the MTV section.

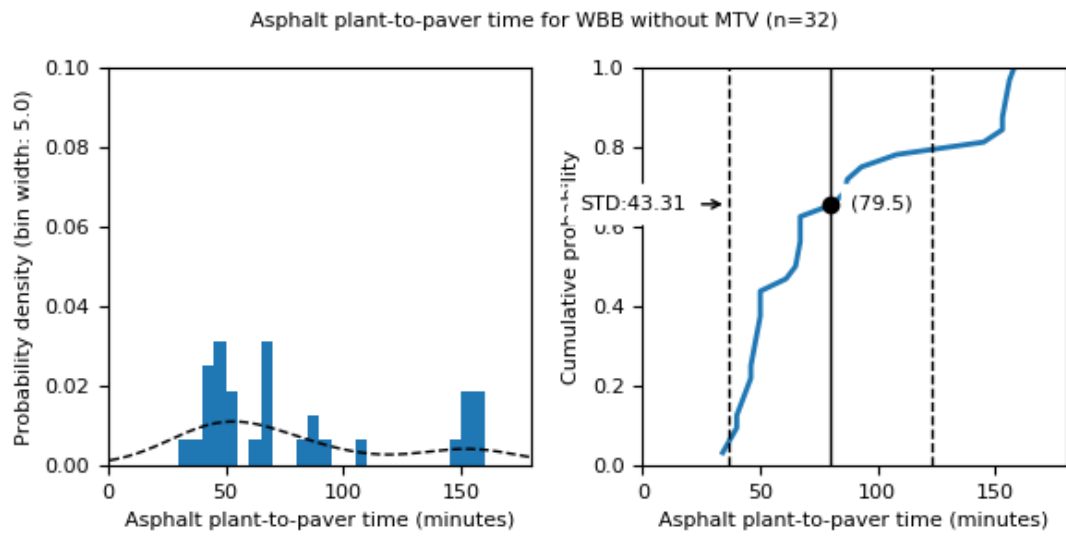


Figure 31 Asphalt plant-to-paver time for the no-MTV section.

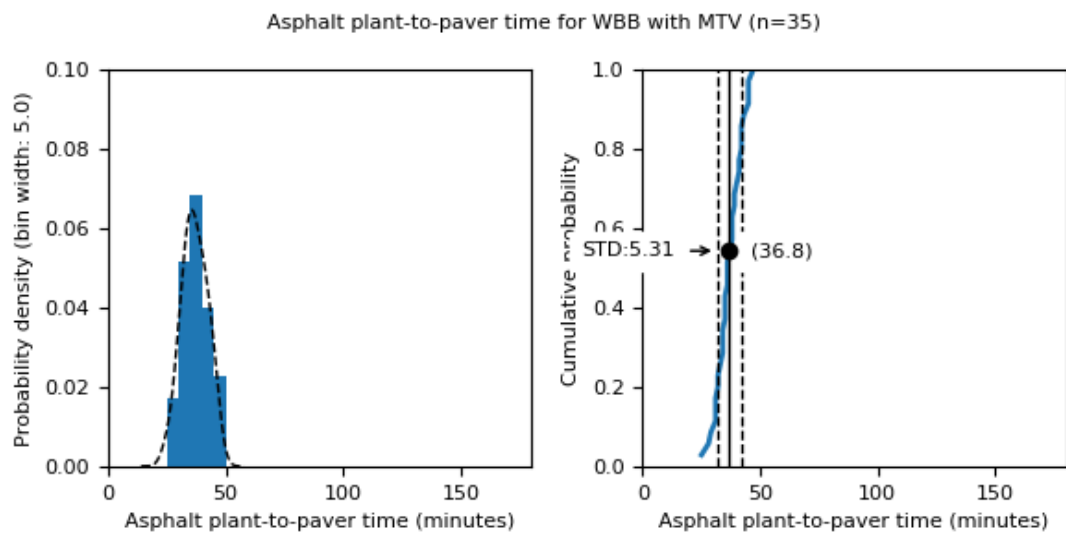


Figure 32 Asphalt plant-to-paver time for the MTV section.

5.3 Effect of local surface properties on $L_{CPX:P1,80}$

The effects of the road surface properties on tyre/road noise are discussed in this section. The investigation is limited to the mean profile depth and surface dielectric constant. No reliable as-built thickness data is currently available.

The sections of road used are limited to the MTV sections (shifts 2–8) with 40 mm nominal thickness.

Table 14 presents the average and standard deviation of $L_{CPX:P1,80}$, mean profile depth and surface dielectric constant. The distributions of each property are plotted in Figure 33 to Figure 35.

Table 14 Summary of available surface properties for WBB project, 40 mm nominal thickness with MTV.

Property	Statistic	Value
$L_{CPX:P1,80}$ (20 metre segments, December 2018)	Mean	93.0 dB
	Std. dev.	1.2 dB
Mean profile depth (20 metre segments, WDM January 2019)	Mean	1.14 mm
	Std. dev.	0.04 mm
Surface dielectric constant (20 metre segments, December 2018)	Mean	4.14
	Std. dev.	0.11

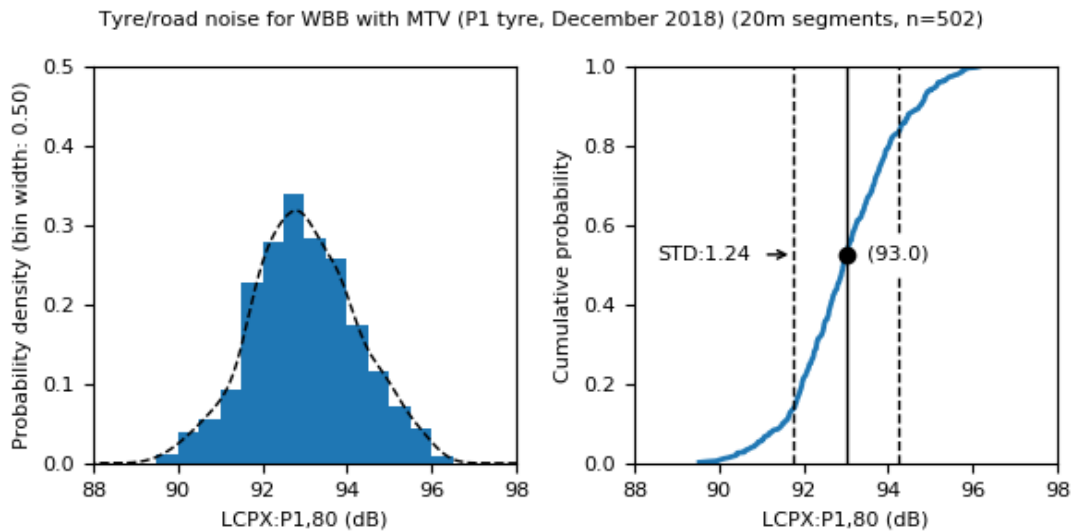


Figure 33 $L_{CPX:P1,80}$ (December 2018) for WBB project, 40 mm nominal thickness with MTV.

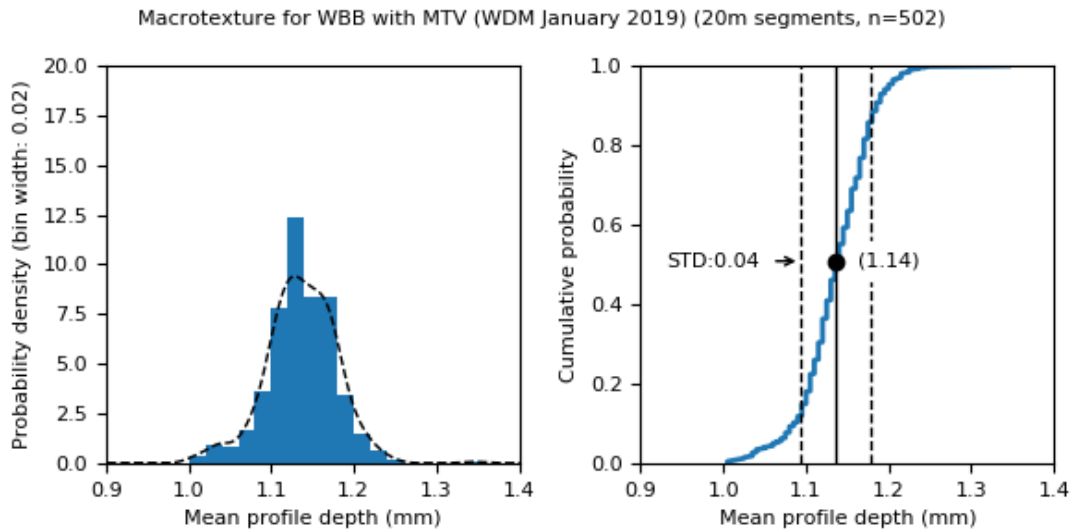


Figure 34 Mean profile depth (WDM, January 2019) for WBB project, 40 mm nominal thickness with MTV.

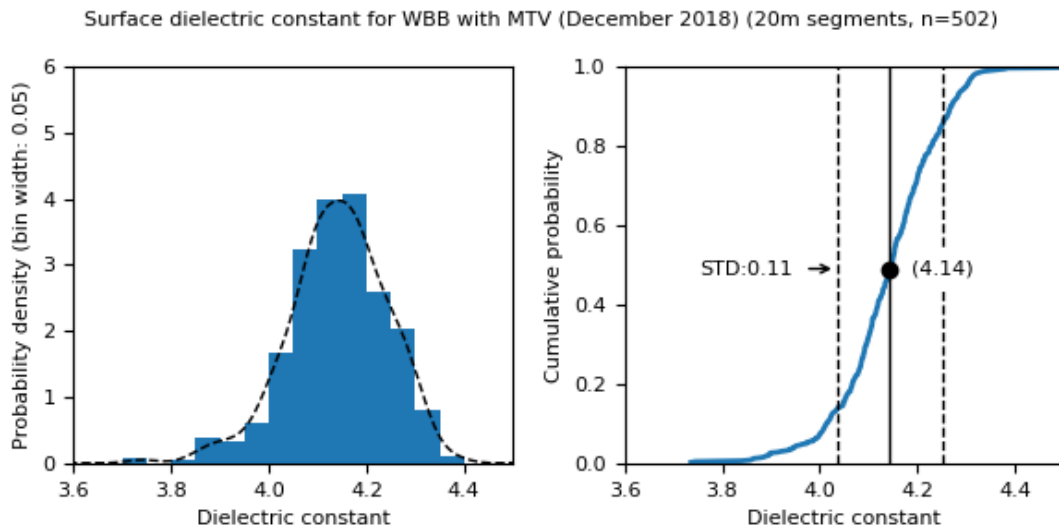


Figure 35 Surface dielectric constant (December 2018) for WBB project, 40 mm nominal thickness with MTV.

Regression analysis

The 20 metre surface property data is presented below as scatter plots. There is no clear relationship between $L_{CPX:P1,80}$ and mean profile depth, and only a weak negative relationship between $L_{CPX:P1,80}$ and surface dielectric constant.

Table 15 presents the results of a multiple linear regression of $L_{CPX:P1,80}$ on mean profile depth and surface dielectric constant.

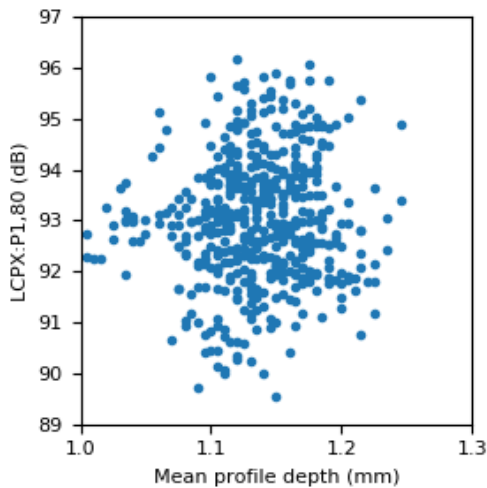


Figure 36 Left wheel path mean profile depth (2019 WDM 10 metre dataset) vs $L_{CPX:P1,80}$ (December 2018).

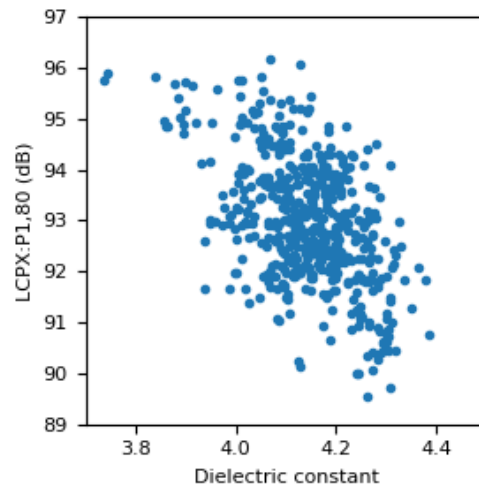


Figure 37 Surface dielectric constant vs $L_{CPX:P1,80}$ (December 2018).

The coefficient of determination (R^2) is low indicating that the majority of variability in $L_{CPX:P1,80}$ remains unaccounted for. This is to be expected given that the thickness variable has not been included in the regression analysis. Based on the results of the thickness trials a 10 mm change in surface thickness can cause a 2.3 dB change in L_{CPX} .

The estimated regression coefficient for the surface dielectric constant variable is highly significant (p -value < 0.001) with a standardised value of -0.4767 . Therefore, there is strong evidence for a negative relationship between surface dielectric constant and $L_{CPX:P1,80}$.

The estimated regression coefficient for the mean profile depth variable has poor statistical significance indicating that $L_{CPX:P1,80}$ does not correlate to mean profile depth. This is contrary to the behaviour observed in the high-void trial sites, which demonstrated a strong positive relationship between mean profile depth and $L_{CPX:P1,80}$. However, it is noted that the high-void trials involved three distinctly different surface mixes (EPA10, EPA10HV and EPA14) with markedly different mean profile depth values, compared to the WBB trials which is concerned with only one surface mix (EPA7).

The width of the mean profile depth 95% confidence is 0.16 mm (see Table 14). Using the mean profile depth to noise relationship from the high-void study, a 0.16 mm change in mean profile depth provides a 0.8 dB change in $L_{CPX:P1,80}$. A 0.8 dB change could be considered a relatively small variation in L_{CPX} . For comparison, the width of the 95% confidence interval for $L_{CPX:P1,80}$ is 4.9 dB over the same section of the WBB project.

It is also possible that any error associated the WDM measurements is high compared to the magnitude of the change in mean profile depth due to small changes in macrotexture on a single surface type. The measurement uncertainty of the WDM system is not known.

Table 15 Effect of available surface properties on $L_{CPX:P1,80}$

	Regression coefficients (std. error)		p-value
	Unstandardised	Standardised	
Surface dielectric constant	-5.423 (0.449)	-0.4767	0.000
Mean profile depth	2.986 (1.151)	0.1024	0.010
Constant	112.08		
R ²	0.229		
N	588		
p-value	0.000		

5.4 Effect of local construction properties on $L_{CPX:P1,80}$

The effects of the construction process and variables on tyre/road noise are discussed in this section. The section of road used is the same as in the previous section (shifts 2–8 with 40 mm nominal thickness).

Table 16 presents the average and standard deviation of the paving temperature and paving speed, along with the total number of paver stops. $L_{CPX:P1,80}$ is included again for reference. The distributions of each property are plotted in Figure 38 to Figure 40.

The asphalt plant-to-paver time has not been included as it cannot be easily mapped onto the 20 metre segments and its effect is expected to be captured by the paving temperature variable. The paver temperature and speed data include the 20 metre segments influenced by a paver stop.

Table 16 Summary of available construction properties for WBB project, 40 mm nominal thickness with MTV.

Property	Statistic	Value
$L_{CPX:P1,80}$ (20 metre segments, December 2018)	Mean	93.0 dB
	Std. dev.	1.2 dB
Paving temperature (20 metre segments, includes stops)	Mean	106.2°C
	Std. dev.	4.5°C
Paving speed (20 metre segments, includes stops)	Mean	6.5 metres/minute
	Std. dev.	1.8 metres/minute
Paving stops (number of 20 metre segments affected by at least one stop)	Total	119 (out of 502 segments)

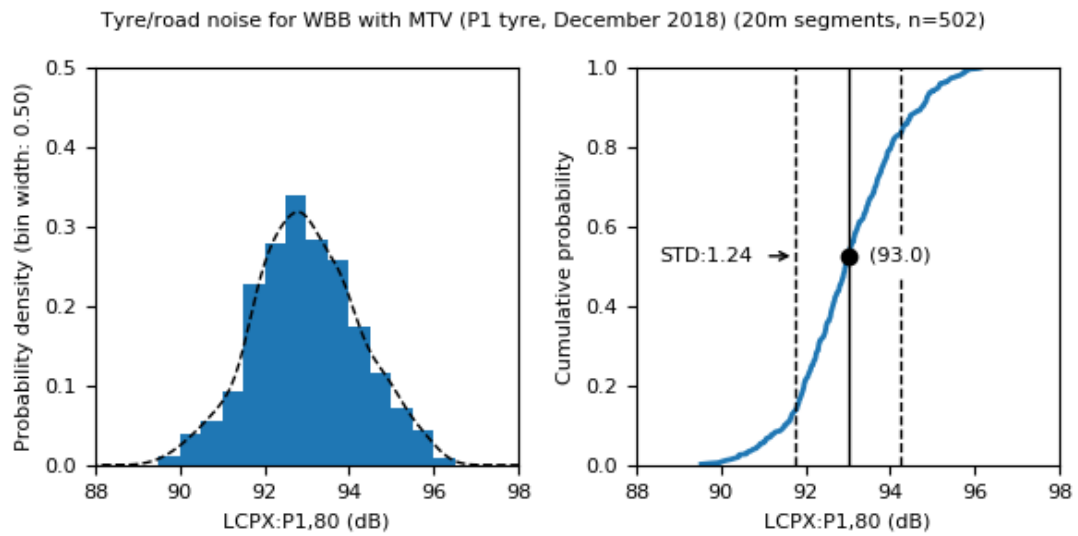


Figure 38 $L_{CPX:P1,80}$ (December 2018) for WBB project, 40 mm nominal thickness with MTV.

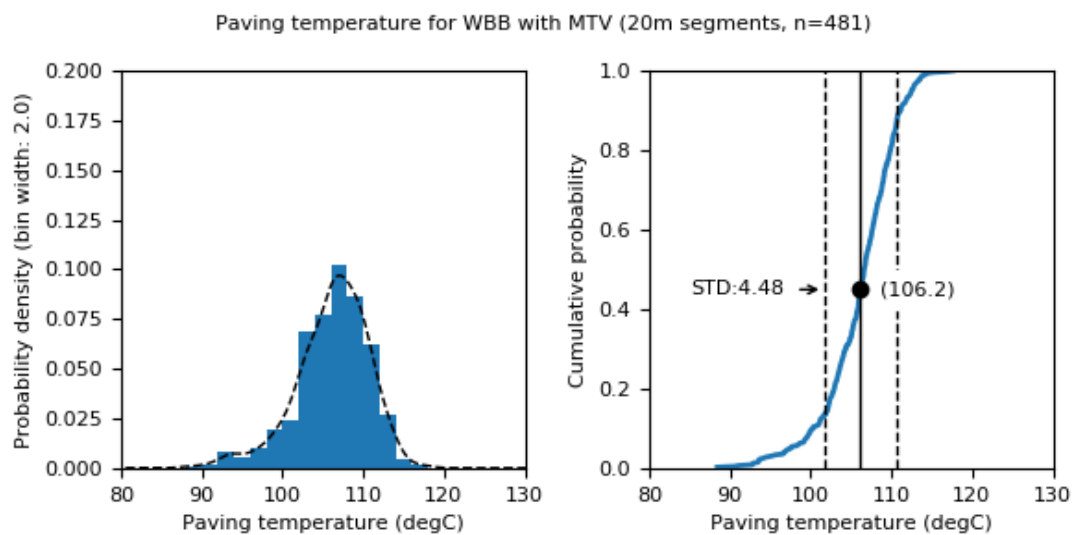


Figure 39 Paving temperature (including stops) for WBB project, 40 mm nominal thickness with MTV.

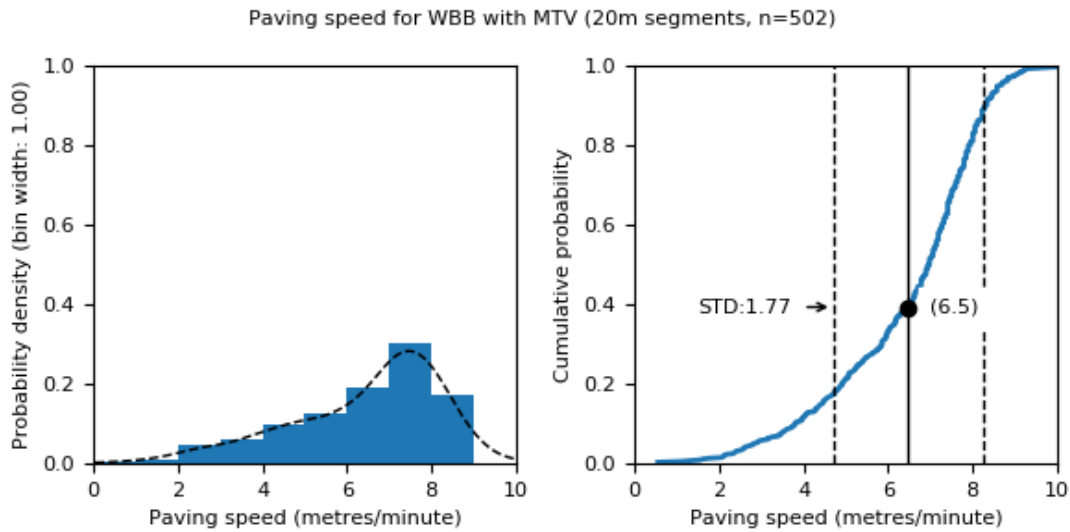


Figure 40 Paving speed (including stops) for WBB project, 40 mm nominal thickness with MTV.

Regression analysis

The 20 metre construction property data is presented below as scatter plots. There is no clear relationship between $L_{CPX:P1,80}$ and paving temperature, paving speed and paver stops. Table 17 presents the results of a multiple linear regression of $L_{CPX:P1,80}$ on paving temperature, paving speed and paver stops. The regression result has a small coefficient of determination ($R^2 = 0.05$) and therefore provides no evidence of a relationship between $L_{CPX:P1,80}$ and the construction properties considered.

Table 17 Effect of available construction properties on $L_{CPX:P1,80}$

	Regression coefficients (std. error)		p-value
	Unstandardised	Standardised	
Paving temperature	-0.035 (0.014)	-0.1253	0.000
Paving speed	0.178 (0.043)	0.2546	0.016
Paver stopped (stop = 1)	0.623 (0.128)	0.2144	0.000
Constant	95.33		
R2	0.05		
N	480		
p-value	0.000		

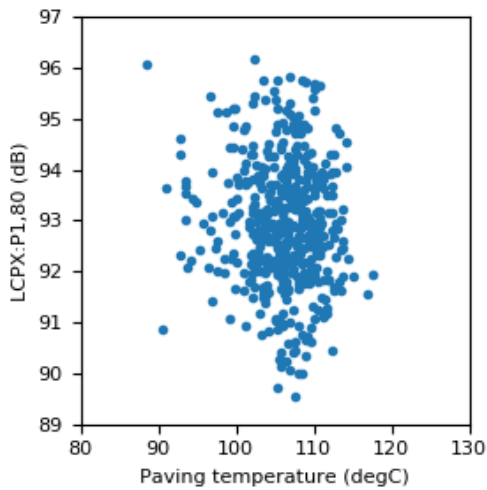


Figure 41 Paving temperature vs $L_{CPX:P1,80}$ (December 2018).

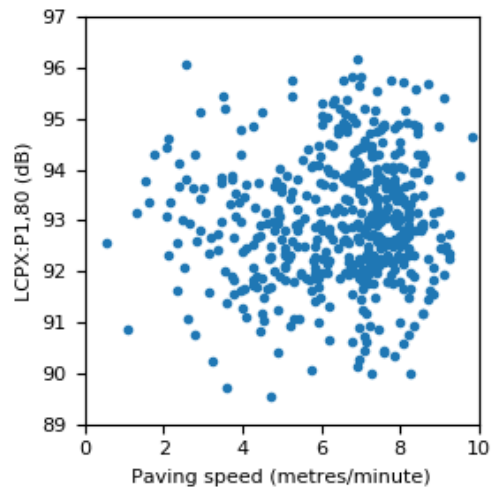


Figure 42 Paving speed vs $L_{CPX:P1,80}$ (December 2018).

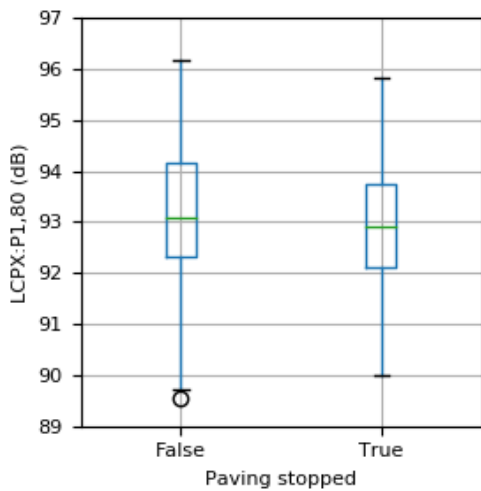


Figure 43 Paver stopped vs $L_{CPX:P1,80}$ (December 2018).

5.5 Thickness as determined by $L_{CPX:P1,80}$

The $L_{CPX:P1,80}$ “heatmap” (Figure 13) shows that there are local areas of high and low tyre/road noise, generally varying between 90 dB and 97 dB. The heatmap also shows the thickness trial sections, with $L_{CPX:P1,80}$ varying over the same 90 - 97 dB range for target thicknesses ranging from 30 mm to 50 mm. Therefore, it is hypothesised that the variations in $L_{CPX:P1,80}$ over the main WBB project (40 mm target thickness) are due to deviations of the as-built thickness from the target thickness.

Without a reliable measurement of the as-built thickness, the presence of deviations of the as-built thickness from the target thickness cannot be verified. Results from the thickness trial sections show distinctly different $L_{CPX:P1,80}$ spectra for each thickness trial section. These differences in spectrum shape can be used to verify changes in thickness.

Figure 44 presents the one-third octave band $L_{CPX:P1,80}$ for the thickness trial sections. All 20 metre segments (across both lanes) have been included in the calculation of the average and 95% confidence interval.

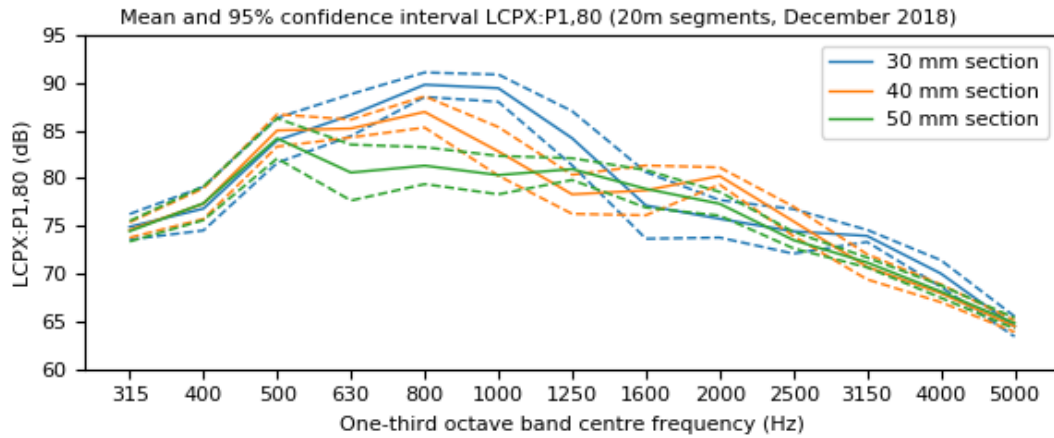


Figure 44 One-third octave band $L_{CPX:P1,80}$ (December 2018) for the thickness sections. 20 metre segments from both lanes have been combined.

Figure 45 shows a selection of 20 metre road segments where deviations from the target thickness are expected due to high and low values of $L_{CPX:P1,80}$. The locations are labelled according to their expected thickness based on the overall $L_{CPX:P1,80}$ for the segment (e.g. location 30A is expected to have a $L_{CPX:P1,80}$ spectrum that matches that of the 30 mm thickness section).

Figure 47 to Figure 55 show the one-third octave band $L_{CPX:P1,80}$ for each location compared to the thickness trial spectra. All locations investigated have spectra that align with the appropriate thickness trial spectrum. This behaviour provides support for the hypothesis that the as-built thickness deviates from the target thickness by up to 15 mm and that the longitudinal variation in $L_{CPX:P1,80}$ is primarily affected by the thickness deviations.

Using the below thickness to $L_{CPX:P1,80}$ (December 2018) relationship, developed as part of the thickness study and rearranged for thickness, the as-built thickness has been estimated. The distribution of the estimated as-built thickness is shown in Figure 46.

$$t = -3.83L_{CPX:P1,80} + 394.33$$

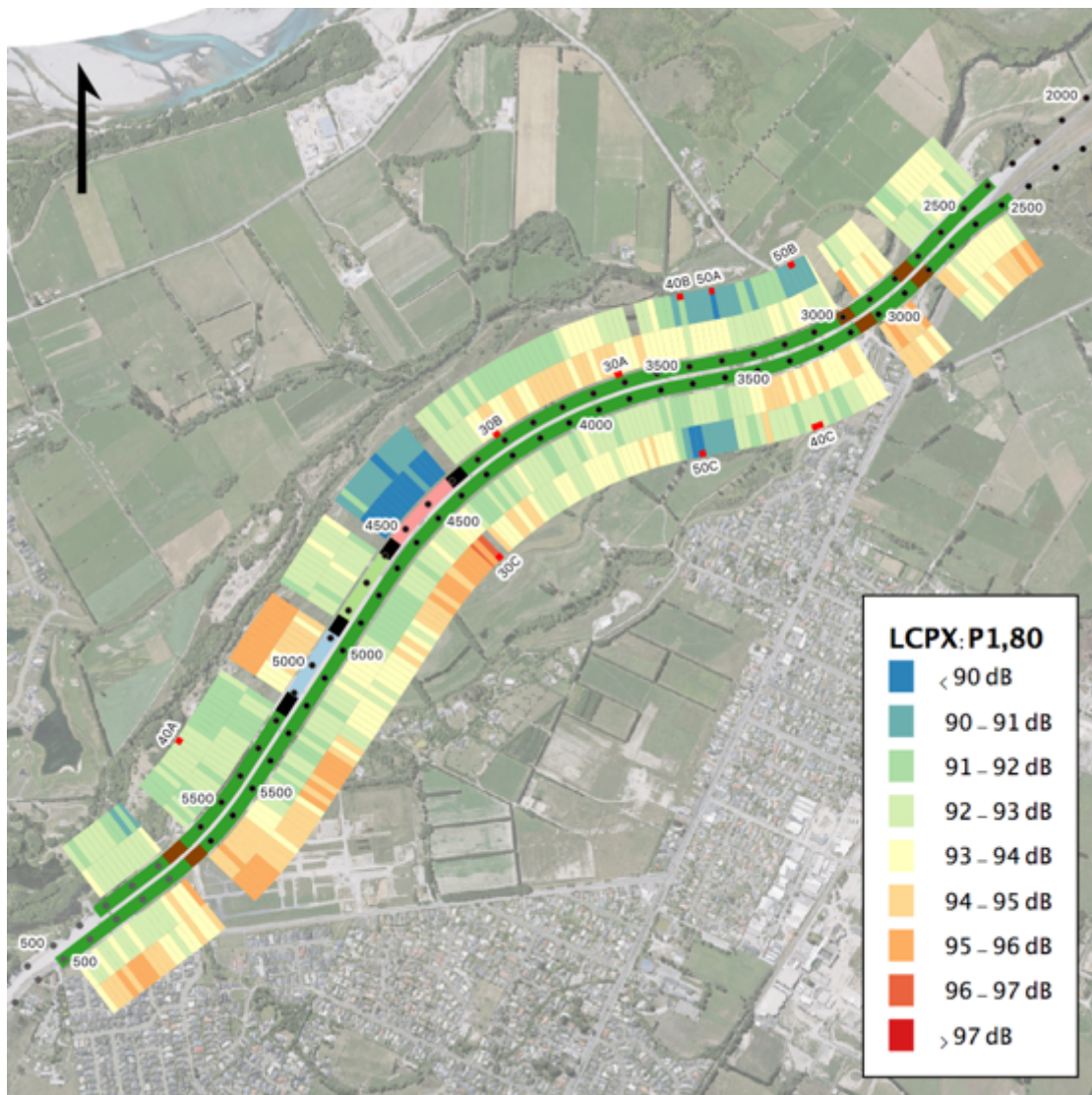


Figure 45 LCPX:P1,80 (December 2018) with one-third octave band locations labelled (20 metre segments).

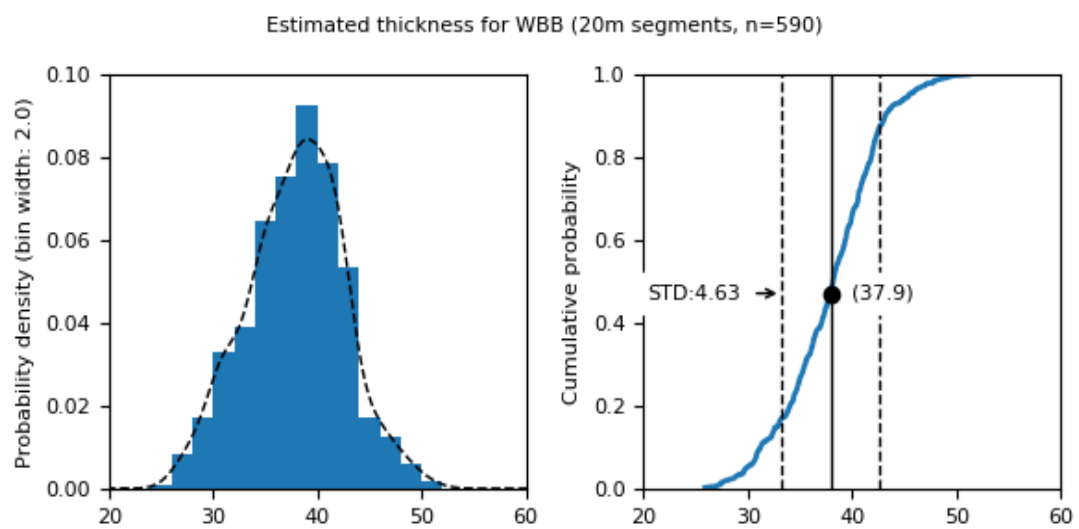


Figure 46 Estimated thickness for WBB (excludes thickness trial sections).

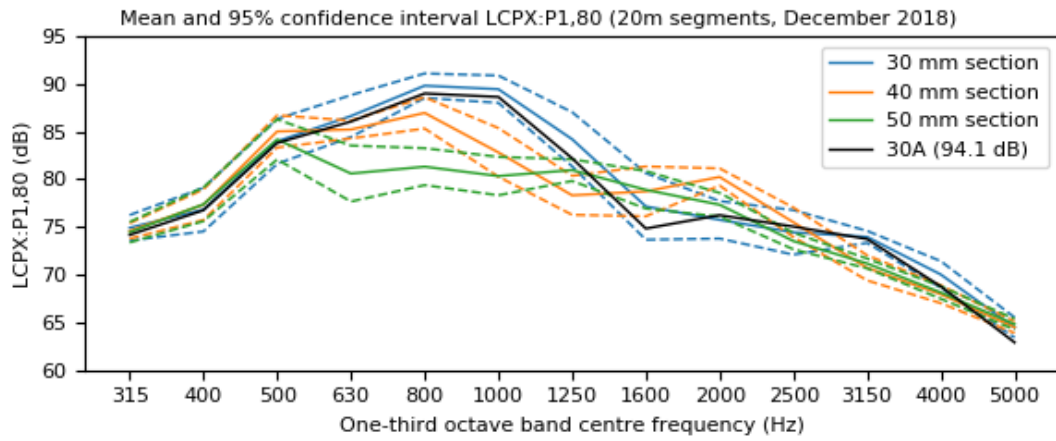


Figure 47 One-third octave band $L_{CPX:P1,80}$ (December 2018) for location 30A.

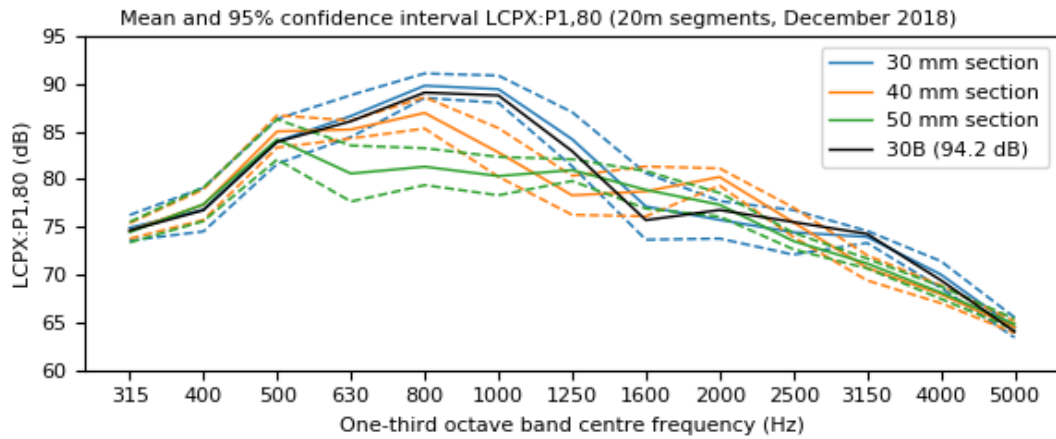


Figure 48 One-third octave band $L_{CPX:P1,80}$ (December 2018) for location 30B

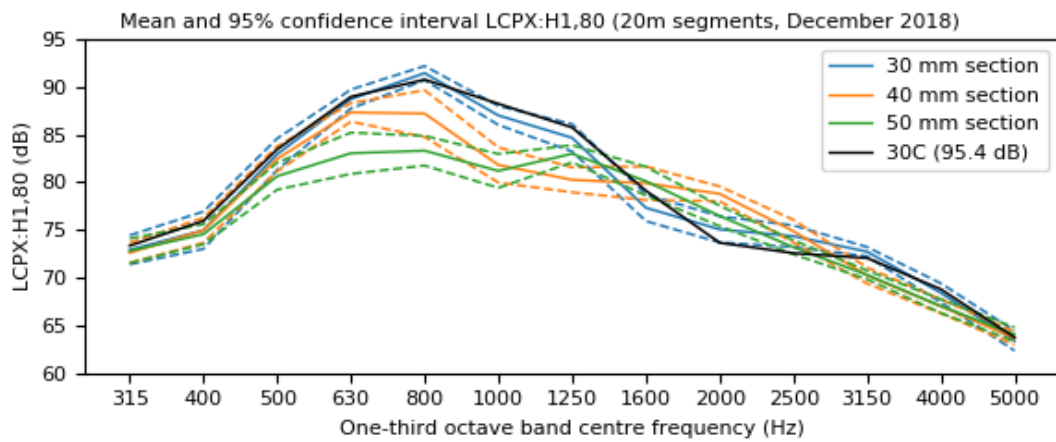


Figure 49 One-third octave band $L_{CPX:P1,80}$ (December 2018) for location 30C.

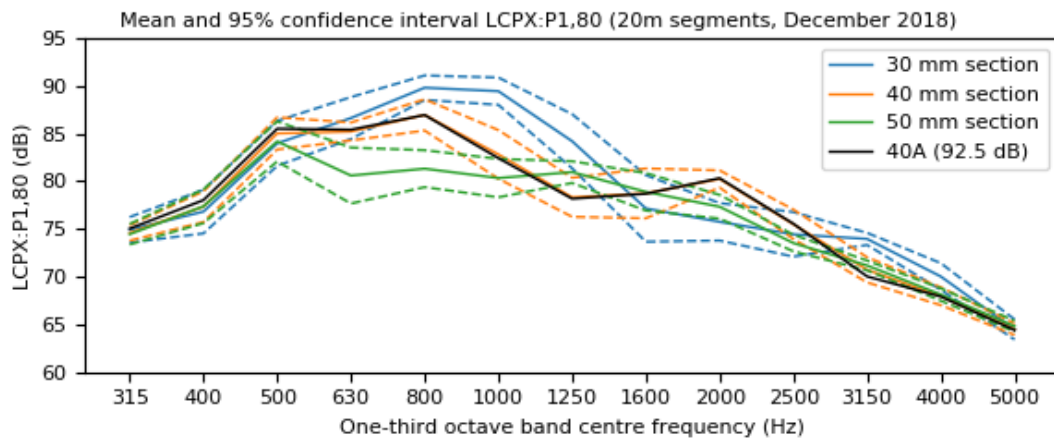


Figure 50 One-third octave band $L_{CPX:P1,80}$ (December 2018) for location 40A.

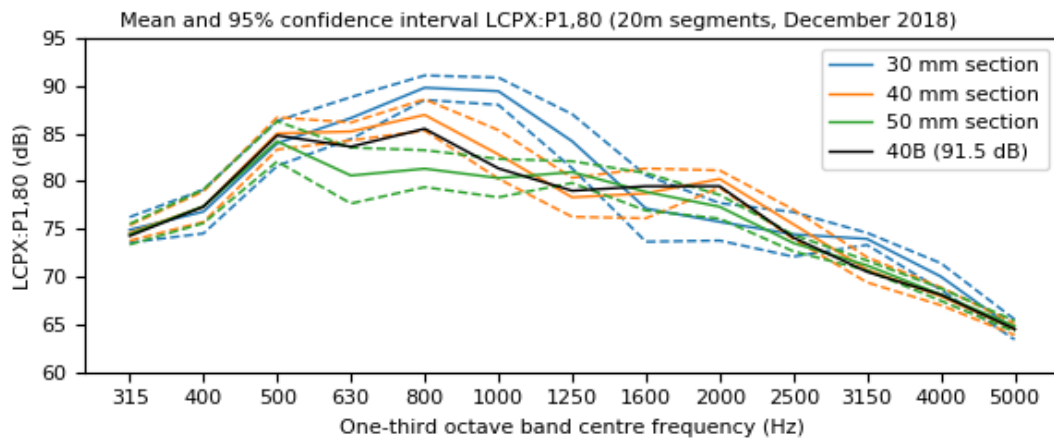


Figure 51 One-third octave band $L_{CPX:P1,80}$ (December 2018) for location 40B.

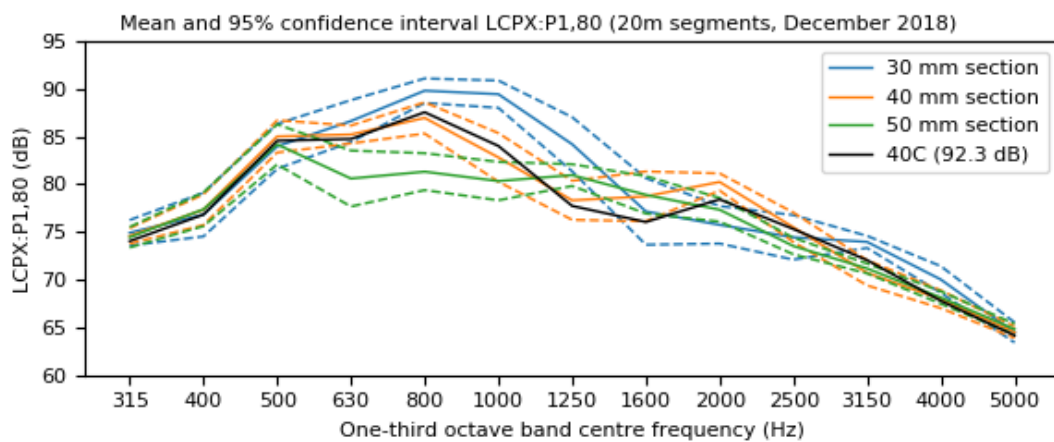


Figure 52 One-third octave band $L_{CPX:P1,80}$ (December 2018) for location 40D.

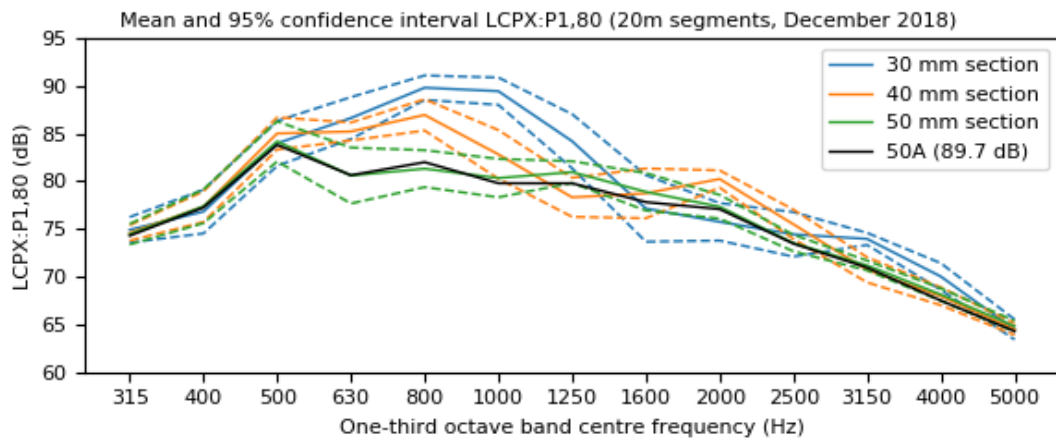


Figure 53 One-third octave band $L_{CPX:P1,80}$ (December 2018) for location 50A.

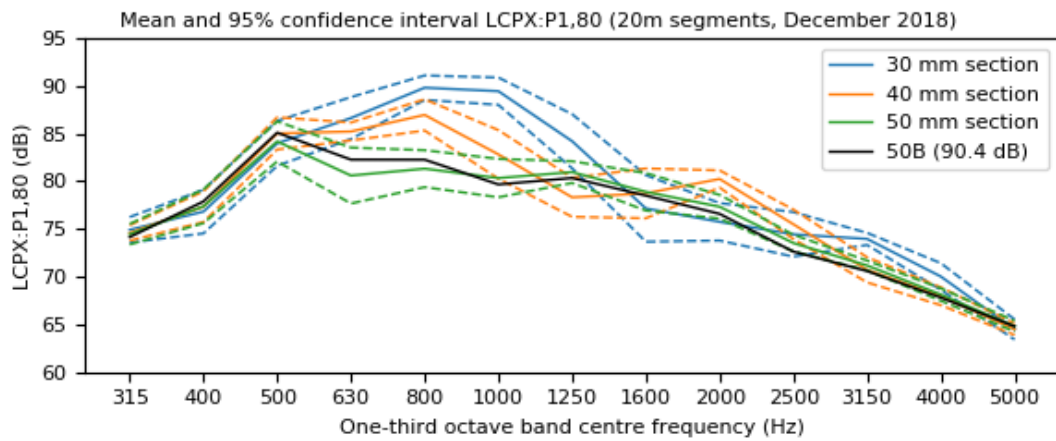


Figure 54 One-third octave band $L_{CPX:P1,80}$ (December 2018) for location 50B.

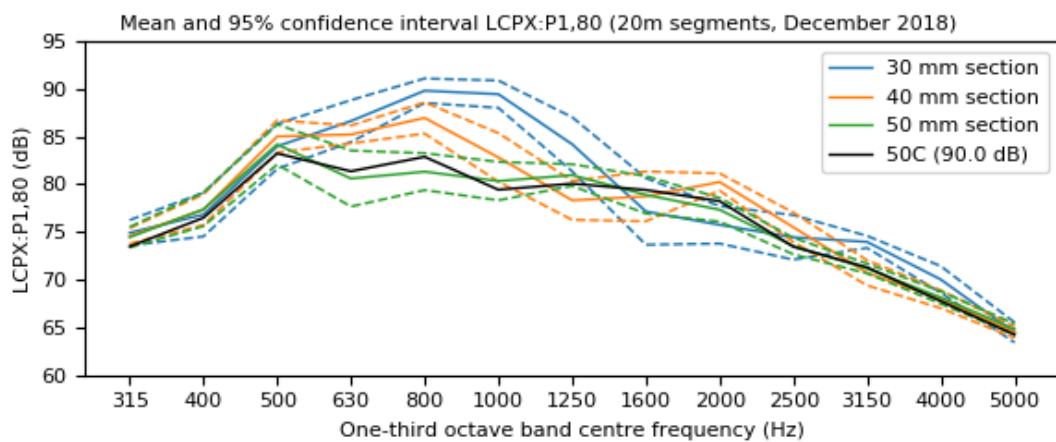


Figure 55 One-third octave band $L_{CPX:P1,80}$ (December 2018) for location 50C.

6 Conclusions

Not all of desired data was available or had been processed at the time of writing; as such, the current analysis represents preliminary findings of the thickness and variability study to-date. In particular, a reliable measure of the as-built thickness was not available and the relationship between dielectric constant and air-void content has yet to be determined. Other collected data such as the roller temperature, roller positions and infrared imagery still need to be investigated. Any new findings will be presented in a revised version of this report.

Thickness study

The overall thickness effect is determined using L_{CPX} and the target thickness of each thickness trial section. The average thickness effect is -2.3 dB L_{CPX} (80 km/h) per 10 mm increase in thickness when considering the measurement results from both the P1 and H1 test tyres (December 2018). Differences in L_{CPX} (80 km/h) of up to 1.4 dB are seen between the lanes; however, the left-right lane differences are not consistent between each thickness section or between the two test tyres. There are no significant variations in mean profile depth between the lanes. Investigation of the one-third octave band $L_{CPX:P1,80}$ shows clear differences between thickness sections; however, the differences in spectra between the lanes are only small and insufficient to confirm the presence of a thickness difference for the same sections.

Effect of material transfer vehicle

The right lane southbound carriageway between Dickey's Road bridge and Groynes Road bridge was used to investigate the effect of the material transfer vehicle as it provided a section of road free from complex features and has consistent traffic behaviour. No significant differences in average $L_{CPX:P1,80}$ and acoustic variability were measured, indicating that use of the MTV during paving has no effect on $L_{CPX:P1,80}$.

Differences in the consistency of the paving temperature were observed, with the MTV section exhibiting a narrower distribution of paving temperatures. There are small differences in mean profile depth and surface dielectric constant between the no-MTV and MTV sections; however, it is unclear whether or not these differences are significant. The no-MTV section involved 40 paver stops, compared to the eight that occurred within the MTV section. This is due to the paver being stopped at every truck change-over for the no-MTV section. The no-MTV section experienced significantly longer average asphalt plant-to-paver times, which is attributed to the start-of-shift delays and complex edge detailing that caused long wait times for the asphalt trucks.

Effect of local surface properties on tyre/road noise

The effect of local surface properties on tyre/road noise was investigated using the 20 metre road segment data. The surface properties considered were limited to the mean profile depth and surface dielectric constant. No reliable measure of as-built asphalt thickness was available for the current analysis.

A regression of $L_{CPX:P1,80}$ on mean profile depth and surface dielectric constant showed a weak but statistically significant negative relationship between surface dielectric constant and $L_{CPX:P1,80}$. For a dry asphalt material an increase in bulk dielectric constant will represent a decrease in air void content; hence, a positive relationship would be expected with lower void content being associated with higher tyre/road noise. The previous high-void trials constructed at Sawyers to Groynes demonstrated that an increase in void content causes an increase in macrotexture, and that the increase in tyre/road noise due to higher macrotexture outweighs any noise reduction due to the increased void content; hence, there is a trade-off between void content and macrotexture, which explains the negative relationship observed in the current study.

No relationship was found between mean profile depth and $L_{CPX:P1,80}$. The previous high-void trials demonstrated a strong positive relationship between mean profile depth and $L_{CPX:P1,80}$ for sections of road having different mix designs. The precision and/or uncertainty of the mean profile depth parameter may be insufficient to detect the relatively small variations in macrotexture between sections of road having the same mix design. Alternate macrotexture parameters should be investigated.

Effect of construction properties on tyre/road noise

The effect of construction properties on tyre/road noise was investigated using the 20 metre segment data. The construction properties considered were limited to paving temperature, paving speed and paver stoppages. Rolling temperature and number of passes were not available for inclusion in the current analysis. The asphalt plant-to-paver time and truck load size could not be easily mapped onto 20 metre segments so were excluded from the 20 metre segment analysis.

A regression of $L_{CPX:P1,80}$ on paving temperature, paving speed and paver stoppage provided no evidence of a relationship between $L_{CPX:P1,80}$ and the available construction properties.

Thickness as determined by $L_{CPX:P1,80}$

The range of $L_{CPX:P1,80}$ across the WBB project (40 mm target thickness) matches the range in $L_{CPX:P1,80}$ found at the thickness trial area and it is hypothesised that the variations in $L_{CPX:P1,80}$ over the main WBB project are due to deviations of the as-built thickness from the target thickness.

Comparisons between the one-third octave band $L_{CPX:P1,80}$ from a selection of 20 metre road segments with the average one-third octave band $L_{CPX:P1,80}$ from the three thickness sections supports the hypothesis, with the higher $L_{CPX:P1,80}$ segments having spectra that align with the 30 mm thickness section spectrum and the low $L_{CPX:P1,80}$ segments having spectra that align with the 50 mm thickness section spectrum. The surface thickness is estimated using the relationship derived in thickness study and provides an average thickness of 38 mm, with values ranging between 25 mm and 50 mm.

Acknowledgements

We would like to thank Geoff Griffiths (NZ Transport Agency), Fulton Hogan and WSP-Opus for accommodating this tyre/road noise study into the Western Belfast Bypass project and agreeing to include the use of the material transfer vehicle. We thank WDM for reprocessing and supplying detailed data from their January 2019 network survey. And finally, the NZ Transport CAPTIF staff for their ongoing support and commitment to the road surface noise research programme.

References

- [1] S. Chiles and J. I. Bull, "Road surface noise research 2016-2018," NZ Transport Agency, 2018.
- [2] NZ Transport Agency, "Close proximity (CPX) road surface noise measurement trailer guide," 2018.
- [3] J. I. Bull and S. Chiles, "Mackays to Peka Peka road surface noise survey," NZ Transport Agency, 2017.
- [4] J. I. Bull and S. Chiles, "SH25 Tairua road surface noise measurements," NZ Transport Agency, 2017.
- [5] R. Jackett, "NZTA road surface noise research programme – Task A: Close proximity versus wayside measurements," WSP-Opus, 2019.
- [6] R. Wareing, "Road surface noise measurements of porous asphalt on the Waikato Expressway and Tauranga Eastern Link," Altissimo Consulting, 2019.
- [7] NZ Transport Agency, "Guide to state highway road surface noise," 2014.
- [8] D. I. Hanson and R. S. James, "Colorado DOT Tire/Pavement Noise Study," Department of Transportation Research, 2004.
- [9] M. Berengier, J. F. Hamet and P. Bar, "Acoustical Properties of Porous Asphalts: Theoretical and Environmental Aspects," *Transportation Research Record*, pp. 9-24, 1990.
- [10] A. Ongel, E. Kohler and J. Harvey, "Principal components regression of onboard sound intensity levels," *Journal of Transportation Engineering*, no. 134, pp. 459-466, 2008.
- [11] "RAMM Software Limited," [Online]. Available: <http://www.ramm.com/>.
- [12] *ISO 11819-2:2017. Acoustics – Measurement of the influence of road surfaces on traffic noise – Part 2: The close-proximity method.*, International Organization for Standardization.
- [13] U. Sandberg and G. Descornet, "Road surface influence on tire/road noise – Part I," in *Internoise*, Miami, 1980.
- [14] J. N. Keeney, *Evaluation of the Repeatability and Reproducibility of Network-Level Pavement Macrotexture Measuring Devices. Masters Thesis*, Virginia Polytechnic Institute and State University, 2017.

Appendix A Results of previous trials

A.1 High void and texture trials

Based on previous pass-by measurements showing potential noise reduction, trials to investigate high void porous asphalt surfaces were organised and laid in February 2017 on the northbound carriageway of State Highway 1 between the Sawyers Arms Road roundabout and the Greywacke Road exit in Christchurch. Four mix designs were initially investigated:

- EPA10 – standard epoxy modified porous asphalt, with 10 mm chips
- EPA14 – epoxy modified porous asphalt, with 14 mm chips
- EPA10HV – epoxy modified porous asphalt, with 10 mm chips and increased void content
- EPA14HV – epoxy modified porous asphalt, with 14 mm chips and increased void content

The EPA14HV mix failed its preliminary laydown test and was excluded from the trials.

The high void trial sections were laid on the right and left lanes on 11 and 12 February 2017, respectively. CPX measurement dates are listed below:

- 21 February 2017 (10 days old)
- 10 April 2017 (8 weeks old)
- 26 April 2017 (10 weeks old)
- 21 March 2018 (13 months old)
- 18 July 2018 (17 months old)
- 17 December 2018 (22 months old)
- 21 March 2019 (25 months old)

The relative performance of each mix and the differences in $L_{CPX:P1,80}$ between the first four test dates are shown below for the left and right lanes. The ranking of each mix is the same for both left and right lanes, with the EPA10 surface exhibiting the lowest $L_{CPX:P1,80}$ values and the EPA14 surface having the highest $L_{CPX:P1,80}$ values.

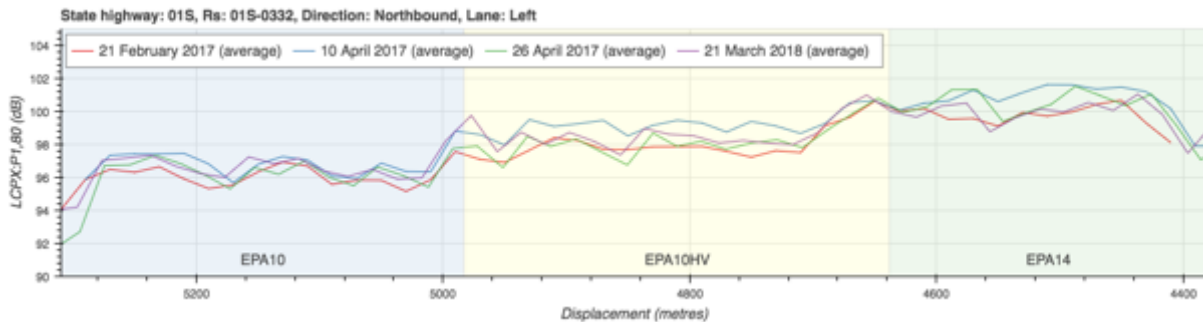


Figure 56 High-void trial sections – left lane

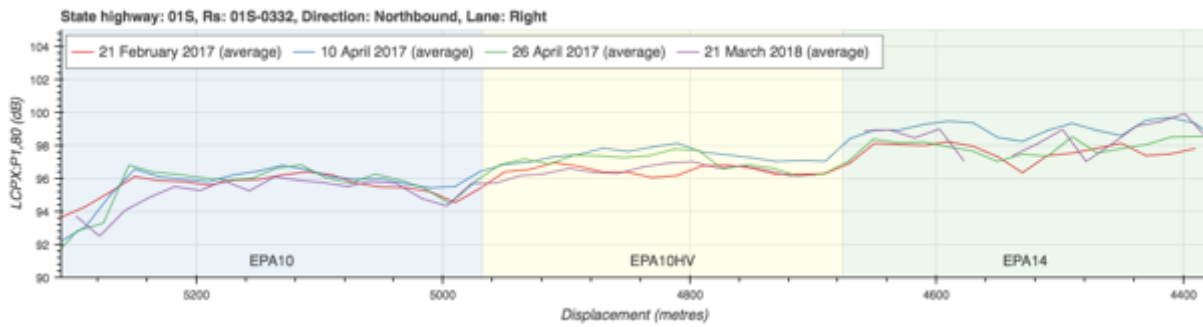


Figure 57 High-void trial sections – right lane

Comparisons between $L_{CPX:P1,80}$ values for the left and right lanes are shown below for first four measurement dates. The results from all measurement sessions show consistently higher $L_{CPX:P1,80}$ values for the left lane, despite identical mixes being used, laid one day apart by the same equipment and crew.

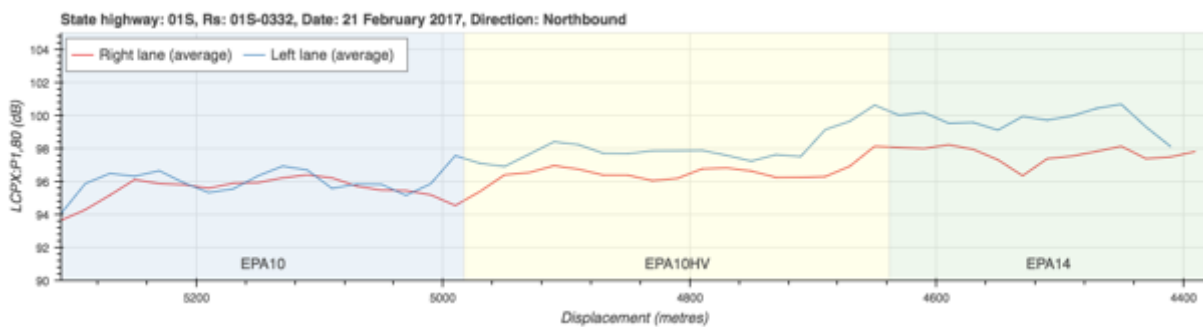


Figure 58 High-void trial sections – 21 February 2017 measurements

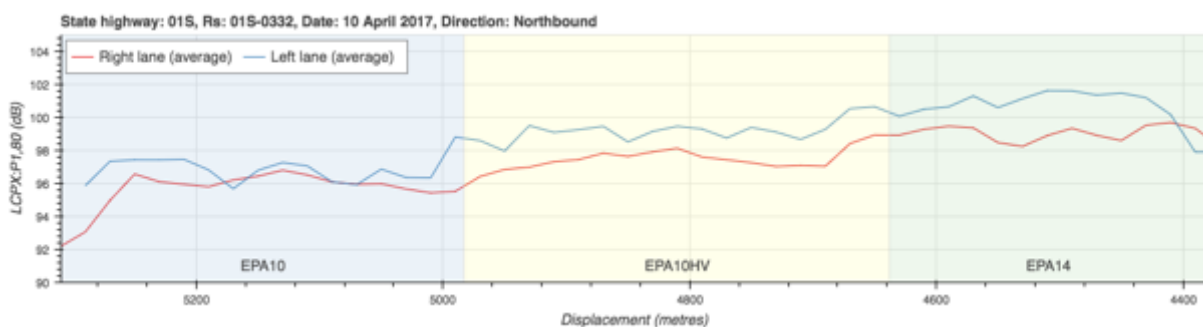


Figure 59 High-void trial sections – 10 April 2017 measurements

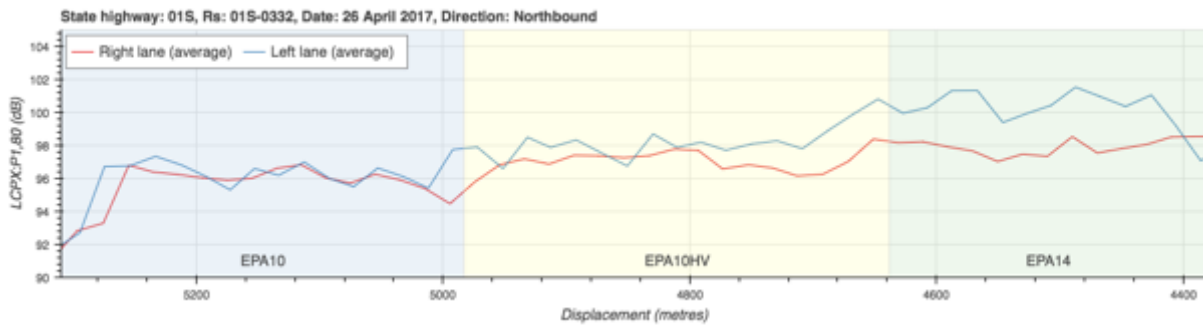


Figure 60 High-void trial sections – 26 April 2017 measurements

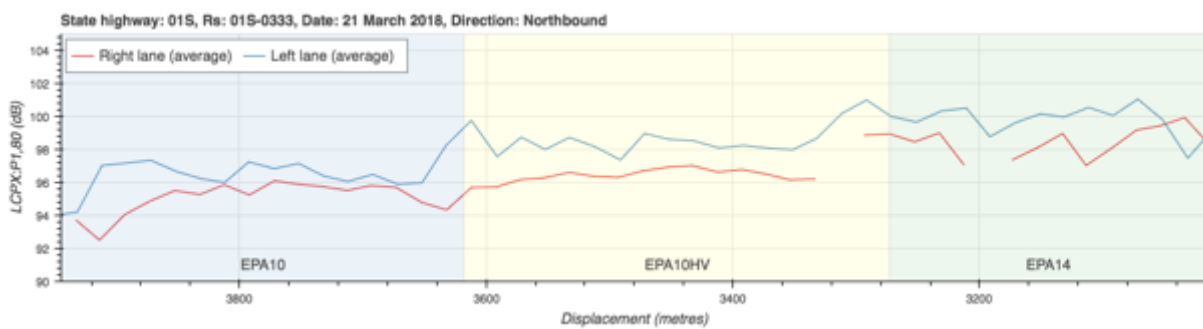


Figure 61 High-void trial sections – 21 March 2018 measurements

Mean profile depth (“MPD”) measurements were taken by Downer on 13 February 2017 for each lane. The $L_{CPX:P1,80}$ and MPD values show a good correlation, with the mean profile depth varying between the lanes and between the mixes (see Figure 62). Discussions with David Alabaster (Transport Agency) and Janet Jackson (Downer) regarding the differing mean profile depth values between the lanes highlighted the differences in traffic management in the 36 hours following paving and differences in the width of paving. These are summarised as follows:

- Right lane paved Saturday, 11 February. Opened to traffic ~18 hours later with temporary traffic management in place. This resulted in well controlled rolling by traffic within the wheel paths during the 18-36 hours following paving. Fully opened to traffic ~36 hours after paving.
- Left lane paved Sunday, 12 February. Fully opened to traffic ~18 hours after paving (no temporary traffic management). Initial traffic was able to wander within the lane reducing the amount of rolling within the wheel paths compared to the right lane.
- Right lane narrower than left lane, and potentially receives a longer duration of rolling by the 7-ton roller during construction, and had the paver screed extensions largely retracted.
- By the time the mean profile depth measurements were taken on Monday, 13 February, the right lane wheel paths had effectively received a longer duration of rolling than the left lane wheel paths, resulting in a smoother surface.

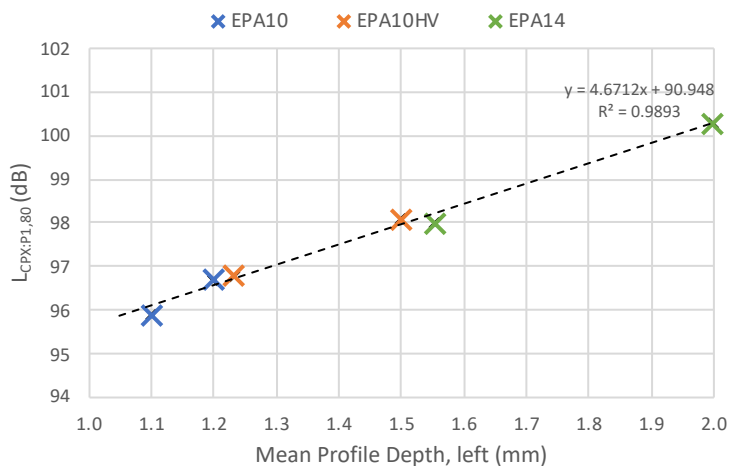


Figure 62 High-void trial sections – relationship between mean profile depth and $L_{CPX:P1,80}$.

Statistical pass-by (“SPB”) testing was performed by WSP-Opus in July 2018 to check for noise reduction effects at the way-side that may not be detectable using the CPX method; no additional way-side noise reduction was observed¹.

The results of the trial demonstrate how macrotexture is a strong driver of differences in tyre/road noise between different porous asphalt mixes. It also shows how an increase in void content results in an increase in macrotexture, and that any noise reduction due to increased void content is insufficient to make up for the increase in noise due to macrotexture.

CPX measurements will continue to be taken for this section of road to investigate age effects.

A.2 WBB pre-construction EPA7 trial

Initial results from the Sawyers to Groynes sections showed that surfaces with higher mean profile depth values (i.e. EPA14 compared to EPA10) produced higher noise levels. It was expected that a reduction in chip size, and hence mean profile depth, would result in a quieter surface.

A section of EPA7 (40 mm nominal thickness) was laid by Fulton Hogan in late 2017 at the southern extent of Western Belfast Bypass to investigate the effect of reduce chip sizes in a porous asphalt surface. CPX measurements were taken on:

- 21 March 2018
- 18 July 2018
- 17 December 2018
- 21 March 2019

The 21 March 2018 results for the left and right lanes are presented in Figure 63.

As was the case with the high void test sections, the EPA7 section shows higher noise levels in the left lane compared to the right lane. Unlike the high void test section, the EPA7 surface was laid before the road was opened to the public, so any degradation of the left lane has occurred after the surface finished curing.

¹ WSP-Opus (2019). NZTA road surface noise research programme – Task A: Close proximity versus wayside measurements.

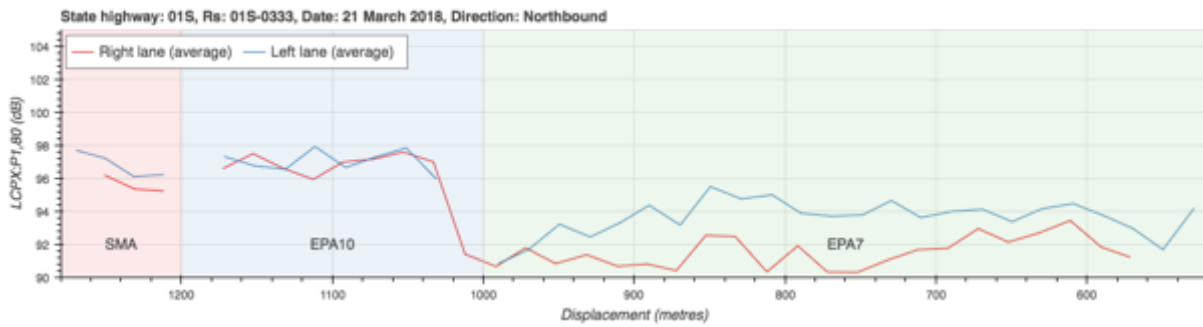


Figure 63 EPA7, Western Belfast Bypass (SH1) – 21 March 2018

Overall, there has been a reduction in noise of 2–4 dB compared to EPA10 sections. CPX measurements will continue to be taken for this section of road to investigate age effects.

A.3 Memorial Ave bridge EPA7 trial

A further section of EPA7 (30 mm thick) was laid by Downer along SH1 at the Memorial Avenue bridge on 7 April 2018 (descending abutment) and 14 April 2018 (ascent abutment).

The 50 km/h speed restriction was in place until May 2018 awaiting completion of the kerb detailing. CPX measurements were taken on 8 June 2018 and showed no improvement over the standard EPA10 mix, with $L_{CPX:P1,80}$ values of 96–97 dB.

The trial site was located on the approaches to the bridge and there is a possibility that the paver behaved differently on the sloped sections of road compared to its behaviour on level sections of road. The CPX measurements may also have been affected by the additional engine noise associated with the tow vehicle travelling uphill.

The limitations of the site were known prior to construction, but the decision was made to go ahead with the site so that it could be determined whether or not these limitations had a significant effect. Due to the site limitations and high initial $L_{CPX:P1,80}$ values only minimal time has been spent analysing the data to date. CPX measurements will continue to be taken for this section of road and will be analysed in detail at a later date.

Appendix B Construction observations

B.1 Shift 1 – Tuesday, 23 October 2018

Carriageway	Southbound
Lane	Right
Start position	01S-0327/02.472-I
End position	01S-0327/04.400-I
Start time	2018-10-23 2206h
End time	2018-10-24 0443h
Weather conditions	Cool and foggy (11°C min)
Length paved	1,798 metres
Average width	4.75 metres
Total asphalt	611 tonnes
Paver	logger-01 (ch1 left wheel path, ch2 right wheel path)
Break-down roller	logger-03
Secondary roller	logger-02

No material transfer vehicle ("MTV") – the ring feeders on the asphalt trucks meant that the trucks could not access the MTV hopper and the MTV was abandoned for shift 1. The ring feeders were removed from the trucks for shift 2.

Notes

A small patch of SMA was repaired at the start of the shift (2040h).

The secondary roller broke down shortly after paving began. The temperature logger unit could not be moved to the back-up roller and as a result secondary roller temperature and position information was only recorded for a small section of road. The secondary roller struggled to keep up with the break-down roller and was generally at least 300 metres behind (on subsequent shifts the secondary roller generally kept up with the break-down roller).

The break-down roller performed a single pass (forward and back) across the lane width. One of the passes was generally under vibration; however, there was no clear pattern to the extent of vibration and it was generally performed in a piecemeal fashion. While the majority of the road experienced a single vibration pass some section will have experience multiple vibration passes. The forward extent of break-down rolling was controlled by contractor QC staff who targeted a maximum surface temperature of 90°C. The break-down roller operator frequently rolled beyond the position specified by the QC staff into the hot (>90°C) area.

There were 5 key-ins on this stretch (shift start and two SMA bridge decks) as well as delays getting paving started due to issues with the asphalt truck ring feeders getting in the way of the MTV hopper. This led to numerous disruptions during the first 600 metres of the shift and many asphalt trucks were delayed in unloading (at most there were 10 trucks waiting on site). The paver stopped on every truck that arrived resulting in a brief pause to paving every 30-40 metres. There was a mechanical fault on the right-hand screed that had to be repaired and caused approximately 30 minute delay.

Traffic management

The lane was opened to traffic (50km/h signs) at 0600h on Wednesday, 24 October. A line of cones was placed between the lanes to protect the asphalt edge. The lane was opened to 100 km/h traffic at 0600h on Thursday, 25 October.

B.2 Shift 2 –Wednesday, 24 October 2018

Carriageway	Southbound
Lane	Left lane
Start position	01S-0327/02.472-I
End position	01S-0327/04.400-I
Start time	2018-10-24 2102h
End time	2018-10-25 0446h
Weather conditions	Light mist from 0100h (8°C min)
Length paved	1,836 metres
Average width	6.35 metres
Total asphalt	840 tonnes
Paver	logger-01 (ch1 left wheel path, ch2 right wheel path)
Break-down roller	logger-03
Secondary roller	Logger-02

Notes

The set-up time for shift 2 was shorter as the construction equipment was already on site. There was some initial coordination between the MTV operators and the paver operator. The paver operator would drive as per usual and the MTV operators would adjust their speed to suit.

There were numerous disruptions to paving due to manual edge detailing, removal of unmixed binder from the asphalt mat, asphalt truck breakdown (approximately 60 minutes), paver hopper overflows and MTV hopper/truck spills.

The secondary roller stayed closer to the break-down roller than during shift 1. The secondary roller performed two slow non-vibration passes over each section of road.

Traffic management

The lane was opened to traffic (100km/h signs) at 0600h on Thursday, 25 October.

B.3 Shift 3 – Friday, 26 October 2018

Carriageway	Southbound
Lane	Right lane
Start position	01S-0327/04.400-I
End position	01S-0333/0.510-I
Start time	2018-10-26 1950h
End time	2018-10-27 0109h
Weather conditions	Cold wind (7°C min)
Length paved	1,802 metres
Average width	4.7 metres
Total asphalt	660 tonnes
Paver	logger-01 (ch1 left wheel path, ch2 right wheel path)
Break-down roller	logger-03
Secondary roller	logger-02

Notes

The shift was delayed until Friday, 26 October due to rain on Thursday.

Paving generally went smoothly. There were four key-ins (Groynes bridge SMA and start/end of shift). There were only a few stops to paving (excluding the bridge key-ins), but these were all limited to 1-2 minutes. The asphalt trucks ran smoothly, and there were never more than three trucks on site at any one time. There was a cold wind for the first few hours of the shift and this caused the asphalt to cool much faster than on previous nights. During this period, the asphalt dropped to rolling temperature (90°C) only 5-10 metres behind the paver. The secondary roller was further behind the break-down roller compared to shift 2.

Even with the MTV there were still times when cold asphalt could be seen in the mat. In one case it was visible to the naked eye. The larger ("Trout River") asphalt trucks appeared to provide a more uniform temperature asphalt than the standard asphalt trucks.

Traffic management

The lane was opened to traffic (50km/h signs) at 0600h on Saturday, 27 October. The lane was opened to 100km/h at 0600h on Sunday, 28 October.

B.4 Shift 4 – Sunday, 28 October 2018

Carriageway	Southbound
Lane	Left lane
Start position	01S-0327/04.400-I
End position	01S-0333/0.507-I
Start time	2018-10-28 2120h
End time	2018-10-29 0300h
Weather conditions	Cold, drizzle prior to paving (10°C min)
Length paved	1,763 metres
Average width	6.2 metres
Total asphalt	806 tonnes
Paver	logger-01 (ch1 left wheel path, ch2 right wheel path)
Break-down roller	logger-02
Secondary roller	logger-03 (with temperature display)

Notes

Note that logger-02 and logger-03 were swapped between the rollers on this shift.

There were a few spots of rain during the setup period, but by the time the paving started the rain had cleared completely. There were four key-ins (Groynes bridge SMA and start/end of shift. There were approximately 6 stops (excluding bridge key-ins). One of the stops was due to running out of asphalt and there was a delay of around 10 minutes until the next truck arrived.

The mat held its heat longer than the previous shift and the break-down roller was generally at least 50 metres behind the paver.

Traffic management

The lane was opened to traffic (100km/h signs) at 0600h on Monday, 29 October.

B.5 Shift 5 – Sunday, 4 November 2018

Carriageway	Northbound
Lane	Right lane
Start position	01S-0333/0.310-D
End position	01S-0327/02.995-D
Start time	2018-11-04 2053h
End time	2018-11-05 0427h
Weather conditions	Clear (5°C min)
Length paved	2,898 metres
Average width	4.8 metres
Total asphalt	1101 tonnes
Paver	01 (ch1 left wheel path (long arm), ch2 right wheel path (short arm), ch3 middle (long arm))
Break-down roller	logger-02
Secondary roller	logger-03 (with temperature display)

Notes

Paving was delayed for a week due to rain.

The lane was narrow meaning slightly longer intervals between trucks, rarely running out of asphalt (only once during the shift) and trucks only waiting a short time to unload (1-2 trucks waiting for most of the shift). The lack of kerb detailing and manhole lids meant a relatively smooth paving run. There were some delays at the very start of the shift that saw 5-7 trucks waiting before paving commenced.

There were four key-ins (Groynes bridge SMA and start/end of shift). The final key-in was at the Dickey's Rd bridge.

The secondary roller took over from the break-down roller when the break-down roller ran out of water. The break-down roller assisted the secondary roller at times.

The break-down roller picked up part of the mat at 01S-0327/04.681-D (within the 40mm trial section). Most of the damage was in the median shoulder, apart from a 2-metre section in the right wheel path about 50 metres behind where the roller first picked up. Observed temperatures reached 103°C immediately before the roller picked-up, however, the high rolling temperature was not uncommon. The cause was attributed to the break-down roller operator feathering the water supply to delay returning to the water truck to refill.

Traffic management

The road was opened to traffic (50km/h signs) at 1000h Monday, 5 November. The lane was opened to 100km/h at 1000h on Tuesday, 6 November.

B.6 Shift 6 – Monday, 5 November 2018

Carriageway	Northbound
Lane	Left lane
Start position	01S-0333/0.310-D
End position	01S-0327/03.624-D
Start time	2018-11-06 0053h
End time	2018-11-06 0814h
Weather conditions	Clear (7°C min)
Length paved	2,274 metres
Average width	6.0 metres
Total tonnes	1102 tonnes
Paver	logger-01 (ch1 left wheel path (long arm), ch2 right wheel path (short arm), ch3 middle (long arm))
Break-down roller	logger-03
Secondary roller	not monitored

Notes

Logger-02 was not working during this shift and logger-03 was moved from the secondary roller to the break-down roller.

The secondary roller took over from the break-down roller when the break-down roller ran out of water. The break-down roller assisted the secondary roller at times.

There were three key-ins (Groynes bridge SMA and start of shift) and numerous stops due to kerb detailing and manhole lids. Paving was intentionally slowed down during the final 90 minutes of the shift to allow the asphalt trucks extra time to negotiate the morning traffic, which minimised stoppage time due to running out of asphalt.

The shift was completed in the daylight. The line markers later commented that the surface was still sticky when they marked the lines mid-morning.

Traffic management

The lane was opened to traffic (100km/h signs) at 1000h on Tuesday, 6 November.

B.7 Shift 7 – Tuesday, 6 November 2018

Carriageway	Northbound
Lane	Left lane
Start position	01S-0327/03.624-D
End position	01S-0327/02.386-D
Start time	2018-11-07 0053h
End time	2018-11-07 0505h
Weather conditions	Clear (6°C min)
Length paved	1,116 metres
Average width	6.2 metres
Total asphalt	562 tonnes
Paver	logger-01 (ch1 left wheel path (long arm), ch2 right wheel path (short arm), ch3 middle (long arm))
Break-down roller	logger-02
Secondary roller	logger-03 (with temperature display)

Notes

The left lane was continued with from the previous shift as it was the longest remaining section. This left the shortest stretch to be paved during the final shift.

The secondary roller took over from the break-down roller when the break-down roller ran out of water. The break-down roller assisted the secondary roller at times.

There were numerous stops due to manhole lid and edge detailing, particularly around the concrete barriers at the bridges. There were six key-ins (two SMA bridges and start/end of shift).

Traffic management

The lane was opened to traffic (50km/h signs) at 1000h on Wednesday, 7 November. The lane was opened to 100km/h at 1000h on Thursday, 8 November.

B.8 Shift 8 – Wednesday, 7 November 2018

Carriageway	Northbound
Lane	Right lane
Start position	01S-0327/02.949-D
End position	01S-0327/02.386-D
Start time	2018-11-08 0010h
End time	2018-11-08 0151h
Weather conditions	Clear (14°C min)
Length paved	494 metres
Average width	5.3 metres
Total asphalt	182 tonnes
Paver	logger-01 (ch1 left wheel path (long arm), ch2 right wheel path (short arm), ch3 middle (long arm))
Break-down roller	logger-02
Secondary roller	logger-03 (with temperature display)

Notes

The shift started at the northern side of the Dickey's Rd bridge. Paving began as soon as the first asphalt truck arrived on site and ran smoothly with some brief stops due to edge detailing on the centre median. There were four key-ins (one bridge and start/end) and the asphalt trucks had to wait while the paver traversed the bridge.

Traffic management

The lane was opened to traffic (100km/h signs) at 1000h on Thursday, 8 November.

Appendix C Ground Penetrating Radar

C.1 Background

General information

Ground penetrating radars (“GPR”) measure the travel time and reflection amplitudes of electromagnetic pulses generated by a horn. Reflections occur due to electrical interferences (changes in a material’s dielectric constant) at the interface between two layers caused by:

- Differences in materials,
- Areas of differing moisture content, and/or
- Areas of differing density or void content.

The dielectric constants of some common materials are listed below². The measured dielectric constant is the volumetric ratio of dielectric constants of the layer’s component materials, meaning that a change in air void content will be seen as a change in dielectric constant.

Table 18 Dielectric constants of common materials

Material	Dielectric constant
Air	1
Asphalt (dry)	2–4
Asphalt (wet)	6–12
Clay (dry)	2–6
Clay (wet)	5–40
Concrete (dry)	4–10
Concrete (wet)	10–20

Figure 64 shows the reflections that occur at various layer interfaces. The recorded signal (measured by the GPR receiver) contains reflection time information (t_1 and t_2) and peak reflection amplitude (A_0 , A_1 and A_2). The reflection time and amplitude information can be used to determine the layer thicknesses (d_1 and d_2) and layer dielectric constants ($\epsilon_{r,1}$, $\epsilon_{r,2}$, $\epsilon_{r,3}$) using the following equations^{4,3}:

$$d_i = \frac{ct_i}{2\sqrt{\epsilon_{r,i}}}$$

$$\epsilon_{r,1} = \left[\frac{A_{inc} + A_0}{A_{inc} - A_0} \right]^2$$

where

- c is the speed of light in free space ($\sim 3 \times 10^8$ m/s),
- i is the layer number,
- A_{inc} is the peak amplitude of the incident wave, obtained by performing a measurement over a metal plate (assumed to be a perfect reflector).

Calculation of the dielectric constants of layers 2 and below (base and subgrade) are based on the calculated dielectric constants for the layers above (equations not included here). These relationships are simplifications and do not account for attenuation within the layer above the

² D.J. Daniels, Ground Penetrating Radar, Institution of Engineering and Technology (2004)

³ Lahour, S. Development of data analysis algorithms for interpretation of ground penetrating radar data. PhD Thesis. Virginia Polytechnic Institute and State University. (2003)

interface. This results in an underestimation of the dielectric constant of the layer below the interface and hence an overestimation of the thickness of the layer below the interface.

Inhomogeneities within a layer due to defects, repairs, moisture accumulation or multiple lifts are also not accounted for. Each feature can cause a small reflection due to a small change in dielectric constant, hence GPR measurements taken on existing roads can be unreliable or difficult to interpret. Inhomogeneity issues are generally less of a concern for GPR measurements taken on newly constructed roads.

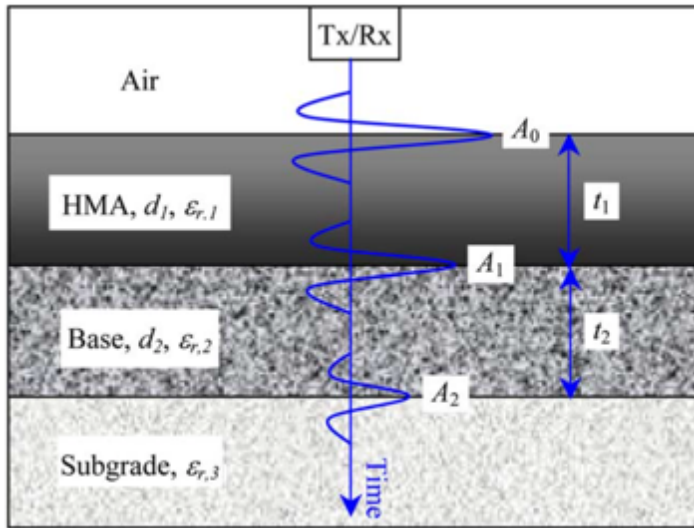


Figure 64 Reflections due to changes in material dielectric constant (from [4]).

Depth resolution limitations

The minimum resolvable layer depth is limited by the width of the transmitted radar pulse, which is a function of the GPR system being used. Layers that are too thin will be obscured by the larger reflection from the interface at the top of the layer.

The minimum resolvable layer depth can be calculated using:

$$\Delta d = \frac{cT}{2\sqrt{\epsilon_r}}$$

where

- *T* is the transmitted radar pulse width in seconds.

The width of the radar pulse for the Fulton Hogan 2.0 GHz GPR system is approximately 1.0 ns. Assuming a typical porous asphalt dielectric constant of 4.0 the minimum resolvable asphalt layer depth will be 75 mm. This rules out use a standard GPR assessment for asphalt thickness measurements in New Zealand where asphalt layers are typically 20-50 mm thick.

Lahouar proposed several solutions to the depth resolution problem and found the power cepstrum and iterative decomposition techniques to be the best performing³. The power cepstrum involves calculating the power spectrum of the logarithm of a signal's power spectrum. The resulting signal is composed of peaks that correspond to the reflection times. The iterative decomposition technique involves the detection and subtraction of the largest

⁴ AL-Qadi & Lahouar, Measuring layer thicknesses with GPR – Theory to practice, Construction and Building Materials 19 (2005)

reflection pulse. This process is continued until the residual signal reaches a predefined threshold chosen based on the original signal noise.

The iterative decomposition technique was chosen for the current Western Belfast Bypass project as the process is easier to understand and hence the results easier to check than the power cepstrum technique.

Coupling pulse

The recorded radar signal includes an initial pulse due to the direct signal travelling from the GPR horn's transmitter to its receiver; this is referred to as the "coupling pulse" (see Figure 65).

The coupling pulse is useful as it defines a fixed point in time and can be used to calculate the height of the GPR horn above the surface; however, the coupling pulse can interfere with the subsequent reflection pulses and must be subtracted from the recorded radar signal before attempting to detect the reflection pulses.

The coupling signal can be found by aiming the GPR horn upwards (towards the sky) and taking a recording. The recorded radar signal will contain the clean coupling pulse (without any surface or sub-surface layer reflections).

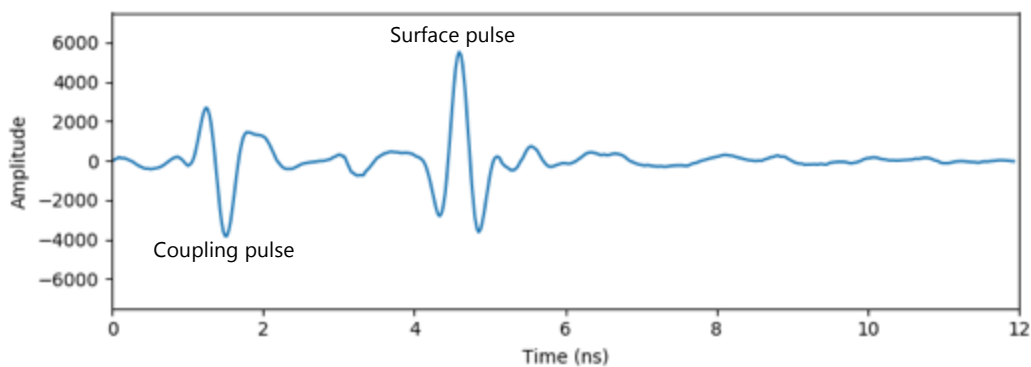


Figure 65 Typical recorded radar signal

Metal plate calibration

In order to calculate the dielectric constant the amplitude of the radar pulse incident on the surface must be found. This is achieved by placing a large metal plate (assumed to be a perfect reflector) on the ground and taking a recording. The peak amplitude of the metal plate reflection is used as the A_{inc} term when calculating the dielectric constant of the first layer.

Fulton Hogan 2GHz GPR system

The Fulton Hogan GPR system is a GSSI SIR20 system with a 2.0 GHz horn. The system is designed to be fitted to a vehicle and driven at road speeds along the survey section (see Figure 66). The system records a "GPR scan" every 0.25 metres along the road resulting in 4,000 scans per 1 km of road surveyed. Each scan is GPS referenced. The measurements are distance-triggered using a wheel encoder attached to one of the rear wheels of the survey vehicle.



Figure 66 Fulton Hogan GSSI SIR20 GPR system with 2 GHz horn fitted to the survey vehicle.

C.2 Raw data processing methods and problems

Coupling pulse removal

The coupling pulse removal process was performed as follows:

1. The clean coupling pulse is found by aiming the GPR horn upwards and taking a recording.
2. The cross-correlation of the clean coupling pulse signal and the recorded ground reflection signal is calculated and the sample offset is calculated.
3. The clean coupling pulse is then zero-padded to match the coupling pulse in the recorded ground reflection signal. This results in the clean coupling pulse being aligned with the recorded ground reflection signal to within one sample point.

4. The clean coupling pulse is then repeatedly shifted by $1/50^{\text{th}}$ of a sample to find the sub-sample shift required to give the best correlation coefficient (see BS EN 1793-5⁵ for a description of the sub-sample shift process).
5. The sub-sample-shifted coupling pulse is then subtracted from the recorded ground reflection signal.

Figure 67 and Figure 68 show the coupling pulse removal process.

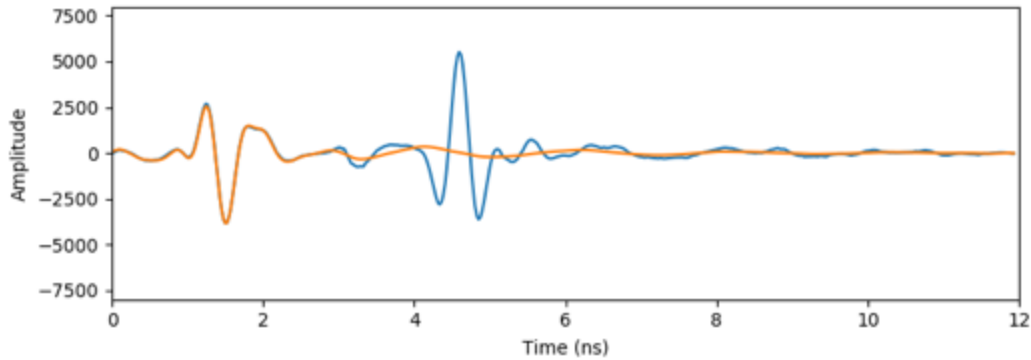


Figure 67 Raw trace with aligned coupling pulse.

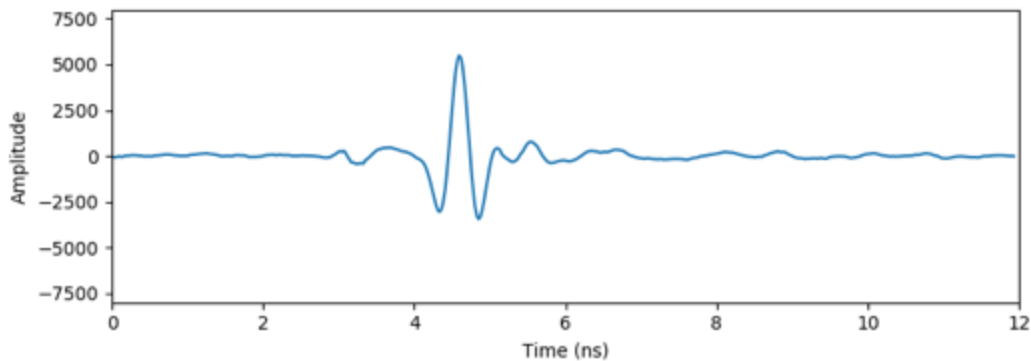


Figure 68 Raw trace with coupling pulse removed, leaving surface and sub-surface reflections.

Incident pulse amplitude

The incident pulse peak amplitude (A_{inc}) is required for determination of the surface layer dielectric constant. The metal plate calibration process provides this value by assuming that the metal plate represents a perfect reflector.

While taking the metal plate calibration measurement it was noted that the metal plate reflection amplitude varied with the height of the GPR horn, suggesting non-trivial attenuation of the radar wave as it travelled through the air. A recording was taken while bouncing the rear of survey vehicle to represent the bumps in the road that would be present during a survey. The results showed a 10% variation in the peak amplitude and that the amplitude was negatively correlated to the sample delay between the coupling pulse and metal plate reflection (GPR horn height) (see Figure 69).

⁵ BS EN 1793-5:2016. Road traffic noise reducing devices – Test method for determining the acoustic performance – Intrinsic characteristics – In situ values of sound reflection under direct sound field conditions.

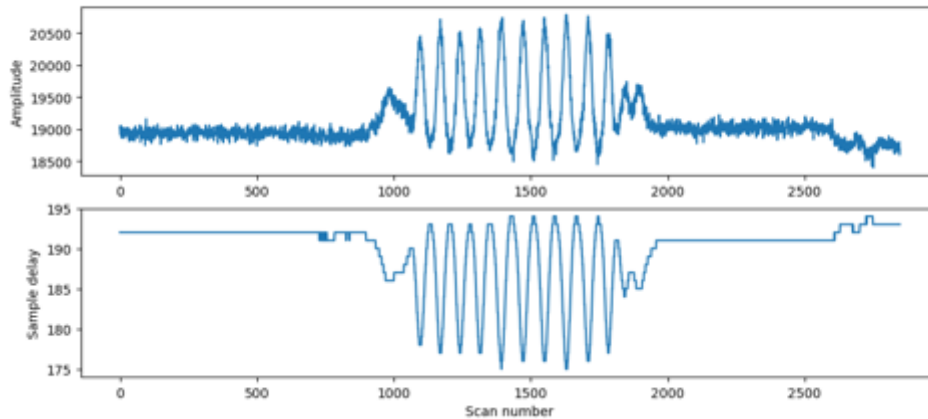


Figure 69 Metal plate peak amplitude (top) and sample delay (bottom) during a bounce test.

Rather than using a constant incident pulse peak amplitude, as is common practice, the decision was made to calculate the effective incident pulse peak amplitude for each GPR trace. Figure 70 shows the linear regression of the metal plate peak amplitude to surface pulse two-way travel time (Δt). The resulting relationship is included below.

$$A_{inc} = -4.4209 \times 10^{12} \Delta t + 32986$$

For the GPR measurements taken on Western Belfast Bypass the effective incident pulse peak amplitude was calculated for each GPR scan using the two-way travel time between the coupling pulse and the surface reflection.

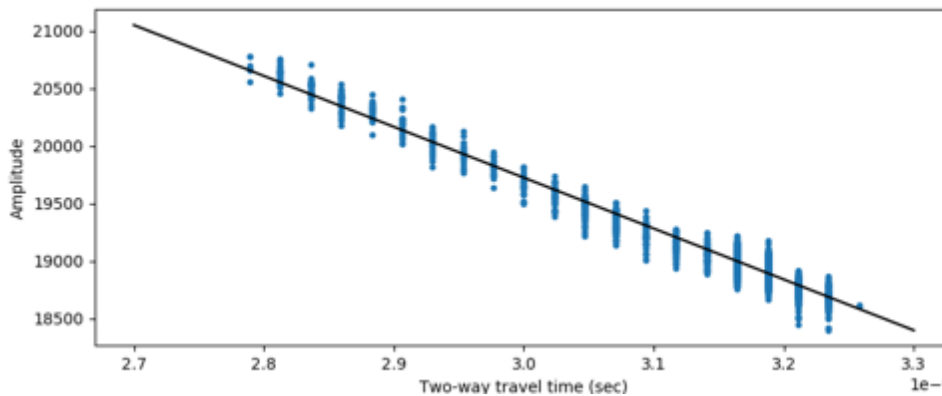


Figure 70 Metal plate amplitude versus coupling pulse to surface reflection two-way travel time.

Subsequent interface reflections and ringing

Interfaces below the asphalt-base interface, such as the base-subgrade interface or an interface between two lifts in the base layer, can obscure the asphalt-base interface in the same way that the surface reflection obscures subsequent interface reflections (i.e. due to the long radar pulse width). A similar problem exists when there is a ringing reflection, which occurs when the radar pulse repeatedly reflects between two layer interfaces. This is a major issue where there are metal objects buried in the ground, but can also cause problems for weaker reflecting interfaces such as the asphalt-base layer interface.

Ringings usually means that the weaker reflecting interfaces beneath a highly reflecting interface are masked by the ringing reflections; however, the ringing reflection can also complicate the detection of the interface causing the ringing where the layer is thin. A ringing reflection from the bottom interface of a thin layer will obscure the initial reflection in the same way that the surface reflection obscures subsequent interface reflections.

In order to detect the desired asphalt-base interface reflection all nearby interface and ringing reflections must be accounted for. Failure to account for these additional reflection pulses will lead to a poor detection of the asphalt-base interface location.

Iterative decomposition

The iterative decomposition was performed as follows for each "GPR scan":

1. Chose a threshold level based on the noise in the raw signal. The iterative decomposition process will stop when the peak amplitude in the residual signal drops below the threshold value.
2. Remove the coupling pulse using the procedure described in the coupling pulse removal section above.
3. Use the cross-correlation and sub-sample shift process (described in the coupling pulse removal section) to synthesise the surface reflection pulse. An inverted version of the coupling pulse is used as the reference pulse. See Figure 71.
4. Remove the synthesised surface pulse from the signal.
5. Use the cross-correlation and sub-sample shift process to synthesise the next most significant reflection pulse (either a ringing reflection or lift-interface within the base layer).
6. Remove the synthesised pulse from the signal.
7. Repeat steps 4 to 6 until the peak amplitude in the residual signal drops below the threshold set in step 1.

Improve each synthesised pulse. For each synthesised pulse:

8. Subtract the other synthesised pulses and coupling pulse from the raw signal.
9. Use the sub-sample shift process to find a new synthesised pulse that better matched the target reflection pulse.

The peak amplitude of the synthesised surface reflection pulse is used to calculate the surface layer dielectric constant. The first synthesised pulse following the surface reflection is assumed to be the asphalt-base interface. The time delay between the surface reflection and the asphalt-base interface reflection is used to calculate the asphalt layer depth.

Figure 72 compares the raw signal (with coupling pulse removed) to a signal comprising of the combination of all synthesised pulses.

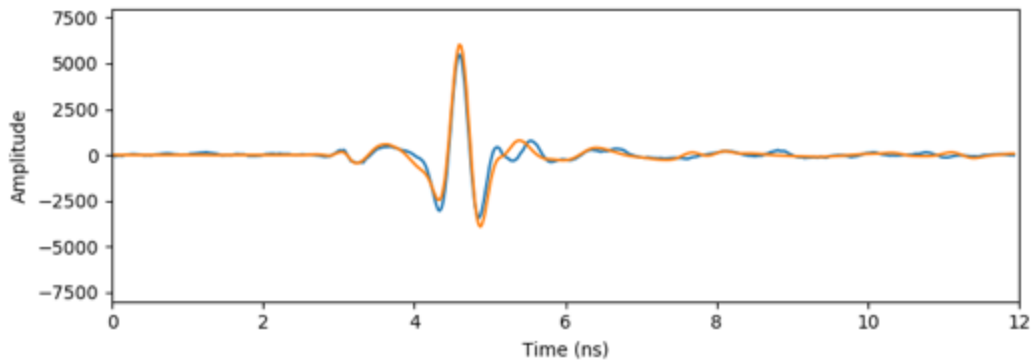


Figure 71 Raw signal with coupling pulse removed (blue) and synthesised surface reflection pulse (orange).

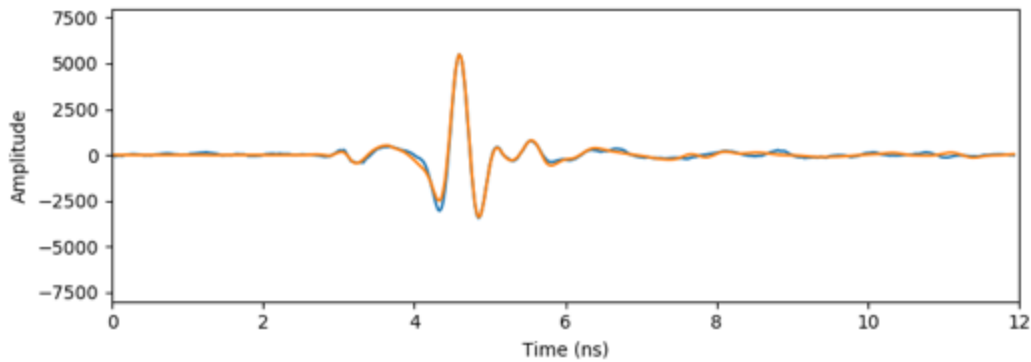


Figure 72 Raw signal with coupling pulse removed (blue) and combination of all synthesised pulses (orange).

While the iterative decomposition technique worked well in removing the surface pulse, problems with ringing reflections and transmitted pulse distortions due to diffraction of the radar wave meant that the asphalt-base interface could generally not be reliably detected.

In most cases the distortion of the transmitted pulse means that the reference pulse, used in the decomposition process, was a poor representation of the target pulse being detected. Subtraction of the synthesised pulse from the target pulse leaves a residual component with a similar shape to the reference pulse. The iterative decomposition process then attempts to synthesise a new pulse representative of the residual pulse, thus effectively splitting the target pulse in two (Figure 73).

The distortion problem does not consistently result in a splitting of the asphalt-base interface reflection pulse in to two synthesised pulses.

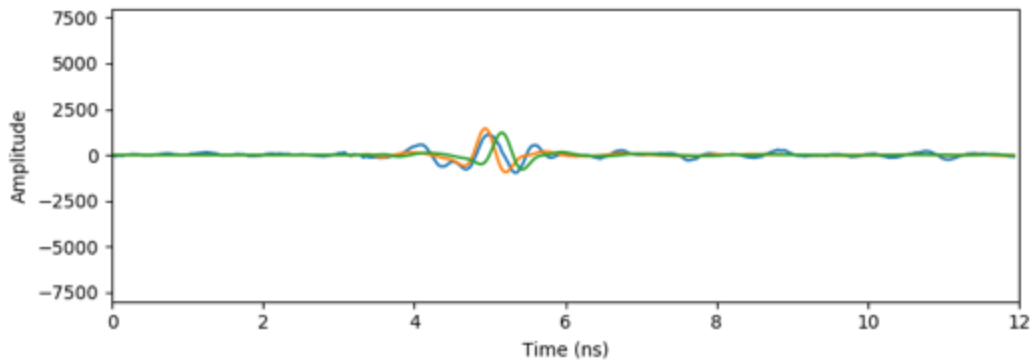


Figure 73 Residual signal after removal of the surface pulse (blue), asphalt-base interface pulse split in to two pulses (orange and green) due to the reference pulse being a poor representation of the target pulse.

C.3 Conclusions and recommendations

Asphalt layer thickness

The use of a ground penetrating radar for asphalt layer thickness measurements has failed to yield reliable results. The main issue being that the surface reflection pulse obscures the reflection pulse of the asphalt-base interface due to the width of the incident radar pulse, which generally limits the minimum resolvable depth to ~75 mm for porous asphalt surfaces.

An iterative decomposition technique was used to remove the surface reflection pulse. While this technique worked well in removing the surface pulse, additional problems with ringing reflections and transmitted pulse distortions due to diffraction of the radar wave meant that the asphalt-base interface could not be reliably found.

Further development and testing of the processing algorithm would be required to yield reliable asphalt thickness values. Specifically:

- Investigate the power cepstrum technique to see if it better deals with the ringing reflections and transmitted pulse distortions.
- Modify the reference pulse used at each stage of the iterative decomposition process to account for the transmitted pulse distortions.

Asphalt layer dielectric constant

The relationship between asphalt dielectric constant and dielectric constant needs to be determined. This can be achieved using a ground-truthing approach, where the dielectric constant is measurement for several sections of asphalt and then the sections of asphalt are cored and the air-void content calculated in the laboratory.

Appendix D Temperature and position loggers

D.1 Background

The temperature and position logger specifications were as follows:

- 1-4 input channels for 4-20mA infrared temperature sensor.
- GPS positioning, synchronised with temperature readings.
- 1 Hz minimum sample rate.
- Stand-alone unit with on-board power supply and SD storage.
- Rugged case.
- Simple mounting arrangement.

No off-the-shelf system was available to perform the temperature and position monitoring at a reasonable cost that would allow three pieces of construction equipment to be equipped; therefore, the decision was made to develop a bespoke system.

Two base options were considered:

DataTaker – Commercial data logging platform

Advantages	Disadvantages
20mA analog input available	No wireless comms on base model.
128MB storage	No built-in GPS receiver.
6A 1.2Ah internal battery	1.5 kg
	High power usage (1.35W or 113mA@12V for 1Hz sampling) probably requiring an additional battery (adding weight).
	Unfamiliar software.

Particle Asset Tracker – Commercial Internet of Things (IoT) platform

Advantages	Disadvantages
Built-in GPS receiver and low-cost accelerometer.	No on-board storage
Built-in 3G modem.	No built-in 20mA sensor input
Small and light.	Requires external battery (but free to choose).
Familiar software and large support network.	

The Particle Asset Tracker was chosen as it provided more flexibility and familiar software, while having a good support network to assist with implementation of the on-board SD storage and 20mA sensor input. The 3G modem also provided a means of verifying correct logger operation during the paving shifts, something that could not be easily done with the DataTaker platform.

Five 4-20mA infrared temperature sensors were purchased and 3D printed plastic clamps were designed to hold each sensor (Figure 74). Magnetic mounts were used to secure the logger enclosure and temperature probes to the construction equipment (Figure 75).

The final bill of materials for the logger units was as follows.

Item
Particle Asset Tracker
20mA sensor circuit board
SD storage circuit board
SD card
Printed circuit board (custom design with power management and signal routing circuitry)
Active GPS antenna
Plastic enclosure
12V lead acid battery

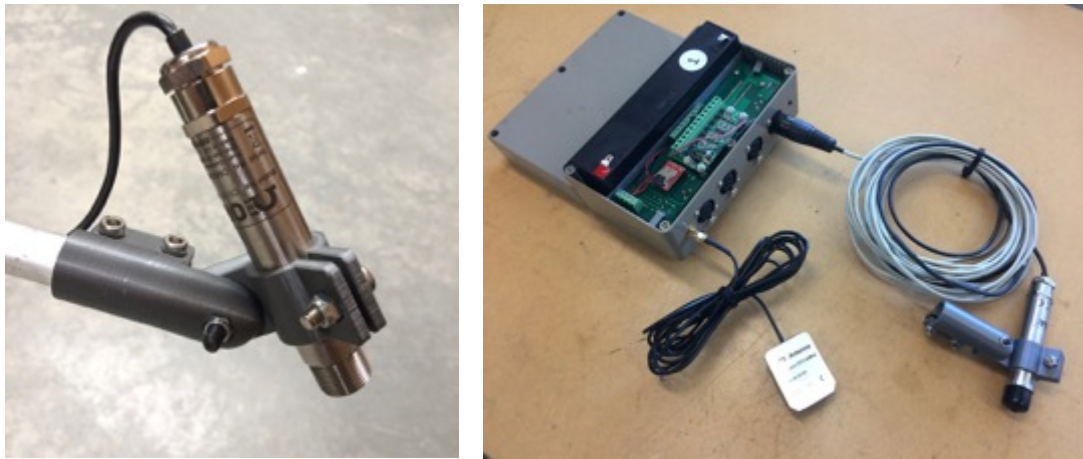


Figure 74 Infrared temperature probes and 3D printed mounts (left), logger unit with GPS antenna and temperature probes connected (right).

D.2 Paver monitoring

D.2.1 Logger and sensor mounting

The logger unit was fixed to the horizontal crossbar that forms part of the pavers roof. The temperature probe signal cables ran along the horizontal crossbar to each vertical roof support where the temperature probes were fixed. The GPS antenna was secured to the roof of the paver. All equipment was removed at the end of each paving shift.

Figure 75 shows the position of the logger unit and temperature probes on the paver.

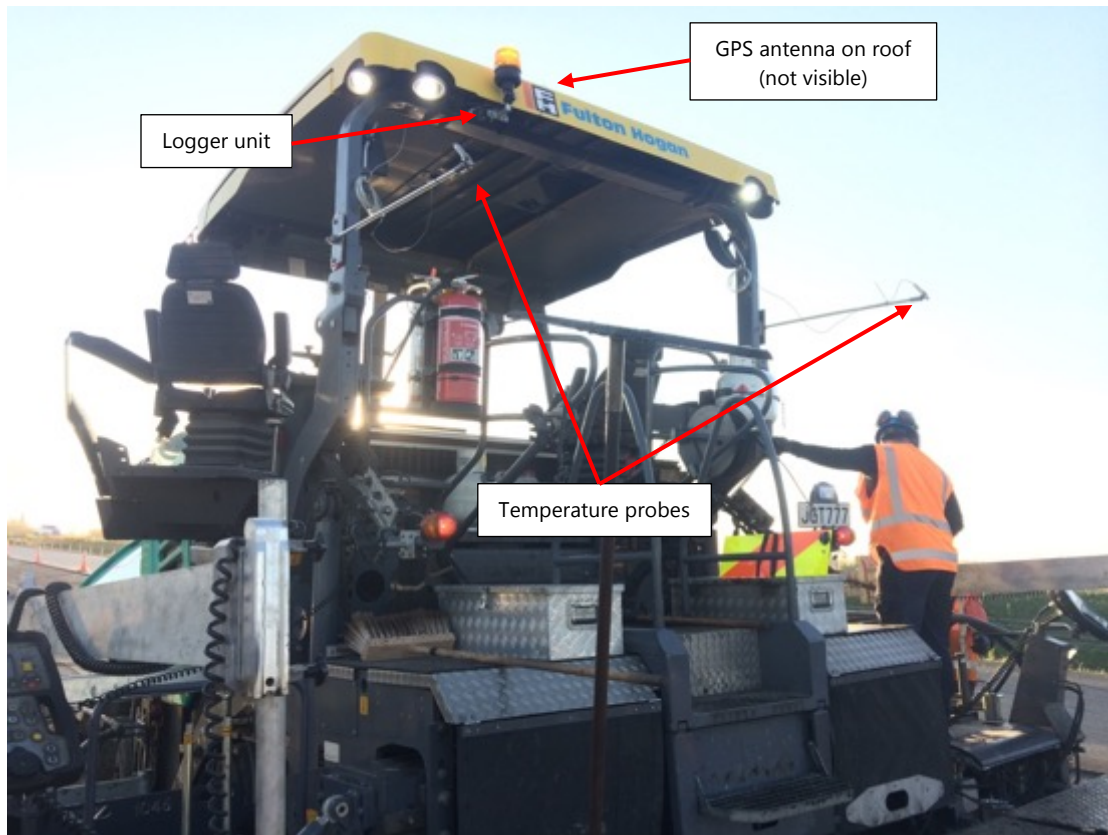


Figure 75 Temperature logger positioning on paver

D.2.2 Data collection and processing

The temperature and position data was collected during eight construction shifts. At least two temperature sensors (aimed at the left and right wheel paths) were used during all shifts. A third temperature sensor was added for shifts 5-8 and this was aimed in the middle of the lane.

The data was processed using the following procedure:

1. The start and end reading number for each continuously paved section of road was found by manually inspecting the data. The start and end reading numbers were stored in the SQL database. E.g. the first continuous run during shift 1 started at the northern extent of the project and ended at the northern edge of Dickies Rd bridge.
2. The GPS coordinates associated with each temperature reading was converted to Rs/Rp positions and the field added to each temperature reading.
3. Two datasets were then created from the base dataset:
 - Screed dataset – screed positions and start/stop points within each continuous paved section. The displacement values were adjusted based on the offset displacement of the GPS antenna from the screed (2 metres in front, see Figure 76). The speed and distance between readings was used to determine where paving was temporarily halted and an "is_stopped" field was added to each temperature reading.

- Temperature dataset – temperature readings. The displacement values were adjusted based on the offset displacement of the GPS antenna from the temperature sensors (4 metres in front, see Figure 76).
4. A uniform 1 metre grid of start and end displacements was then built and the minimum, maximum, mean and standard deviations of temperature readings within each 1 metre segment were calculated.
 5. Since the temperature sensors are aimed behind the screed, when the paver stops there is a section of asphalt between the screed and temperature sensors that starts to cool. The temperatures of this cooled section will be read when the paver starts to move again, however, these later values are invalid as the asphalt has been cooling for a variable period of time. An additional field was added to note whether each 1 metre road segment held valid data.
 6. In some cases a person or object obscured the sensor's view of the asphalt mat and resulted in low readings. The validity field was updated to remove any readings below 80°C and any readings where the channel 1 (left wheel path) and channel 2 (right wheel path) data differed by more than 10°C.

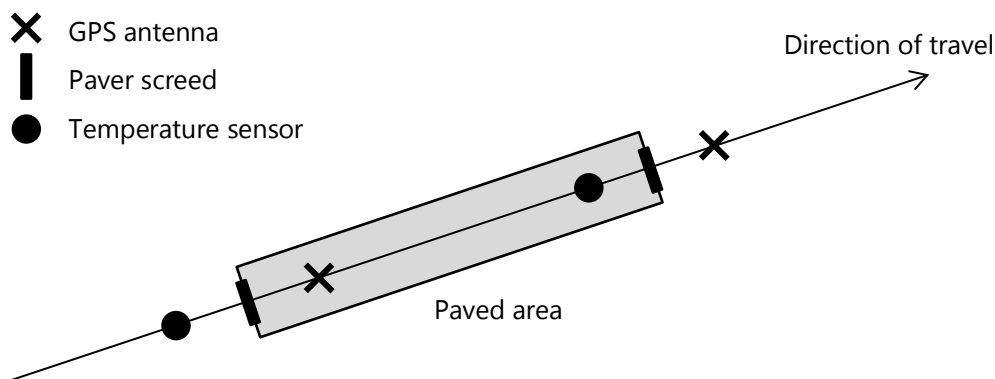


Figure 76 Diagram showing the position of GPS antenna, paver screed and temperature sensors during paver monitoring.

D.3 Roller monitoring

D.3.1 Logger and sensor mounting

The logger unit was installed inside the cab of each roller. The temperature probe signal cable and GPS antenna cable ran out the driver's door. The temperature probes were fixed to the front of each roller and the GPS antenna was secured to the roof. The logger units were removed at the end of each paving shift. The temperature probes and GPS antenna were left attached to the rollers between shifts (each temperature probe was covered with a plastic bag to protect it from rain).

Figure 77 shows the position of the logger unit and temperature probes on one of the rollers.



Figure 77 Temperature logger positioning on roller

D.3.2 Data collection and processing

The temperature and position data was collected during the eight construction shifts. No measurements were recorded for the secondary roller during shifts 1 (due to roller breakdown) and shift 6 (due to a faulty logger unit).

At the time of writing the processing methodology for the roller temperature data has yet to be developed.

Appendix E 3D Lidar Scan Data

Lidar data was provided for the chipseal and asphalt surfaces as separate "las" files. The data was processed using the following procedure:

1. The "las" files were processed into "tiff" files with 0.2 metre resolution and loaded into QGIS.
2. The 2018 HSD survey lane centrelines were used as the reference centrelines. The reference centreline provided the mid-lane position.
3. The mid-lane position was offset by 0.8 metres to the left, to give the left wheel path line.
4. Cross-sections of each surface were taken using the left wheel path lines for each lane. The resulting cross-section was a set of points where the polyline crosses a surface triangulation line (i.e. it is an interpolated version of the original "tiff" surface).
5. By using the same polyline as the basis for the cross-section on both the chipseal and asphalt surfaces, the height points were taken at identical positions. The thickness was calculated by subtracting the chipseal surface height from the asphalt surface height.
6. The GPS coordinates for each point were then converted to Rs/Rp positions.
7. A uniform 1 metre grid of start and end displacements was then built and the minimum, maximum, mean and standard deviations of the thickness readings within each 1 metre segment were calculated.

Appendix F 1 metre Mean Profile Depth Data

The 1 metre mean profile depth (MPD) readings were provided by WDM for the northbound carriageway and the final ~400 metres of the southbound carriageway. The files also covered the remainder of Rs 01S-0333, however, these areas were not required as part of this study.

The data was provided as displacement – mean profile depth pairs. The relationship between the displacement and the Rs/Rp reference system was determined by manually inspecting the mean profile depth trace and identifying surface transitions. The following tables provide details of the alignment; the highlighted rows were used as the datum point and “rubber-banding” was performed using the calculated scaling factor. The mean profile depth values were then mapped (interpolated) back on to a 1 metre grid.

Table 19 Northbound

		Northbound, left lane	Northbound, right lane
	Measurement name	S1D034419_S10_190126163127	S1D034419_S10_190126163127
Start	Surface transition	WBB southern extent (SMA10 to EPA7)	WBB southern extent (SMA10 to EPA7)
	MPD displacement	10,385 metres	10,413 metres
	Rp displacement	316 metres (road_id: 3656)	316 metres (road_id: 3656)
End	Surface transition	WBB northern extent (EPA7 to SMA10)	WBB northern extent (EPA7 to SMA10)
	MPD displacement	13,990 metres	14,021 metres
	Rp displacement	2,404 metres (road_id: 1715*)	2,404 metres (road_id: 1715*)
	MPD distance	3,605metres	3,608 metres
	Rp distance	3,590 metres	3,590 metres
	Difference	15 metres	18 metres
	Scaling factor	0.9958	0.9950

* Road id 1715 ends at Rp displacement 5,678 metres.

Table 20 Southbound

		Southbound, left lane	Southbound, right lane
	Measurement name	S11033319_S10_190127080316	S11033319_S10_190127091130
Start	Surface transition	Groynes bridge (EPA7 to SMA10)	Groynes bridge (EPA7 to SMA10)
	MPD displacement	40 metres	40 metres
	Rp displacement	5,750 metres (road_id: 1716*)	5,750 metres (road_id: 1716*)
End	Surface transition	WBB southern extent, after ramp SMA (SMA10 to EPA10)	WBB southern extent, after ramp SMA (SMA10 to EPA10)
	MPD displacement	884 metres	879 metres
	Rp displacement	830 metres (road_id: 3650)	830 metres (road_id: 3650)
	MPD distance	844 metres	839 metres
	Rp distance	849 metres	849 metres
	Difference	5 metres	10 metres
	Scaling factor	0.9941	0.9882

* Road id 1716 ends at Rp displacement 5,769 metres.